DEVELOPMENT AND CHARACTERIZATION OF BIODEGRADABLE SUTURES MADE OF ELECTROSPUN FIBERS WITH AMPICILLIN

by

HANG LIU

(Under the Direction of Dr. Karen K. Leonas)

ABSTRACT

Surgical sutures are one of the most frequently used devices in emergency rooms and operating theatres. Due to the large number of surgical site infections caused by suture implantations, there is an increasing need for the application of sutures with antimicrobial properties, especially biodegradable sutures with the controlled release of antimicrobial agents. A study was carried out to develop these suture fibers by electrospinning and evaluate selected properties of the fibers. As electrospinning is a relatively new spinning method and fundamental understanding of the technique has not been established, the spinning process and the influence of the processing parameters on the fiber properties were studied as well.

Polycaprolactone, a biodegradable polymer used in biomaterials approved by the Food and Drug Administration (FDA), was the polymer selected. The antimicrobial agent, which was incorporated in the polymer solution to provide the produced fibers with antimicrobial properties, was ampicillin sodium salt. The selected fiber properties included physical and mechanical properties, antimicrobial properties, and the release of ampicillin from the fibers, as well as biodegradation properties.

One of the major goals of the study was to establish methodologies to collect and characterize electrospun nanofibers, which could be physically manipulated as required for suture applications. The use of a thin disk as the electrospinning collector to collect nanofiber bundles has been proved to be a feasible method to achieve this goal.

Other findings of the dissertation included the following. Fibers with a wide range of diameters and percentages of crystallinity could be produced by varying the polymer solution properties (the polymer concentration and the addition of ampicillin sodium salt) and the spinning processing parameters (voltage, feedrate, and the distance from the needle tip to the collector). The as-spun fibers showed antimicrobial effectiveness on both *S. aureus* and *K. pneumoniae*. The ampicillin release was completed in 96 hours. The mass loss of degraded fibers was less than 3% in 12 weeks, but surface morphological changes were observed in samples that had been exposed to the biodegradation environment for six weeks.

INDEX WORDS: Electrospinning, Surgical sutures, Antimicrobial properties, Degradation properties, Nanofibers

DEVELOPMENT AND CHARACTERIZATION OF BIODEGRADABLE SUTURES MADE OF ELECTROSPUN FIBERS WITH AMPICILLIN

by

HANG LIU

B.S., China Textile University, China, July 1999

M.S., DongHua University, China, March 2002

A Dissertation Submitted to the Graduate Faculty of The University of Georgia in Partial Fulfillment of the Requirements for the Degree

DOCTOR OF PHILOSOPHY

ATHENS, GEORGIA

2008

DEVELOPMENT AND CHARACTERIZATION OF BIODEGRADABLE SUTURES MADE OF ELECTROSPUN FIBERS WITH AMPICILLIN

by

HANG LIU

Major Professor: Karen K. Leonas

Committee: Helen H. Epps
Joy B. Doran Peterson
Guigen Zhang
Yiping Zhao

Electronic Version Approved:

Maureen Grasso
Dean of the Graduate School
The University of Georgia
August 2008

DEDICATION

The dissertation is dedicated to my dear parents: Liu, Huizhong and Yu, Wenqing for their selfless and forever love.

ACKNOWLEDGEMENTS

There are so many people that I would like to thank, who paved the way along with me to make this dissertation a success.

Foremost, sincere thanks to my major professor, Dr. Karen Leonas, for her great insight in the planning of the research and her substantial assistance and guidance throughout my entire course of study at the University of Georgia, especially for her long-distance direction from Pullman, Washington in the last year.

Special thanks to my committee members, Dr. Helen Epps, Dr. Joy Peterson, Dr. Guigen Zhang and Dr. Yiping, Zhao, who have provided valuable suggestions, ideas and supports from various aspects. Thanks for their willingness to assist me in the past three years.

I am grateful to the faculty and staff in the department of Textiles, Merchandising and Interiors and the researchers and students in Dr. Yiping Zhao's research group for their kindness and assistance.

I would also like to thank AATCC Research Foundation for providing financial support for this project.

My deep appreciation goes to my lovely families, my parents for their love and endless support, my sister for taking care of our parents to give me a peace mind from halfway around the globe. At last but not the least, I would like to thank my husband Ting Chi, for his emotional support and confidence on me.

Without the help of any of them, it would not be possible for me to successfully complete the dissertation. THANKS!

TABLE OF CONTENTS

Page

LIST OF TABLES

Page

LIST OF FIGURES

Page

Chapter 1. Introduction

Since the inception of biomaterials approximately a half century ago, they have developed rapidly, and today are widely used in medicine, dentistry, and biotechnology. Surgical sutures, one of the earliest recorded and most frequently used surgical devices in operating theaters and emergency rooms, have been extensively studied during the last fifty years.

A suture, by definition, is a thread-like material used to sew tissue together or to stitch a wound closed [1]. The main function of sutures is to hold the wound together and support the injured tissue until it returns to its own strength and can withstand daily tensile forces. According to Meyer and Antonini [2], the earliest material used as sutures was flax, around 3000 B.C. Historically, a variety of materials have been used and/or are still being used as suture materials, including dried gut, tendon, horse hair, cotton, silk, bark fibers, iron wire, gold, silver, and synthetic polymer fibers, such as polyester, polypropylene, and nylon. Significant developments that have impacted the materials available for sutures were the synthesis and introduction of biodegradable polymers in the 1970s. These provided the advantages of both sutures made from animal tissues and those of synthetic polymers, i.e., biodegradation and biocompatibility, respectively. Biodegradable sutures degrade in the body, and the degradation products can enter metabolic pathways and be excreted from the body. These sutures are also referred to as absorbable sutures. Biocompatible sutures induce less tissue reaction than natural tissue materials. Ever since these absorbable sutures were introduced to the market, they have received a great deal of attention [3]. Absorbable sutures have replaced some nonabsorbable sutures when used in locations where the removal of sutures is undesirable or difficult, and a secondary

invasive procedure is avoided. Today, approximately 42% of the sutures used worldwide are synthetic absorbable sutures [4], 41% are synthetic non-absorbable sutures, and 13% are natural sutures [5]. The use of natural sutures is decreasing due to their inconsistent properties and inflammatory tissue reactions.

All sutures degrade in the harsh environment inside the human body as a result of its aqueous nature and the presence of enzymes, extreme pH, and ions. The strength loss of sutures during degradation always occurs faster than the mass loss. Once sutures lose their strength completely, they are no longer functional. Therefore, the classification of absorbable and nonabsorbable sutures is based on their loss of strength. Sutures that lose their strength completely in two to three months are classified as absorbable sutures, while those that lose their strength completely in more than two to three months are classified as nonabsorbable sutures [6]. Common absorbable polymers used today include polyglycolide (PGA), poly(glycolide-lactide) random copolymer (PLGA), poly-p-dioxanone, poly(glycolide-trimethylene carbonate) block copolymer, polycaprolactone (PCL), poly(glycolide- ε –caprolactone, and glycolide-trimethylene carbonate) block copolymer.

In terms of their physical configuration, sutures are divided into two categories, monofilament and multifilament. Multifilament sutures are made of monofilaments that are braided or twisted together. Each category has advantages and disadvantages when compared to the other. For example, generally, monofilament sutures induce less inflammation and less tissue drag than multifilament sutures; on the other hand, multifilament sutures have higher tensile strength and better handling properties compared to monofilaments. In most cases, multifilament sutures are coated to create a false monofilament, which improves the handling properties and reduces tissue drag [6]. Beeswax, paraffin wax, silicone, and poly(tetrafluoroethylene) are

nonabsorbable coatings used on nonabsorbable sutures, while water-soluble and hydrolytic materials are coating materials commonly used for absorbable sutures. For example, Dexon® Plus, an absorbable suture, is covered with poly(oxyetylene-co-oxypropylene), which is a water-soluble surfactant; Dexon II, another absorbable suture, is coated with a hydrolytic polymer, polycaprolactone [6].

Whether the sutures are absorbable or nonabsorbable, monofilament or multifilament, as foreign materials present in body, all suture implantations may initiate the host's natural defense mechanisms. One of the most common defense mechanisms is local tissue reaction demonstrated as acute inflammation, chronic inflammation, necrosis, and neoplastic transformation [7]. The degree of the host's defense depends primarily on the properties of the sutures.

1.1 Statement of Problem

The designed purpose of surgical sutures is to facilitate wound and tissue healing by holding the open incision together. However, currently, sutures are vehicles that can carry microorganisms into wounds, which may be potential pathogens that will impede the healing of the tissues, and even lead to patients' morbidity and mortality. In addition to the potential to act as a vehicle to transport microorganisms into surgical sites, the use of sutures has also been shown to lower the critical number of bacteria needed to cause infection. Elek and Conen demonstrated that with the presence of silk sutures, the number of bacteria required to cause infection was reduced 10,000-fold of that needed without sutures [8]. To establish infection, 7.5 x 10^6 *S. aureus* were needed without silk suture implantation; with the silk implant suture, only 300 bacteria were enough. Furthermore, sutures can work as substrates on which bacterial biofilms form, which enhance the survival mechanisms of bacteria against antibiotics and body

defense systems. It has been accepted that the implantation of sutures increases the susceptibility of surgical site infections (SSIs).

There are about 2.4 million cases of hospital-acquired infections each year in the United States alone, of which approximately 15% are surgical site infections (SSIs) [9, 10]. Around 66% of these SSIs are confined to the incision, either superficial or deep [11, 12]. Although advanced infection control practices have been recommended by the Centers for Disease Control (CDC) and are practiced by most hospitals, the hospital-acquired infection rate has not decreased, and, instead, has increased by 36% during the past 20 years [13].

SSIs result in longer hospital stays, extra financial costs, and increased physiological and psychological burdens on patients and their families [14]. It was estimated that 10 additional days of hospital stay and $2,000 in additional costs were caused by SSIs in 1980. In 1992, the numbers were 7.3 days and $3,152, respectively [10]. King [15] reported that each year more than 1 million patients were affected by infections caused by hospital-acquired suture implantation and more than $2.5 billion was spent on their health care.

Above all, new suture materials with antimicrobial characteristics, preferably with controlled release of antimicrobial agents, are needed. This would help inhibit the adherence and colonization of bacteria on sutures, thereby preventing the formation of biofilms [5, 16].

The most common production method used for suture materials today is melt spinning. Due to the high temperature necessary to melt polymers, the addition of bioactive agents and temperature-sensitive antimicrobial agents to polymers before extrusion is prohibited, as they will lose their bioactivities when exposed to high temperatures. An emerging technique, electrospinning, eliminates the use of high temperatures by dissolving polymers in a solvent, which is then removed by evaporation after filament formation. The small diameter of

electrospun fibers allows for the complete evaporation of the solvent. Furthermore, the excellent mechanical properties of electrospun fibers make this spinning method an ideal choice for use in this study.

1.2 Objectives

The purposes of this study were as follows: 1) to develop new fiber materials to be used as sutures or other biomedical materials by electrospinning. The fibers needed to have an antimicrobial function by incorporating an antimicrobial agent in polymer solutions and biodegradability by using biodegradable polymers; 2) to evaluate various properties of the fibers, especially antimicrobial properties and biodegradation properties; and 3) at the same time, to study the spinning process and the influence of the processing parameters on the fiber properties. These were essential since electrospinning is a relatively new spinning method and fundamental understanding of the process have not been yet established.

There were several specific objectives of this research, as listed below.

1) Establish proper spinning setup to serve the purpose of this study.
2) Investigate the influences of electrospinning parameters on fiber properties. The electrospinning parameters include solution concentration, voltage, feedrate, and distance between the spinning jet and the fiber collector.
3) Study the influence of the incorporation of antimicrobial agents on electrospun fiber properties.
4) Investigate the *in vitro* antimicrobial efficacy of the fibers and the release of antimicrobial agents.
5) Study the *in vitro* degradation properties of fibers, including the changes in mass and surface morphology.

Chapter 2. Literature Review

This is a complex project, and three fundamental components will be included in this literature review: 1) sutures, 2) antimicrobials, and 3) electrospinning. For the reader to have a thorough understanding of the project, providing background for each of these components is essential.

2.1 Sutures

Over the more than 5,000-year history of sutures, although the function of sutures has remained the same, their chemical components, physical forms, and properties have changed significantly. The earliest materials used for sutures included flax and catgut. With the rapid development of polymer science and biomaterials over the last several decades of the 20th century, especially with the application of biodegradable polymers in biomaterials, there have been major improvements. Extensive studies on sutures, including their raw materials, manufacturing methods, various properties, and finishing, have been completed because sutures are some of the most frequently used biomaterials, and the implantation of sutures into bodies induces post-surgery complications [17, 18].

2.2 Sutures Commercially Available on the Market

Today, in the United States, Europe, and the Pacific, there are several leading suture manufacturers, including Ethicon, Davis and Geck, US Surgical, and Société Steril Catgut [3, 19]. In 2002, Chu summarized all the commercial suture materials available in the United States, Europe, and the Pacific. He noted their generic and trade names, physical configurations, and manufacturers. There were four natural absorbable sutures, 10 synthetic absorbable sutures, and

39 nonabsorbable sutures listed. Two sutures were introduced to the market in 2002 or later, which are not included in the list. One is Vicryl* Plus, a synthetic absorbable suture introduced to the market by Ethicon in 2002. Vicryl* Plus sutures are IRGACARE MP*(triclosan)-coated polyglactin 910 sutures with antibacterial functions[20]. The other is Vicryl* Rapide, which is also a coated polyglactin 910 suture. Vicryl* Rapide loses its strength completely in two weeks. This suture was designed for rapidly healing tissues, such as mucosa gingival, and for periocular skin closure [20]. Table 2.1 lists all synthetic absorbable sutures currently available on the market with their generic and trade names, physical forms, surface treatments, and manufacturers.

2.3 Properties of Sutures

With numerous choices available, the type of suture that should be used in a specific surgery depends on the properties of the suture and the types of tissues being closed. Different tissues have different strengths and different healing rates [21-23]. Capperauld believed there were three phases in a normal wound healing process [18]: 1) the lag or substrate phase, 2) the proliferative phase, and 3) the remodeling phase. The first phase lasts one to four days after surgery. At this stage, the sutures hold the wound together and keep it from opening. The wound itself has no intrinsic strength. The second stage lasts for five to 20 days after surgery, at which period the collagen is laid down, and all clots and debris are removed. The tissue begins to gain some strength, and the sutures contribute to the strength in a decreasing manner. The third stage, remodeling, lasts from 21 days after surgery until healing is fully completed. Collagen matures and gains tensile strength during this phase. After stage three, the sutures act as foreign bodies. Therefore, an ideal suture should provide an initial strength the same as the undamaged tissue and gradually lose strength at the same rate at which the healing tissue gains strength. The

degradation products should be eliminated as soon as possible; otherwise, they serve as a source of irritation and niduses for persistent infection [23].

At the same time, a suture should not induce any complications, including inflammation, damage, carcinogenicity, allergy, immunogenicity, irritation, toxicity, or mutagenicity. Studies have not found any sutures that induce cancer or mutation thus far, but inflammation is commonly associated with the use of sutures. In addition, when using a suture, it should be possible to tie a knot easily, and the knot should be able to hold the tissue closed [21].

Unfortunately, some surgeons select sutures based on personal preferences and not on scientific facts [24, 25]. Meyer pointed out that many dentists choose the sutures that were used in the institutions where they were trained [2]. A full understanding of the properties of various sutures is the basis for educated suture selection. An ideal suture should satisfy the needs of four critical property categories, which are as follows: 1) physical and mechanical properties, 2) handling properties, 3) biological properties, and 4) biodegradation properties [3, 26].

Table 2.1. Commercially Available Synthetic Absorbable Suture Materials

Generic Name	Trade Name	Physical Configuration	Surface Treatment	Manufacturer
Polyglycolic acid	Dexon "S"®	Braided multifilament	None	Davis & Geck
Polyglycolic acid	Dexon Plus®	Braided multifilament	Poly(oxyethylene-oxypropylene)	Davis & Geck
Polyglycolic acid	Dexon II®	Braided multifilament	Polycaprolate	Davis & Geck
Polyglycolic acid	Medifit®	Braided multifilament	None	Japan Medical Supplies
Poly(glycolide-lactide)(polyglactin 910)	Vicryl*	Braided multifilament	Polyglactin 370 and calcium stearate	Ethicon
Poly(glycolide-lactide)(polyglactin 910)	Vicryl* Plus	Braided multifilament	IRGACARE MP*	Ethicon
Poly(glycolide-lactide)(polyglactin 910)	Vicryl* Rapide	Braided multifilament	Coated	Ethicon
Poly(glycolide-L-Lactide)	Panacryl®	Braided multifilament	None	Ethicon
Poly(glycolide-L-Lactide)	Polysorb®	Braided multifilament	Coated	US Surgical
Poly-*p*-dioxanone	PDS II®	Monofilament	None	Ethicon
Poly(glycolide-co-tri methylene carbonate)	Maxon®	Monofilament	None	Davis & Geck
Poly(glycolide-co-ε-Caprolactone)(poliglecaprone 25)	Monocryl®	Monofilament	None	Ethicon
Glycomer 631	Biosyn®	Monofilament	None	US Surgical

2.3.1 Physical and mechanical properties

Physical and mechanical properties that relate to suture performance include all those related to tensile properties, stiffness, viscoelasticity, size, physical form (monofilament or multifilament), coefficient of friction, and capillarity.

I. Tensile properties

Tensile properties include straight strength and elongation as well as knotted strength and elongation. These properties have been studied the most among all the physical and mechanical properties. When a suture is in use, the weakest point of the suture is the knot, and the second weakest point is the portion immediately adjacent to the knot [26]. Therefore, knotted strength and elongation of sutures best represent the tensile properties of a suture in use. But the tensile properties of straight sutures are usually studied to give a fundamental characterization. Chu [27], Holmlund [28], Capperauld [18], Thacher [29], Stone [30], von Fraunhofer [31], and many others have investigated or reviewed the tensile properties of various sutures. In general, catgut and cotton sutures have the lowest tensile strength, and stainless steel sutures have the largest straight pull and knot pull break strength. Monocryl® possesses the largest percentage of break elongation, which ranges from 67% to 96% [19]. Among the absorbable sutures, both natural and synthetic, polyglactin 910 sutures (Vicryl*) have medium straight strength and knot strength. Polyglycolide (Dexon® and Dexon Plus®) has relatively high straight strength and knot strength. Some of the mechanical properties of absorbable sutures are listed in Table 2.2 [32].

Table 2.2. Mechanical Properties of Absorbable Sutures[a]

Generic Name	Commercial Name	Break Strength (Straight Pull) (Mpa)	Elongation at Break (%)
Catgut / regenerated collagen		310-380	15-35
Poly-*p*-dioxanone	PDS®, PDSII®	450-560	30-38
Poly(glycolide-co-tri methylene carbonate)	Maxon®	540-610	26-38
Poly(glycolide-lactide)(polyglactin 910)	Vicryl*	570-910	18-25
Poly(glycolide-co-ε-Caprolactone)(poliglecaprone 25)	Monocryl®	91000[b]	39
Polyglycolic acid	Dexon S®	760-920	18-25
Glycomer 631	Biosyn®	3.7-4.4 kg	44-47

a. Mechanical properties are for sizes 0 to 3-0.
b. Data are in psi of 2/0 size.

II. Stiffness

The stiffness of a suture relates to several properties, including knot tying, knot security, package memory, and handling; thus, stiffness is both objective and subjective. A stiff suture is difficult to tie and requires more throws to maintain tissue approximation. Furthermore, high stiffness leads to greater package memory (the tendency of sutures to retain kinks after being unpacked), which is unfavorable. A study by Chu [33] demonstrated that multifilament sutures were generally more flexible than monofilament sutures and coated sutures were stiffer than their corresponding uncoated ones. Stiffness increases with increasing suture size [32].

III. Viscoelasticity

Viscoelasticity is a property shared by all polymeric materials, including all natural and synthetic sutures. Creep (change in elongation under a constant tension) and relaxation (change in tension under constant strain) are two aspects of viscoelasticity. There are a limited number of studies related to the viscoelasticity of sutures. Metz [34] studied the stress relaxation behavior

of three commercially available sutures, Prolene®, PDS®, and Dexon®. He found that all exhibited stress relaxation; Prolene® (polypropylene suture) had the greatest value, i.e., approximately 40% of its initial load. On one hand, viscoelasticity may cause problems of ligatures around a vascular pedicle, but on the other hand, viscoelasticity may alleviate the over-tight approximation of skin and fascia.

IV. Size

The size of a suture refers to its diameter and can be expressed in code numbers by one of two different standard systems, the United States Pharmacopoeia (USP) system and the European Pharmacopoeia (EP) system. A small range of suture diameters is permitted for each code, as shown in Table 2.3 [6]. In the USP system, the code of nonsynthetic absorbable sutures is different from that of nonabsorbables and synthetic absorbables even though they have the same allowable range of diameters. In the EP system, the code numbers range from 0.1 to 10 as the diameter of the suture increases; there is no differentiation of synthetic absorbable from nonsynthetic absorbable sutures. The minimum diameter (in mm) of a suture in the range of a specific EP size code can simply be obtained by dividing the code number by 10.

The tensile strength of the suture material increases with the increase in suture size. When sutures are selected, the suture should be as small as possible to minimize the amount of material drawn through the surface of the tissue as well as inside the body [3]. In addition, the amount of foreign material should be as small as possible to minimize complications. An increase in suture size leads to a large increase in volume. Van Rijssel et al. [35] and Trimbos et al. [36] reported that the knot volume increased more than four to six folds the increase in the suture size. Therefore, small sutures are desirable if other requirements have been met.

Table 2.3. Suture Size Classification [6]

USP Size Codes		**EP Size Codes**	**Suture Diameter (mm)**	
Nonsynthetic absorbable materials	Nonabsorbable and synthetic absorbable materials	Absorbable and nonabsorbable materials	Min.	Max.
	11/0	0.1	0.01	0.019
	10/0	0.2	0.02	0.029
	9/0	0.3	0.03	0.039
	8/0	0.4	0.04	0.049
8/0	7/0	0.5	0.05	0.069
7/0	6/0	0.7	0.07	0.099
6/0	5/0	1	0.10	0.14
5/0	4/0	1.5	0.15	0.19
4/0	3/0	2	0.20	0.24
3/0	2/0	2.5	0.25	0.29
2/0	0	3	0.30	0.39
0	1	4	0.40	0.49
1	2	5	0.50	0.59
2	3	6	0.60	0.69
3	4	7	0.70	0.79
4	5	8	0.80	0.89
5	6	9	0.90	0.99
6	7	10	1.00	1.09

V. Physical configuration

There are two different physical configurations of sutures that are common, monofilaments and multifilaments. The physical configuration of a suture influences its tensile strength, handling properties, knot security (the ability of retaining the knot as tied), coefficient of friction, and capillarity. Braided and twisted are the two forms of multifilament sutures available. Cotton and regenerated gut materials are twisted, while all synthetic multifilaments are braided. Generally speaking, the handling properties of multifilament sutures are better than the handling properties of monofilament sutures in terms of flexibility, knot security, and package memory. On the other hand, the knot tie-down, capillarity, and tissue drag properties of monofilament sutures are attractive.

VI. Coefficient of friction

The friction between the tissue and the suture, and between sutures, influences tissue drag and knot tie-down as well as knot security. A higher coefficient of friction benefits knot security, resulting in a more secure knot. But at the same time, it is problematic at the knot snug down because it may take more time and energy to tie a knot. Furthermore, a higher coefficient of friction increases tissue drag, which may result in more traumatic wounds and a more severe inflammation response. Rodeheaver [37] compared the knot efficiency and the resistance to passage through tissues of polyglycolic acid sutures and polyglactin 910 sutures. The results showed the knot efficiency of dry polyglycolic acid sutures was higher than that of polyglactin 910, whereas the resistance to passage through tissue of polyglactin 910 was higher.

VII. Capillarity

Capillarity is the action of “wetting fluids rising in narrow tubes if immersed, a phenomenon called ‘capillary ascension’ that is the consequence of molecular activity (adhesive

or cohesive force) between adjacent bodies." (page 381) [38] Since the human body is an aqueous environment, the capillarity of suture materials is an issue to be considered. No capillarity is desired in any case of suture application due to the spread of microorganisms with the body fluid in between the fibers in multifilament sutures [16]. In terms of capillarity, monofilament sutures are desirable because of the lack of wicking effect. Geiger studied the transportation of colorant and bacteria along sutures [38]. He found that none of the studied monofilaments transported either colorant or bacteria in 30 days. Some of the pseudomonofilament (coated multifilament sutures) and braided multifilament sutures transported both colorant and nonmotile *Escherichia coli*, and a majority of the multifilaments (both coated and noncoated multifilaments) transported motile *Proteus mirabilis*. These results agreed with a previous study by Lilly [39].

To eliminate the nondesirable capillary effect, the surface of the sutures can be made hydrophobic or the interfiber capillaries can be filled. In Sergeev's study, several coating materials, including polyurethanes, organosilicon substances, film-forming phenol-polyvinyl acetal composites, polyamide varnish, and isoprene rubbers, were tested and organosilicon rubber SKTN-G and phenyl-polyvinyl acetal (PPVA) were the best in terms of the capillarity and physiomechanical properties of the resulting sutures [16].

2.3.2 Handling properties

Handling properties of sutures refer to how easy or difficult it is for surgeons to handle the sutures, for example, to tie a knot at the end or bend them. Many of the properties previously discussed in this literature review relate to the handling properties, including stiffness, knot tie-down, knot security, packaging memory, coefficient of friction, and tissue drag. Among all

natural and synthetic sutures, silk has been widely accepted as having exceptional handling characteristics, which are the standards to which other sutures are compared [40].

2.3.3 Biocompatibility

With the implantation of any biomaterial, including sutures, a two-way interaction is initiated at the time of the contact of the biomaterials with tissues. Biomaterials affect surrounding tissues, and the tissues affect the properties of biomaterials [7, 26]. This two-way interaction is referred to as the biocompatibility of biomaterials. The impact of biomaterials on tissues can be local or systemic, but usually a nonspecific inflammation results. “To a great extent, these interactions arise from alterations of physiological (normal) processes (e.g., immunity, inflammation, blood coagulation) comprising host defense mechanisms that function to protect an organism from the deleterious external threats (such as bacterial and other microbiologic organisms, injury and foreign materials).” (page 293) [7]

Tissue response or cell host response to injury includes inflammation, wound healing, and foreign body reaction. Inflammation is the immediate response of vascularized living tissue to local injury and serves to contain, neutralize, dilute, or wall off the injurious agent or process. Neutrophils are predominate during acute inflammation, which occurs in the first 24 to 48 hours after the implantation. Then macrophages, monocytes, and lymphocytes dominate during chronic inflammation with the proliferation of blood vessels and connective tissue. The appearance of foreign body giant cells and fibroblasts indicate foreign body reaction. The measurement of the presence and density of these cells at a surgical site is one common and widely used method to access the biocompatibility of biomaterials. Another commonly used method to study the biocompatibility of biomaterials is the enzyme histochemistry method, which measures the presence of a variety of enzymes associated with cellular response in tissues [26].

Tissue reaction to sutures depends on several factors, including the chemical nature of the suture material, the physical form of the suture, the amount of suture in the tissue (suture size and knot volume), and stiffness [26]. Among these, the chemical composition of the suture is considered the most important factor [3]. Usually, natural suture materials, such as catgut, provoke more severe tissue reactions than synthetic sutures due to the availability of acceptance sites on some natural suture materials for the enzymes to react with sutures. Most of the test results on the biocompatibility of synthetic sutures were satisfactory. For example, in an *in vivo* study by Shishatskay [41], two types of polyhydroxyalkanoate (PHA) sutures, polyhydroxybutyrate (PHB) sutures and hydroxybutyrate and hydroxyvalerate (PHV) copolymer sutures, were compared to silk and catgut sutures in terms of tissue reaction. The results showed the compatibility of PHB and PHV were comparable with that of silk, and all were much better than catgut sutures. Another study [42] found that synthetic, nonabsorbable Novafil®, Monolene®, and Gore-tex® sutures induced minimal tissue reaction, which proved their high biocompatibility. Molea et al. [43] investigated the biocompatibility of three monofilament sutures, PDS®, Monocryl®, and Biosyn®, in *in vivo* studies of rats and found that all three sutures showed optimum biocompatibility. Smit et al. evaluated tissue reactivity of 10 suture materials *in vivo* on rats (silk, plain catgut, chrome catgut, Tevdek®, Ticron®, Ethibond®, Vicryl*, Dexon®, Maxon®, and Prolene®) using the histological method [44]. Their results showed that there was no significant difference in tissue reaction among the 10 different sutures and the surgical trauma had a greater influence on tissue reaction than the material itself.

In addition to the influence of the chemical nature of sutures, the physical form and the amount of suture material enclosed in the wound have also been shown to influence the compatibility of sutures. Karaca et al. studied the *in vivo* tissue reactions of silk, polyester,

polyamide, and polypropylene sutures and found that all showed tissue reaction to some extent, but in general, braided sutures induced more tissue reaction than monofilament sutures [45]. The same results were obtained by Rodeheaver et al. [46]. The stiff ends of monofilament sutures tended to elicit different levels of tissue reaction. The larger the volume of sutures being enclosed in the wound, the more severe the tissue reaction. By comparing the tissue reaction with different size sutures, van Rijssel found that "the use of thick-gauge suture material adds much more to the total amount of foreign body and tissue reaction in the wound than the addition of extra throws to the knot and might, therefore, be deleterious to optimum wound healing." (page 64) [35]

Polylactide, polyglycolide, and their copolymers, as well as polycaprolactone, have been widely used as sutures, drug release systems, and fracture fixation pins [47, 48]. The biocompatibility of these materials has been examined, and most of the results showed both locally and systemically nontoxic. Although inflammation, foreign body reaction, and cell lysis have been reported, these have been within acceptable limits. *In vivo* studies on animals showed that polylactic acid (PLA) and PGA sutures induced no tissue reaction in rats and guinea pigs [49], less inflammation reaction than catgut, silk, or Dacron® in rabbits [50, 51], and minimal inflammatory reactions in monkeys [52]. When poly(l-lactic acid) (PLLA) was used as drug release in soft tissue, *in vivo* studies of rats indicated that PLLA provoked very moderate foreign body reactions [53, 54]. For biodegradable polymers, the degradation products may induce tissue reaction as well. Cutright and Hunsuck found that degraded sutures induced giant cell reaction [55].

2.3.4 Biodegradability

Biodegradability is a property exclusive of sutures that can be degraded and absorbed by the human body. The degradation of biomaterials in tissues is the other side of the two-side biomaterial-tissue reaction, which is the influence of tissues and other environmental conditions on biodegradable biomaterials.

There are natural biodegradable and synthetic biodegradable sutures. Examples of natural biodegradable suture materials are catgut and reconstituted collagen. Examples of synthetic biodegradable suture materials are PGA, PLA, and PLGA. All the currently used synthetic biodegradable sutures are made of aliphatic polyesters and are based on one or more of these cyclic monomers: glycolide, L-lactide, trimethylene carbonate, *p*-dioxanone, and ε–caprolactone [5]. These polymers or copolymers are degraded by the hydrolysis of aliphatic ester bonds. The end products of hydrolysis are water and carbon dioxide. While the degradation of natural sutures, such as catgut, is based on enzyme degradation, this is not desirable as the degradation rate is not predictable due to the different enzymatic activities of different people.

The degradation of sutures leads to loss of tensile strength, loss of mass, and change in fiber morphology. The degradation rate of these synthetic polymers is influenced by a wide variety of intrinsic and extrinsic factors [26, 56]. The intrinsic factors include the morphology of biomaterials, chemical composition, molecular chain orientation, stereochemical structure, molecular weight, and distribution of polymers. In sutures, which have a unique fibrous structure (i.e., molecular chain orientation and crystallinity), the fiber microstructures play an important role in determining the rate of degradation. By comparing the degradation of PGA in the fiber form to that in pellet or chip forms, it was found that the different physical forms degraded in different manners even though they had the same chemical composition [57]. This is because the

accessibility of water into the polymer bulk depends on the portion of the amorphous region to the crystalline region as well as the molecular chain orientation [58-60]. Studies indicated that the degradation always started from an amorphous region. This was determined by measuring the crystallinity of the sutures. Results showed that the percentage of crystallinity first increased with the degradation and reached its maximum, then dropped down to zero.

Since hydrolysis is the reaction between water and the functional groups on polymer molecular chains, it is apparent that the hydrophilicity of biomaterials affects their degradation rate as well. Water can readily penetrate hydrophilic polymers, and therefore more readily react with functional groups on these polymers. However, water cannot penetrate hydrophobic polymers as easily as in the case of hydrophilic polymers. A study by Shikanov et al. showed that with both hydrophilic and hydrophobic components in a copolymer, the degradation rate was higher than that of either of the two monopolymers [56].

For synthetic biodegradable suture materials, the degradation rate can be tailored to different applications. The rate of suture degradation can be controlled by selecting polymers with hydrophilic or hydrophobic properties, changing the monomer percentage of a copolymer, and adjusting spinning parameters when fibers are produced to alter their microstructures.

The extrinsic factors that influence the degradation rate include the presence of moisture, enzymes, pH, temperature, microorganisms, stress applied to biomaterials in use, and sterilization methods used. The effects on the suture degradation of those factors that have been extensively studied are discussed. These include the pH of the degradation environment, electrolytes in degradation environment, applied stress to sutures during degradation, addition of drugs and plasticizer to the suture polymer, and sterilization of sutures.

I. Effect of pH

The pH of the human body ranges from 1.0 (gastric juice in the stomach) to around 8.5 (pancreatic juice in the duodenum). The hydrolytic reaction rate is affected by the pH of the surroundings. Therefore, it is important to understand how sutures react to environments with different pHs. Chu has completed several studies and found that the degradation of both Dexon® and Vicryl* sutures was pH-dependent [61-64]. The maximum retention of the tensile strength of Vicryl* occurred in an environment with a neutral pH. In alkaline conditions, Vicryl* and Dexon® sutures degraded faster than when in acidic conditions. The same results were obtained by Tomihata et al. [65] in their study of Monocryl®, Maxon®, and Biosyn®. But in another *in vitro* study evaluating the degradation of nine suture materials (Vicryl*, Vicryl* Rapide, Monocryl®, Dexon®, Safil®, Biosyn®, Polysorb®, PDSII®, and Maxon®) by Freudenberg [25], the results were different from the results of Chu's studies. PDSII® was the only suture in which the degradation rate was influenced significantly by changing the pH from 2 to 7.4 and 8. Other sutures studied in Freudenberg's study did not show a significant difference in degradation in environments with different pHs.

II. Effect of electrolytes

The presence of electrolytes in the degradation environment influences the water uptake of absorbable polymers by altering the icatrisa sphere surrounding biomaterials, thereby influencing their degradation rate [66]. The human body consists of various ions in body fluid, such as Na, Ca, Mg, and K. Studies showed that the electrolytes decreased the degradation rate of PGA and PLGA sutures [67].

III. Effect of applied stress

When in use, sutures are subjected to both stress and strain. The amount of stress and strain depends on the tissue being closed and the initial strain applied by surgeons during surgeries. Stress may induce several changes in sutures so that the degradation pattern is altered when compared with that of unstressed sutures. These changes include stress-induced chemical reactions, stress-reduced alterations of the morphological structure, and stress-reduced accelerated diffusion of small molecular species [66]. Chu [68], Zhong [69], and Miller [70] found that the applied stress and strain accelerated the degradation of sutures.

IV. Effect of the addition of drugs and plasticizers to the polymer

The presence of small molecules or oligomers in polymers increases the mobility of the polymer molecular chains and decreases their crystallinity. In this sense, the addition of drugs or plasticizers to polymers should increase their degradation rate. However, several studies on the degradation of drug carriers showed more complicated results, and the resulting degradation behavior of the polymer depended on many factors, including the properties and concentration of the drugs. In research on a controlled delivery carrier for paclitaxel, Shikanov et al. found that the incorporation of a hydrophobic drug in the hydrophobic polyester anhydride polymer decreased the degradation rate of the polymer [71]. Guinchedi et al. studied the degradation of two diazepam-loaded poly-D,L-lactides of different molecular weights and a diazepam-loaded 50/50 poly-D,L-lactide-co-glycolide [72]. The results showed a faster degradation rate for the drug-loaded polymers than the pure polymers. Miyajima et al. investigated the release of basic drugs, acidic drugs, and neutral drugs from a PLGA matrix and found basic drugs reacted with the carboxylic group of the polymer, so that the functional group in the polymer for hydrolysis was shielded; thus, the degradation was slowed down [73]. The acidic and neutral drugs had only

weak interactions with the polymer, and the drugs precipitated out quickly during degradation. As a result, these drugs had almost no effect on the hydrolysis of the polymer. The concentration of the incorporated material also influenced the degradation rate of the polymer based on the study by Li et al. [74].

V. Effect of sterilization

All biomaterials need to be sterilized to destroy microorganisms present before implantation, therefore minimizing the risk of infection and associated complications. The commonly used sterilization methods include steam, dry heat, radiation (ionizing radiation and γ radiation), ethylene oxide gas, or a combination of these methods [75]. Both dry heat and steam may cause degradation and deformation of biomaterials. Radiation is commonly used in the sterilization of most biomaterials, including sutures. Radiation may induce early degradation and/or cross-linking of polymer chains. Usually, γ-radiation is used to sterilize sutures. However, its effect on absorbable sutures is undesirable because the degradation rate/pattern of sutures is changed by the radiation [66]. Because of its toxic nature, ethylene oxide gas sterilization needs a lengthy process of degassing to ensure all of the toxic gas is eliminated before use.

2.4 Surgical Site Infections and Biofilm Formation on Sutures

2.4.1 Biofilms

As stated earlier, the presence of suture materials increases the probability of surgical site infections. The body's natural defense systems are interrupted by implantations. Biomaterial-associated infections have several unique characteristics. These are the following: "(1) They often have indolent pathogenic patterns with alternating quiescent and acute periods. (2) There may be an initial response to antibiotic therapy, but relapses are frequent. (3) While these infections are often polymicrobial, the predominant bacteria are either common members of the

autochthonous skin or bowel flora or common environmental organisms that are often only pathogenic in immunocompromised patients. (4) Bacteria may be difficult to recover from adjacent fluids when the device is in place and from the device itself when it is removed." (page 443) [76] All of these characteristics indicate the involvement of biofilms in the infections.

Van Leeuwenhoek, who examined the "animalcules" in the plaque on his teeth, was the first to describe biofilm [77, 78]. But it was not until the 1970s that the formation of biofilms and bacteria characteristics in biofilms were widely studied. Marrie et al., who examined a failed medical device and found biofilm forming on the surface [79], introduced biofilms into medical microbiology. By definition, biofilm is "a microbially derived sessile community characterized by cells that are irreversibly attached to a substratum or interface or to each other, are embedded in a matrix of extracellular polymeric substances that they have produced, and exhibit an altered phenotype with respect to growth rate and gene transcription." (page 168) [77]

Biofilms provide sessile bacteria with a safer environment to survive compared to planktonic bacteria by limiting the access of antibiotics, bacteriophage, phagocytic, eukaryotic cells, and any other agents that can kill the bacteria. In addition, biofilm formation triggers phenotypic changes in enzymatic activity, cell wall composition, and surface structure, which lead to changing the targets of biocides and antibiotics, and the accessibility of these agents.

Biofilm formation on suture implants has been widely reported. A recent *in vivo* study of bacterial colonization by Otten et al. [80] isolated bacteria from the biofilm formed on Monocryl® and Deknalon® after eight days of implantation in intraoral dentoalveolar surgery. One hundred and fourteen aerobic and 115 anaerobic strains of bacteria were isolated.

2.4.2 Bacterial adherence on biomaterials

To form a biofilm, bacteria need to first adhere to the surface of biomaterials and then subsequently colonize. The initial adhesion is the critical event in the pathogenesis of infection [81].

The adherence of bacteria to biomaterials depends on the properties of the biomaterials and the bacteria as well as environmental factors. Biomaterials properties include chemical composition, surface charge, hydrophobicity, surface roughness, and physical configuration. In a study of the adherence of *Staphylococcus aureus* and *Escherichia coli* on 10 different sutures, Chu and Williams [82] found PDS® II had the lowest affinity toward the adherence of both bacteria, while Dexon® had the highest affinity. In general, the adherence of *Staphylococcus aureus* was higher than that of *Escherichia coli*. This might be due to the cell wall differences between gram-positive and gram-negative bacteria. The high adherence to the Dexon® suture was confirmed by Katz et al. [83]. Environmental factors affecting adherence to sutures include temperature, pH, local concentration of electrolytes, the time of exposure, concentration of bacteria, and the presence of antibiotics [81].

The most direct and effective method to prevent adherence, and the subsequent formation of biofilm on biomaterials, is to kill the bacteria that come in contact with implantations using antimicrobial agents.

2.5 Antimicrobial Agents and Their Working Mechanisms

Antimicrobial agents function in various ways to kill or inhibit the growth of microorganisms. Those antimicrobial agents that can kill organisms are cidal, while those that only inhibit the growth are static. According to the range of effectiveness, there are narrow-spectrum agents (effective only against a limited variety of pathogens) and broad-spectrum

agents (attack many different kinds of pathogens). Broad-spectrum antimicrobial agents are ideal for use in biomaterials due to the wide variety of bacteria that can possibly contaminate wounds.

To effectively inhibit the growth of microorganisms, the antimicrobial agents must interrupt the microorganisms' growth cycle. Studies have indicated that the important targets to attack in the growth cycle include the cell wall, cytoplasmic membrane, protein synthesis, and nucleic acid synthesis [84, 85].

The antibacterial agents that inhibit cell wall synthesis work by one of three mechanisms. Mechanism one is the inhibition of the transpeptidation enzymes, which play roles in the cross-linking or the polysaccharide chains of bacterial cell wall peptidoglycan. An example of this kind of agent is penicillin, which works best on gram-positive bacteria because of the large amount of peptidoglycan content in the cell wall. Mechanism two is the binding to the D-ala-D-Ala terminus and inhibition of the transpeptidation. Mechanism three is the inhibition of cell wall synthesis by disabling the transport function of Bactoprenol to transport cell wall precursors across the plasma membrane. Antifungi agents inhibit the synthesis of chitin, glucan, or mannoprotein to prevent the formation of a fungi cell wall. Examples of this kind of antimicrobial agent are beta-lactams (penicillins and cephalosporins), semisynthetic penicillin, carboxypenems, and glycopeptides.

Protein synthesis inhibitors work by binding with one of the ribosome subunits to inhibit protein synthesis. Some inhibitors bind to the 30s subunit and some bind to the 50s subunit of the ribosome complex to interfere with the steps of the protein synthesis. By binding with the 30s subunit, antimicrobial agents can cause the misreading of mRNA or can interfere with aminoacyl-tRNA binding; by binding with the 50s subunit, peptide bond formation can be blocked, or peptide chain elongation can be prevented. Because of the different ribosome size,

70s for prokaryote and 80s for eukaryote, the toxicity of antimicrobial agents is selective. Antimicrobials that belong to this category include aminoglycosides, lincomycins (clindamycin), tetracyclines, and macrolides.

Nucleic acid synthesis inhibitors combine with DNA gyrase or RNA polymerase, thereby interfering with DNA replication, transcription, and other activities involving DNA or RNA synthesis. These kinds of antimicrobial agents are broad-spectrum agents. An example of an antimicrobial in this group is rifamycin.

Competitive inhibitors or metabolic antagonism work by blocking metabolic pathways through competitively inhibiting the use of metabolites by key enzymes. Sulfonamide is an example.

Today, these antimicrobial agents have been applied to various textile materials to impart antimicrobial properties to the materials or to protect them from being degraded by microorganisms.

2.6 Sutures with Antimicrobial Properties

As early as 1957, Echeverria and Olivares [86] proposed the importance of using sutures with antimicrobial functions. In these researchers' study, braided, non-capillary silk sutures were treated with 1.5 wt% Aureomycin or 1.5 wt% Aureomycin plus 0.5 wt% Neomycin and cotton sutures were treated with 1.5 wt% Aureomycin. The treatment methods were not clarified in the paper. The results of the *in vivo* studies indicated that the antibiotic-treated sutures accelerated the icatrisation process with no active inflammation, while untreated sutures produced excessive cicatrices; the exudative inflammation persisted for eight days.

Although the significance of antimicrobial sutures has been known for at least 50 years, there have been only a limited number of reported studies that provide information on sutures

with these antimicrobial properties. Most of these studies evaluated sutures with topical coatings of antimicrobial agents.

2.6.1 Coating method

Antimicrobial agents were added to coating materials, and applied to the surface of sutures. The coatings could be nonabsorbable or absorbable materials. In the case of nonabsorbable coatings, antimicrobial agents are released by migration; in the case of absorbable coatings, both migration and exposure by the degradation of coatings may have led to the release of antimicrobial agents into the environment. In both cases, the antimicrobial agents should not change or be changed by the coating.

In 1987, Chu et al. incorporated a silver compound in the coating of a nylon braided suture and examined the *in vitro* bactericidal properties of the modified sutures toward both fresh bacterial species and established bacterial colonies [14]. In both cases, the sutures exhibited very good to moderate antibacterial effectiveness. A study by Blaker et al. investigated the effect of silver ions on the bioactivity, dynamic mechanical properties, and thermal properties of bioactive glass-coated polyglactin 910 and non-resorbable Mersilk® surgical sutures [87]. It was shown that the addition of silver ions did not influence these properties, so that sutures with bioactive and bactericidal properties could be obtained with this coating.

Decamethoxin (DMO) is a quaternary ammonium compound, a broad-spectrum antimicrobial. Several studies have used DMO as the biologically active compound to coat sutures. A group of scientists (Kovtun, Sergeev, Plygan, Baglei, Vagin et al.) selected a phenyl-polyvinyl acetal (PPVA) composite from several others to use as a coating material in a series of studies [16, 88-90]. DMO was added to PPVA as the coating material to apply to sutures. The studies of the *in vitro* kinetic release of DMO showed that 70% to 100% of the drug was released

in 13 days. At the same time, the release kinetics indicated that no bond formed between the drug and PPVA. The rate of release decreased in time, and the highest rate was observed in the first two days. The highest concentration of DMO released did not exceed the standards for use in medicine issued by the Pharmaceutical Committee. The release of DMO was studied by two methods: 1) A direct method, the extraction-spectrophotometric method, which measured the quantities of DMO released into the aqueous medium, and 2) an indirect method, the gravimetric method, which calculated the release of DMO by determining the weight loss of the sutures in the aqueous medium. In one study, the effect of DMO was compared to 11 other antimicrobials with different composites as coating materials on PCA sutures. In terms of *in vitro* antimicrobial effectiveness on *Staphylococcus aureus*, yeast-like fungi, and *Escherichia coli*, DMO with PPVA coating was regarded as the best. Further studies indicated no other properties were considerably changed by the coating except that capillarity was decreased significantly. Furthermore, the stability of modified sutures in biological medium was satisfactory based on *in vitro* studies.

Vicryl* Plus and Vicryl* Rapide antibacterial sutures

The antibacterial effectiveness of Vicryl* Plus and Vicryl* Rapide was achieved by coating a synthetic, braided absorbable suture, i.e., polyglactin 910 suture, with triclosan. To date, Vicryl* Plus and Vicryl* Rapide by Ethicon Co. are the only commercially available antibacterial sutures approved by the U.S. Food and Drug Administration (FDA). In terms of ease of passage through tissues, first-throw knot holding, knot tie-down smoothness, knot security, surgical handling, and overall evaluation by surgeons, *in vivo* studies showed that there was no distinguishable difference between Vicryl* Plus and Vicryl* sutures [11, 91].

The antimicrobial effectiveness of Vicryl* Plus has been reported in several studies. The *in vitro* zone of inhibition tests by Gómez-Alonso and Garcia-Criado [12] demonstrated the bactericidal effect of the coating on gram-positive bacteria and bacteristatic effect on gram-negative *Escherichia coli. In vivo* animal study results showed the advantages of Vicryl* Plus sutures over Vicryl* in modulating the inflammatory response when surgical site infection presented. The antibacterial effect against wild-type and methicillin-resistant *Staphylococcus aureus* and *Staphylococcus epidermidis* could last up to seven days with aqueous immersion, knotting, and passage through subcutaneous and facial tissues, according to Rothernburger et al. [92]. An *in vivo* study of guinea pigs demonstrated that the antibacterial Vicryl* Plus sutures inhibited bacterial colonization on sutures by 30.5-fold less than that of Vicryl* [93]. As to the effect on human bodies, it was reported that the occurrence of edema at surgical sites treated with Vicryl* Plus was much lower than that of Vicryl*, 23% for Vicryl* Plus versus 42% for Vicryl*. At the same time, 57% of the patients treated with Vicryl* Plus reported pain compared with 89% of those treated with Vicryl* [94].

However, there were two *in vivo* studies in which different results were observed. Storch et al. examined the influence of these two sutures on wound healing and found there was no statistically significant difference ($p > 0.5$) based on the cellular response, collagen formation, and orientation in guinea pigs [95]. A study of humans by Defazio et al. demonstrated that around 8.7% and 10.3% of the patients showed signs of infection or inflammation with Vicryl* and Vicryl* Plus sutures, respectively [96]. However, the cost of the 3-0 Vicryl* suture was $55.47 per box (three dozen), and that of Vicryl* Plus was $348 per box, more than six times the price of Vicryl*.

2.6.2 Other methods to provide textile materials antimicrobial properties

Although no published research on methods other than coating to provide sutures with antimicrobial functions was found, antimicrobial finishing on textile materials has been an active area of study for a long time. Antimicrobial agents can be applied to all stages of textiles during their production, including applications to fibers, yarns, fabrics, and other end products [97]. If antimicrobials are added to the polymer solution before extrusion for synthetic or regenerated fibers, or added in spinning baths of fibers that are wet spun, the fibers produced will have inherent antimicrobial characteristics. For natural fibers, antimicrobial functions can be obtained by grafting functional groups (homopolymers and/or copolymers) onto the fibers' molecular chains. Microencapsulation, a physicochemical technique, disperses microcapsules containing antimicrobial agents within the fiber matrix. The microcapsules serve as a reservoir of antimicrobial agents that can be released gradually.

For yarns, fabrics, and other end products, the pad-dry-cure method, a commonly used textile finishing method, can be used for antimicrobial finishing. In this process, antimicrobial agents are dissolved in water to form solution or suspension. Then textile substrates are passed through the solution and then pad rollers, which force the liquid into fabric, yarns, and fibers. The substrate is then dried. Sometimes the dried products are processed further with higher temperatures, a process called curing. The purpose of curing is to improve the durability of the finishing by using high temperature to activate crosslinking between antimicrobial agents and fibers or among the incorporated crosslinking agents themselves.

Bide et al. reported on using the method of dyeing polyester with disperse dyes to apply antimicrobial drugs to polyester woven fabrics due to the similarities of drugs to disperse dyes [98]. These similarities included limited water solubility, small molecular size, and shape. Two

fluoroquinolones drugs, ciprofloxacin (Cipro) and ofloxacin (Oflox), were used. Both exhaustion and pad-dry procedures were investigated. The *in vitro* results of the release of drugs showed that Cipro was lost from samples finished by exhaustion after 48 hours, while the pad-dry-treated samples retained around 20% of Cipro even after 96 hours and continued to release it slowly. For Oflox, release from pad-dried samples was slower than from those samples finished with the exhaustion method, but there was no long-term release in either case. The same group of scientists also applied Cipro to silk woven fabrics, nylon woven fabrics, polyurethane A (a modified polyurethane with carboxylic acid groups), and polyurethane B (a commonly used polyurethane) to achieve antimicrobial functions by the exhaust dyeing and the pad-dry dyeing procedures [9, 99].

2.7 Manufacturing of Synthetic Sutures

The production method currently used for almost all synthetic sutures is melt spinning. In this process, polymer chips or pellets are melted using heat, and then the molten polymer is forced through a spinneret to form filaments. Immediately after the filaments are extruded from the spinneret, cool air passes through and solidifies the filaments. The fibers can be drawn before and after being solidified to obtain the desired degree of molecular chain orientation, crystallinity, and desired fiber diameter. The diameters of fibers produced by melt spinning range from 10 μm to 50 μm. This production method prohibits the incorporation of bioactive agents and temperature-sensitive antibiotics as the high temperatures necessary to melt the polymers may cause these agents to lose their functional activity. Therefore, a spinning method that does not use high temperature is required for the purpose of this research. An emerging technique, electrospinning, will be examined.

2.8 Electrospinning

2.8.1 Introduction to electrospinning

The traditional spinning methods, including dry spinning, wet spinning, and melt spinning, use only mechanical forces to produce fibers from a polymer melt or solution. However, in electrospinning, both mechanical and electrical forces are applied to produce fine fibers. In this process, a high voltage supply is applied to produce a strong electric field. The polymer solution or polymer melt is contained in a syringe with a thin tip. It is from the syringe tip that polymers are drawn into fibers. Usually, either a metal needle tip is used or a metal wire is inserted into the polymer solution at the tip of the syringe to charge the polymers positively or negatively. As a result, the polymer solutions or polymer melt at the tip is subjected to both surface tension and mutual charge repulsion. The direction of the surface tension opposes the direction of the mutual charge repulsion. As the intensity of the electric field is increased, and the mutual charge repulsion of the liquid overcomes the surface tension, the solution at the tip of the capillary is ejected. The fibers are formed upon the evaporation of the solvent or upon the cooling of the polymer melt. The diameters of fibers manufactured by electrospinning range from several microns to several hundredths of a micron or even several nanometers [100, 101]. A schematic diagram of a typical electrospinning apparatus is shown in Figure 2.1 [102].

The electrospinning process was first patented in 1934 by Formhals, who filed four additional patents in the following 10 years. In these patents, an experimental setup was described for the production of polymer filaments using electrostatic force [103-107]. But this technology did not gain extensive research attention immediately due to the lack of understanding of the process and parameter control techniques. Interest has resumed in recent years as a result of the increased special needs of military, medical, and filtration applications

using nanofibers [108]. According to Huang et al., more than 100 polymers have been electrospun to produce ultrafine fibers [100]. Most of these polymers were dissolved to form a solution; others were heated to form a liquid or melt.

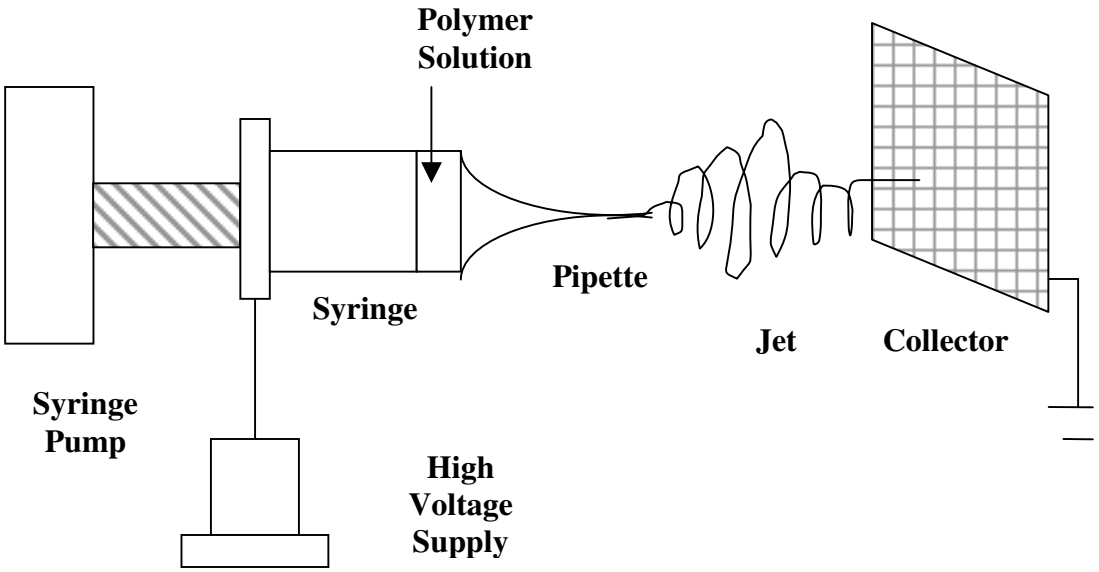

Figure 2.1. Schematic of Electrospinning Setup
(Revised from http://www.umassd.edu/engineering/textiles/research/electrospinning)

I. Parameters

Electrospinning is a versatile spinning method. The spinning process can be modified readily to produce fibers with the desired morphology and properties. In addition to commonly used round smooth fibers, fibers with various cross-section shapes can also be made by electrospinning, including porous fibers, ribbon-like fibers, branched fibers, helical fibers, and hollow fibers [109-113]. The parameters that can be manipulated to produce fibers with different morphologies and properties can be grouped into three categories: polymer solution properties, processing conditions, and ambient environment.

Polymer solution properties

Solution properties include viscosity, surface tension, and conductivity. The solution viscosity is a critical factor that influences the diameter and morphology of the electrospun fibers. The viscosity should be large enough to hold the polymer at the tip of the capillary without electrical force, maintain a continuous solution jet with electrical force during electrospinning, and yield smooth fibers without beads [111, 114]. At the same time, problems in drawing the polymer solutions into fibers rise with viscosities that are too high due to the difficulties in pumping the solution through the syringe needle and quick drying of the solution at the tip of the needle [115, 116]. The solution viscosity increases with increasing polymer molecular weight and solution concentration. Ramakrishna et al. [117] listed those boundary conditions of polymer concentration to form uniform fibers and beaded fibers that have been reported in the literature. The values varied significantly among different polymers.

All liquids have surface tension, which is the force required to increase their surface area. The higher the surface tension of a liquid, the more likely the liquid will form beads to decrease its surface area. In electrospinning, solutions with high surface tensions are more likely to form beaded fibers. Fibers with even diameter are required for sutures. The surface tension of the polymer solution is determined by the solvent used. Zeng et al. studied the effect of adding several surfactants to the polymer solutions to reduce the surface tension and found that the smoothness of the fibers improved [118].

Most of the solvents used to dissolve the polymers used in electrospinning are organic. Many organic solvents have some conductivity although they are generally known to be non-conductive. The conductivity facilitates the drawing of fibers, which influences the molecular chain arrangement of fibers and fiber diameter. The higher the conductivity, the more stretched

the fibers, which leads to thinner fibers with higher crystallinity. To increase the conductivity of solutions, ions, such as NaCl, KH_2PO_4, and NaH_2PO_4, have been added to polymer solutions by Fong [114], Huang [119], and Zong [120]. They found that the addition of salts resulted in fibers with smaller diameters.

Processing conditions

Processing conditions include voltage, feedrate, and the distance between the syringe tip and the collector. Adjustments of the processing conditions can be made easily and contribute to making electrospinning a versatile technique.

High voltage is applied in electrospinning, which generates the electrical force to initiate and maintain solution jets. The minimum voltage required depends on the polymer solution viscosity, surface tension, and feedrate, but in general, voltage of more than 6 kV can initiate the solution jets [121]. The electrical field charges solutions with positive or negative charges; consequently, the columbic repulsive force overcomes surface tension, and a jet is formed. The voltage influences the stretching and the acceleration of the jet, thereby influencing the diameter and microstructure of fibers. With the increase in voltage, the stretching rate increases, leading to fibers with higher crystallinity and more oriented molecular chains. But for a given distance between the tip and the collector, the crystallinity reaches its peak value with increasing voltage to a specific point. Beyond this point, the crystallinity decreases again due to the insufficient flying time (the time needed for the spinning jet to travel from the needle tip to the collector) of the solution jets before they are deposited on collectors [113]. The diameters of the fibers are reduced at a higher voltage [111, 122], but a greater tendency of bead formation is also demonstrated [116, 123].

Feedrate is the amount of solution that is available for jet formation at the tip of the syringe in a given time period. Feedrate influences fiber diameter and bead formation. As the feedrate increases, the diameter of the fibers and the tendency of bead formation increase [116].

The distance between the tip of capillary and the collector determines the electrical force and the jet flying time. For a given voltage, the effect of increasing the distance equals the effect of decreasing the voltage. For electrospun fibers to have enough strength, the jet requires sufficient flight time to be stretched, which means the distance should not be too small.

Ambient parameters

The environmental conditions of temperature, humidity, surrounding atmosphere, and pressure surrounding the electrospinning jet may influence the electrospinning process. Most of the electrospinning processes reported were carried out in the usual lab environments. The effect of humidity on the surface morphology of polysulfone electrospun fibers was studied by Casper et al., who indicated that humidity higher than 50% resulted in porous fibers [124]. Only a few studies have investigated how different atmosphere and pressure influenced the electrospinning process [110, 111].

II. Applications

As a versatile spinning method, electrospun products are advantageous in a wide variety of applications, such as high-performance filters, barriers in protective apparatus, wound dressing materials, scaffolds in tissue engineering, and reinforcement in composite materials [125-127]. Having a large surface-area-to-volume ratio, electrospun nanofiber webs have significantly higher filtration efficiency than the webs usually used and nonwoven fiber webs. Tsai et al. compared the filtration efficiency of conventional meltblown fabrics with that of electrospun polyethylene oxide nanofiber webs [128]. The results showed that the nanofiber

webs with 3 g/m^2 density had filtration efficiency similar to that of the meltblown webs with 35 g/m^2 density to filter NaCl aerosol containing 100-nm particles. Ultra-Web®, a commercial nanofiber filter by the Donaldson Company, USA, was made of 10-μm cellulose fibers and 250-nm nanofibers.

The filtration efficiency along with the high breathability of electrospun nanofiber webs make the materials a good barrier candidate for protective gear, including face masks, surgical gowns and drapes, and other equipment used in protective applications. Graham et al. applied polyamide nanofiber webs to a Joint Service Lightweight Integrated Suit (JSLIST) and examined the aerosol barrier efficiency and Frazier permeability of the achieved composites [126]. The results showed 98% efficiency on a two-micron particle and acceptable Frazier permeability.

The large surface area of nanofibers also provides a huge base for chemical groups or antimicrobial agents to react with toxic gases and chemicals or to kill or inhibit the growth of microorganisms. Due to the increasing concern about chemical and biological warfare agents, interest has increased in this topic. Graham [117] included a catalyst in the polyurethane solution, and Acatay [129] incorporated quaternary ammonium salt in perfluorinated polymers. Interestingly, Lee and Belcher fabricated M13 viruses in 1,1,1,3,3,3-hexafluoro-2-propanol nanofibers, which had the ability to infect bacterial hosts [130]. The incorporation of antimicrobial agents in electrospun fibers, such as silver nanoparticles and Mefoxin®, was investigated by Xu et al. [131] and Kim et al. [132], respectively. In the study by Xu et al., 10 wt% PLLA was dissolved in dimethylformamide and dichloromethane (1/9 vol/vol) with $AgNO_3$. The spinning was carried out with a voltage of 15 kV. Scanning electron microscope (SEM) and energy-dispersive spectroscopy (EDS) images showed an even distribution of silver particles across the fibers. The *in vitro* tests indicated that antibacterial efficacy as high as 94%

to 98% was achieved within 12 hours, and the antimicrobial effect lasted longer than 20 days. In the case of Mefoxin®, PLGA (75/25) was the substrate, and *N,N*-dimethyl formamide (DMF) was the solvent. Five percent by weight of the drug was added into the scaffold. It was found that the morphology of the electrospun fibers depended on the concentration of the drug due to its hydrophilic salt nature. The maximum *in vitro* release of the drug was at one hour incubation at 37°C. The drug was completely released after six hours. The introduction of the amphiphilic poly(ethylene glycol)-b-poly(lactide) (PEG-b-PLA) copolymer into PLGA extended the release time to around one week. Good antibacterial efficacy was observed against *Staphylococcus aureus* growing in static and dynamic environments based on *in vitro* studies.

Drug delivery systems using electrospun fibers have also been an active area of research recently due to the advantages of on-site drug delivery over the conventional systematic delivery. Zeng et al. incorporated both rifampin (a drug for tuberculosis) and paclitaxel (an anti-cancer drug) into poly(L-lactic acid) (PLLA) electrospun fibers [118]. The solvent used was 2:1 in volume mixture of chloroform and acetone. The polymer concentration was 3.9% by weight. A voltage as high as 35 kV to 40 kV was applied during spinning. The release of drugs into Tris-HCl buffer solution was measured *in vitro* by a UV-visible spectrophotometer at the wavelength of 473 nm. The results showed a constant release of the drugs without an initial burst release.

In many recent studies, electrospinning was also used to fabricate nanofiber matrices used as tissue engineering scaffolds. Due to the morphological similarity between the nanofiber matrix and the extracellular matrix (ECM) of natural tissues, this new method to prepare tissue engineering scaffolds is being studied extensively. Many studies have reported on improving the biocompatibility of electrospun nanofiber matrices by physical blending, coating, and grafting

proteins or growth factors onto them [117]. Other applications of this matrix include bone tissue engineering and therapeutic application in gene delivery.

III. Methods of collecting filament fibers

All of the applications mentioned above are based on electrospun nanofiber webs, and the alignment of fibers in the webs is not a critical issue. However, in applications where mechanical properties are important, such as fiber reinforcement materials and suture materials, fibers need to be well aligned when collected. A few reported applications used individual fibers or fiber bundles due to the technical difficulties of controlling the instability of spinning jets. Huang et al. pointed out that so far there are no means to easily achieve the three ideal targets of electrospinning, which were "1) the diameters of the fibers be consistent and controllable, 2) the fiber surface be defect-free or defect-controllable, and 3) continuous single nanofibers be collectable." (page 2230) [100] But several groups of researchers have attempted different techniques to align electrospun fibers or to collect fiber bundles. These include methods using rotating cylinder collectors, disks with sharp edges, frame collectors, auxiliary electrical fields, two opposite jets, and a parallel collector.

Cylinder collector

Boland and Matthews used cylinders rotating at high speeds, up to thousands of revolutions per minute (rpm), to wind poly(glycolic acid) electrospun fibers and type I collagen fibers, respectively [100, 117]. Using this method, there is a strict requirement regarding the rotating speed of the cylinder, which should be the same as the speed of the jet reaching the surface of the collector. If the speed is too slow, the fibers may randomly deposit on the cylinder. On the other hand, if the speed is too high, the jet may be broken apart due to the overdrawing of the spinning jet.

Improved cylinder collector

One drawback of the rotating cylinder method is that the whole surface of the cylinder is charged, so that the fibers spread out on the surface of the cylinder. Two methods, a disk with sharp edge and a sharp pin inside the cylinder, are improvements of the rotating cylinder collecting method.

A disk with sharp edge

Using a rotating disk with a sharp edge to collect fibers is an improvement based on the rotating cylinder method used by Theron et al. (Figure 2.2). By narrowing the width of the cylinder, the fibers collected had better alignment. In this study, a rotatable table collector was installed on the edge of the disk to collect nanofiber webs. Well-aligned polycaprolactone fibers were achieved [133].

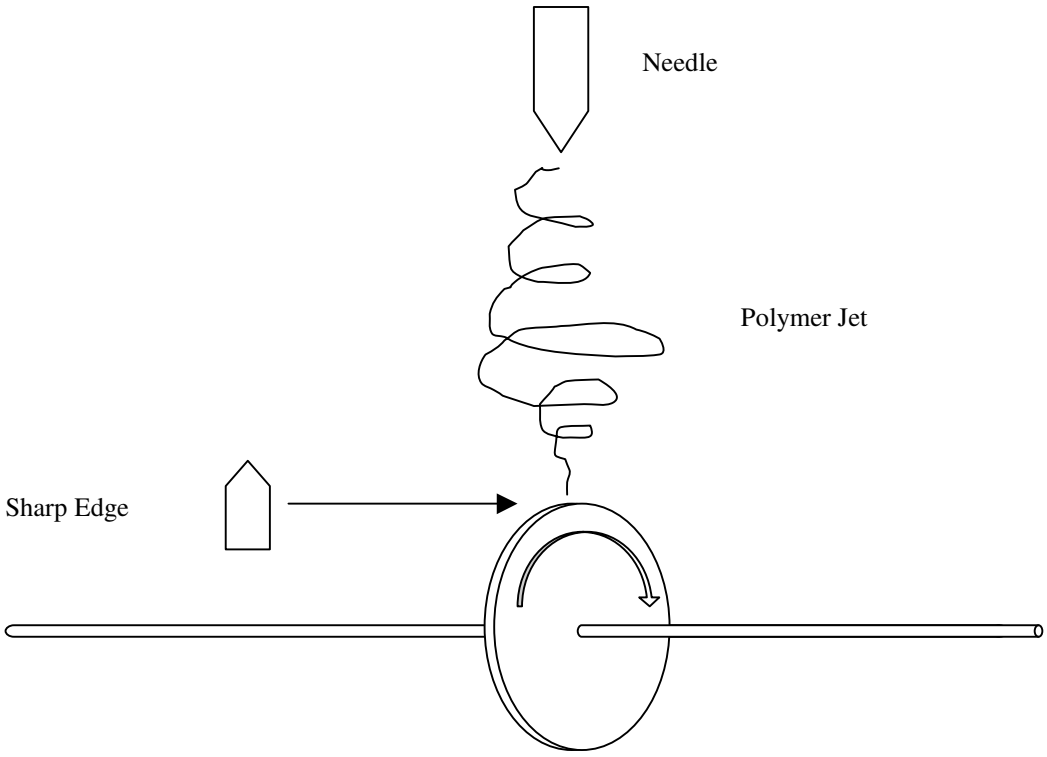

Figure 2.2. A Disk with a Sharp Edge as a Fiber Collector
(Revised from Theron et al. (2001))

A sharp pin inside the cylinder

A sharp conductive pin carrying opposite charges to those carried by the polymer jet was installed inside the rotating cylinder collector to direct the deposit of the spinning jet. This was used by Sundaray et al. to produce continuous aligned polystyrene fibers [134].

An auxiliary electrical field

The direction of the spinning jet can be controlled by manipulating the electric field. Several different auxiliary electrical field methods have been used. A nonconductive rotating cylinder was placed in front of parallel conducting strips by Bornat (Figure 2.3) [117, 135]. The strips carried opposite charges to those of the solution jet, so that fibers were collected in the direction of the orientation of the strip. Teo et al. replaced the strip with parallel knife-edged bars [117].

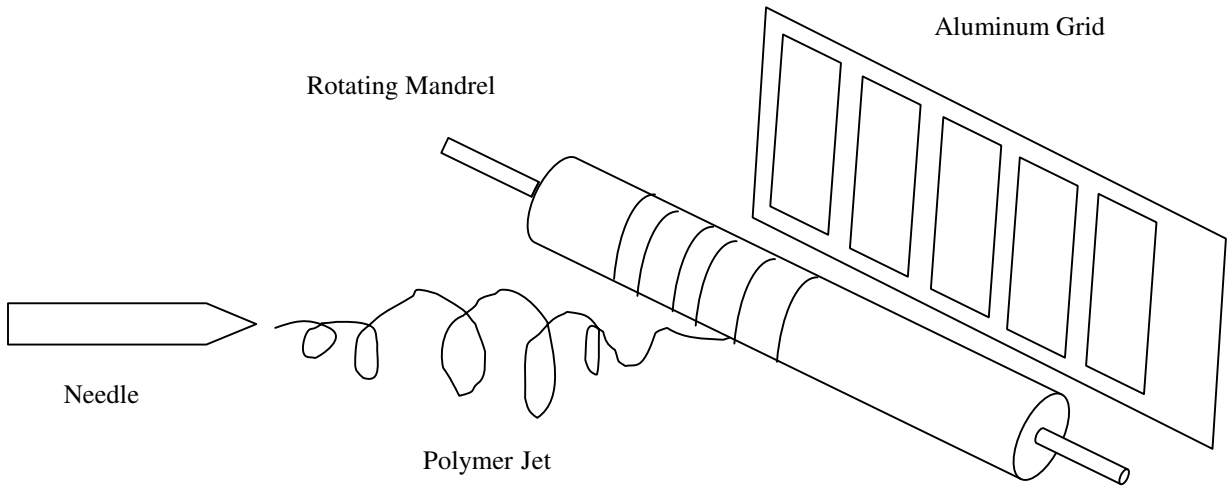

Figure 2.3. Parallel Conductive Strips as an Auxiliary Electrical Field
(Revised from Bornat (1987))

The above method used electric force to attract the jet to deposit fibers in a desirable manner. Deitzel et al. used electric force to propel the jet to deposit on a small area using several copper rings that carried the same charges as the polymer jet (Figure 2.4) [136]. When the electrospinning jet passes through the rings, it is forced to the center of the rings, therefore reducing the chaos of the jet.

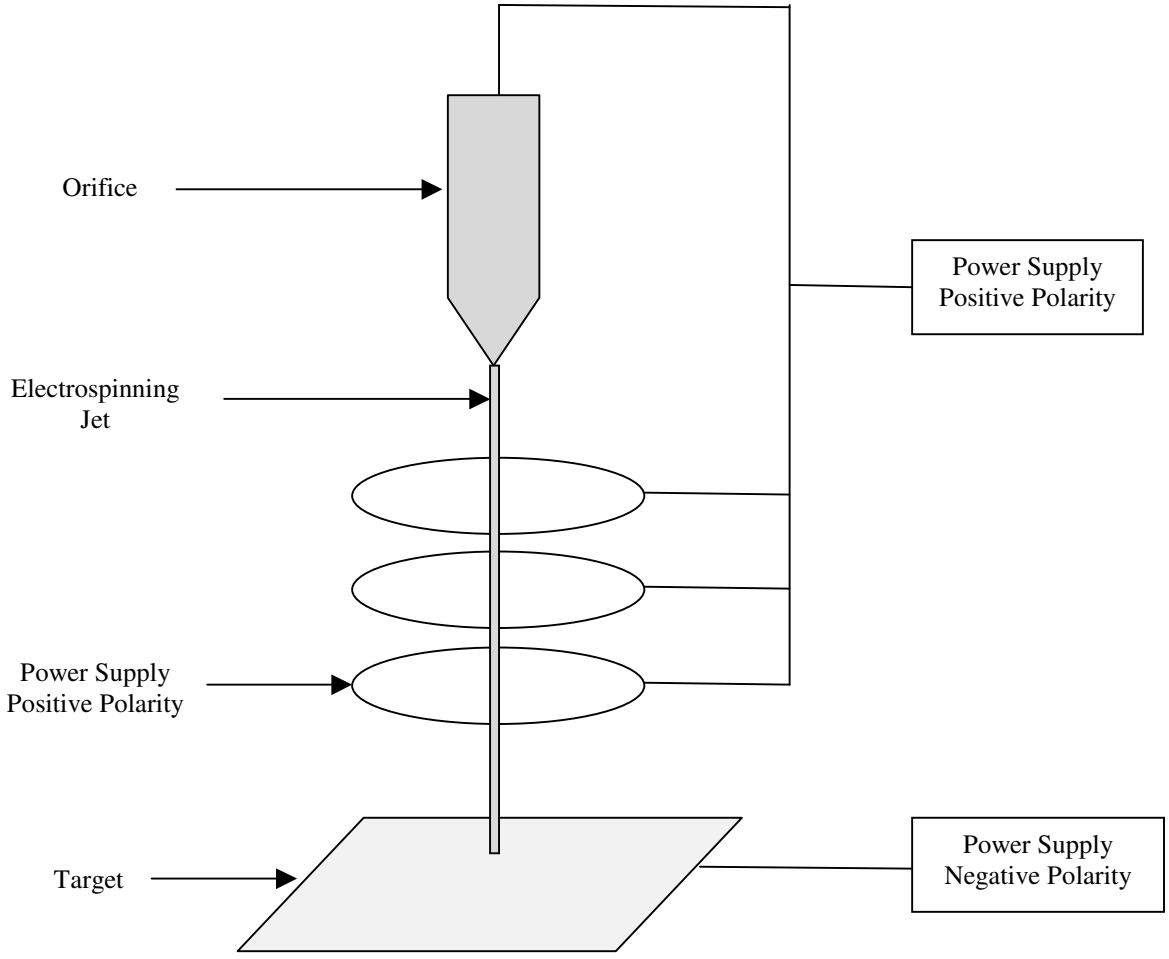

Figure 2.4. Using Copper Rings as an Auxiliary Electrical Field
(Revised from Deitzel (2001))

A frame collector

To collect individual fibers for experimental characterization, Huang et al. invented a method that applied a rotating rectangular frame under the spinning jet, as shown in Figure 2.5 [100]. Results indicated that the aluminum frame resulted in better alignment than the wood frame. More studies evaluating the influence of frames of various sizes and shapes are ongoing.

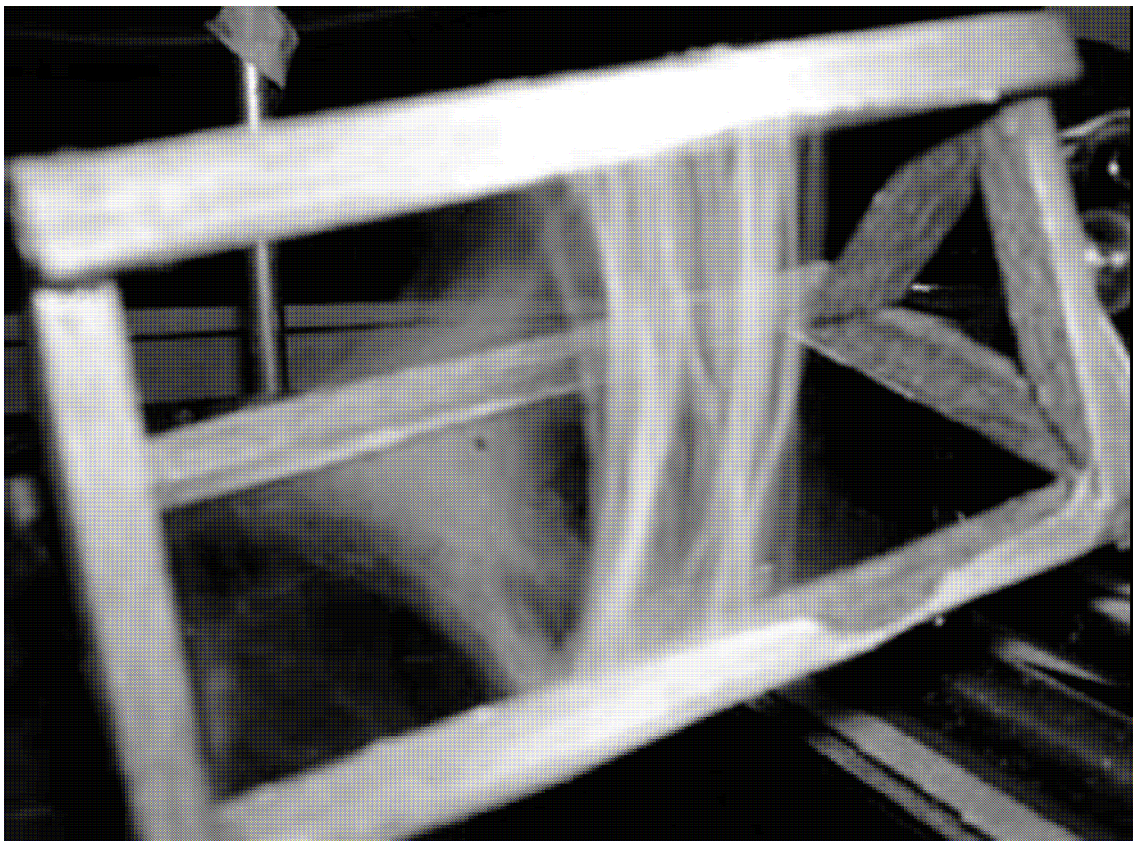

Figure 2.5. A Frame Collector [100]

Two jets method

The difficulty in collecting electrospun fibers lies in the charges that fibers carry. Fibers with the same charges repel each other, which results in the chaos of the polymer jets. In a recent study, a two-jets collecting method solved the problem by neutralizing the jets before collection

[137]. Two syringe pumps charged with the same amount, but opposite charges, were placed toward one other. When the two jets from the two pumps met, the fibers combined to form a yarn due to the attraction of the opposite charges, as shown in Figure 2.6. A cylinder rotating at high speed wound the neutral yarn with very good alignment.

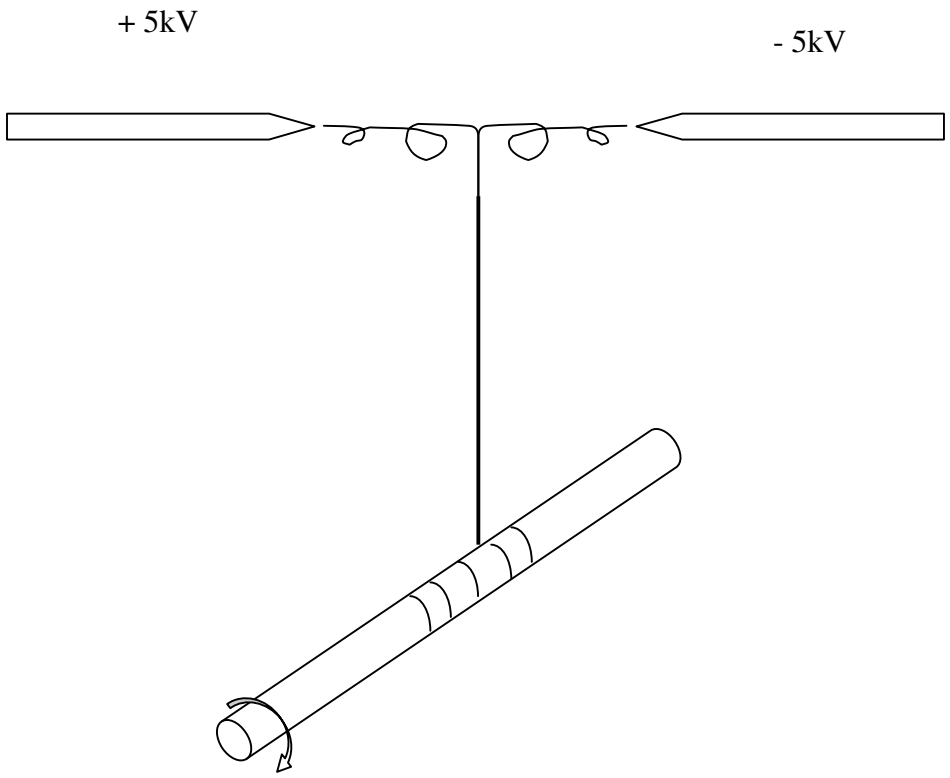

Figure 2.6. A Two Jets Method to Collect Continuous Electrospun Fibers
(Revised from Pan et al. (2006))

Parallel collector method

In the study by Li et al., two parallel-grounded silicon strips were used as the collector to align fibers (Figure 2.7) [138]. The electric field produced a guide for fibers that deposited in the

gap between the two silicon stripes. The fibers collected were well aligned, but the length was limited to the distance between the two strips, which could not be more than several centimeters.

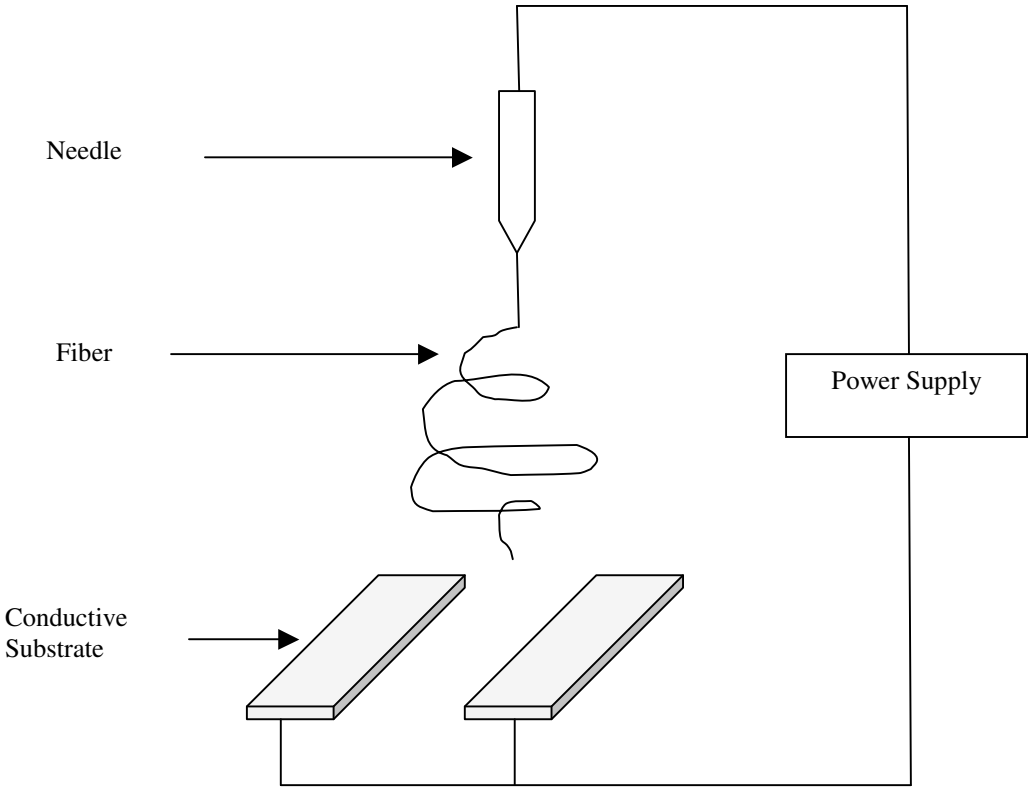

Figure 2.7. Parallel Conductive Substrates as the Fiber Collector
(Revised from Li et al. (2004))

Water bath collector

The water bath collecting method is the same as the traditional wet spinning method. As fibers exit from the spinneret, they are deposited in a liquid bath that extracts solvent and precipitates the fibers. The fibers were wound on a take-up roller. Smit et al. used this method and obtained continuous nanofiber yarns (Figure 2.8) [139].

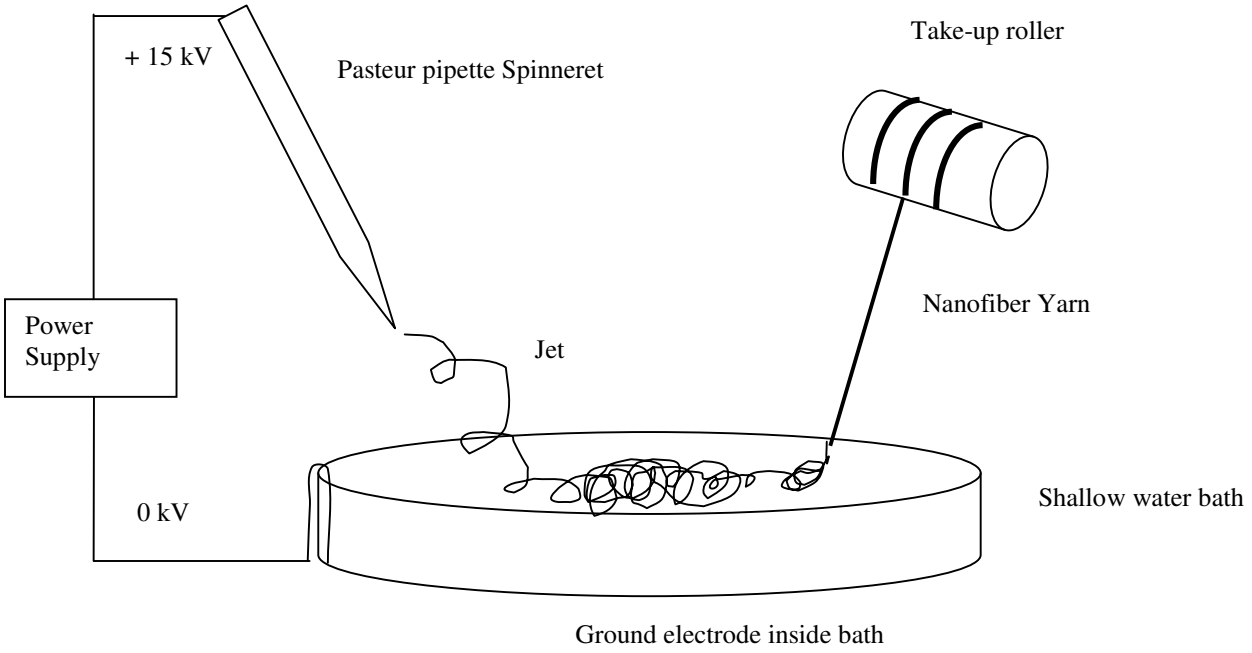

Figure 2.8. Using a Water Bath to Collect Fiber Bundles
(Revised from Smit et al. (2005))

Opposite ring collector

To produce twisted yarns, Dalton et al. used two conductive rings, as shown in Figure 2.9 [140]. Fibers were collected in between the two rings in the same way as the parallel collector method. Then the fibers were twisted into yarns by rotating one of the rings, as shown in Figure 2.9 (b). The length of the yarns produced was limited to several centimeters.

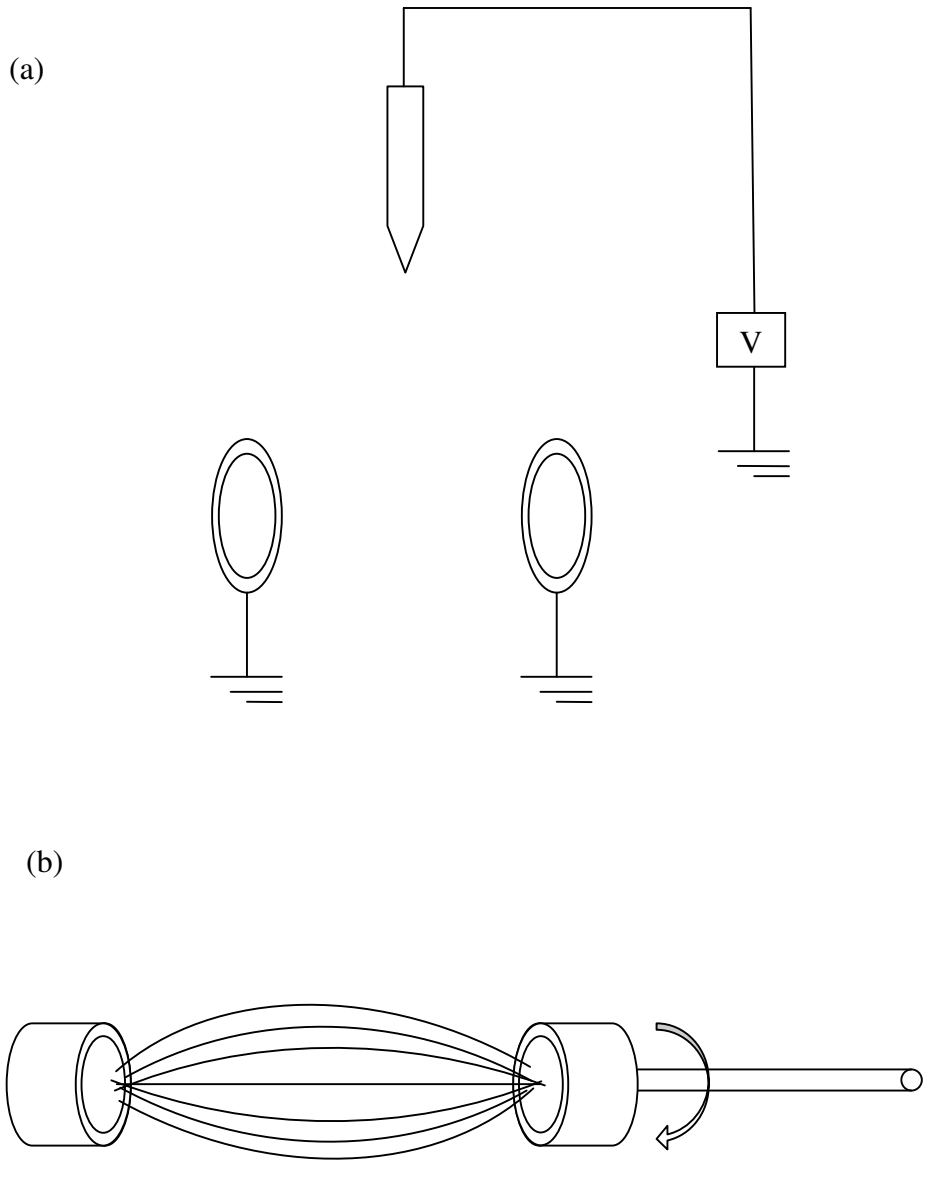

Figure 2.9. Opposite Ring Method to Produce Electrospun Twisted Yarns (a) Schematic of Electrospinning Setup; (b) Twisting of Fibers into Yarns. (Revised from Dalton et al. (2005))

Chapter 3. Materials and Methods

3.1 Methodology

This project was divided into three sections: 1) the design and construction of electrospinning equipment to be used in this study, 2) antimicrobial electrospun fiber development, and 3) characterization of the fibers. The overall goal of each of these is discussed below followed by a detailed description of how each was accomplished.

3.1.1 Design and construction of electrospinning equipment

Because there is no standard equipment for electrospinning, and each research group uses their own design, some preliminary work was completed to design and build the electrospinning setup that served the purpose of this study. The function of the equipment was to produce and collect continuous individual fibers or well-aligned filament fiber bundles.

3.1.2 Fiber development

In this section, the question of how to produce fibers with ideal properties was studied. Some preliminary work was completed initially to determine the practical ranges of polymer solution properties and spinning processing parameters. The polymer solution properties included polymer concentration and viscosity. The spinning processing parameters were feedrate, voltage, and distance. Second, within these ranges, the parameters were varied to study their influence on the properties of the fibers produced. The effects of adding the antimicrobial agent to the polymer solution on fiber properties were also investigated. The fiber properties of interest were fiber diameter and fiber alignment.

3.1.3 Fiber properties characterization

After the initial fibers were produced, the selected fiber properties were measured. These properties included physical and mechanical properties, antimicrobial properties, release of antimicrobial agents, and biodegradable properties. The specific properties tested and the methods used are listed following the materials section.

3.2 Materials

3.2.1. Polymer

Polycaprolactone (PCL) is a biodegradable polyester polymer, which degrades in a physiological environment by the hydrolysis of ester bonds. PCL has a low glass transition temperature of approximately –60°C and a melting point of approximately 60°C. PCL is an FDA-approved polymer for biomaterials, such as sutures and drug delivery carriers. The PCL used in this research was purchased from Sigma-Aldrich Chemical (Batch No.: 12331AB). The molecular weight of the polymer (Mn) is around 80,000. The chemical structure of PCL is shown in Figure 3.1.

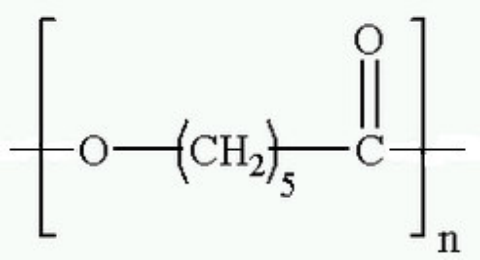

Figure 3.1 Structure of PCL

3.2.2. Solvent

I. Chloroform

Chloroform is also known as trichloromethane, methane trichloride, or formyl trichloride. It is a commonly used solvent and reagent. The physical properties of chloroform are listed in Table 3.1 [141]. Chloroform is a good solvent to dissolve PCL. The chemical structure of PCL is shown in Figure 3.2. The chloroform used was purchased from Fisher Scientific (Lot No.: 024068).

II. Methanol

Methanol is a type of polar solvent, so that it can dissolve ampicillin sodium salt. The physical properties of methanol are shown in Table 3.1 [142], and the chemical structure is shown in Figure 3.3. The methanol used in this study was purchased from Fisher Scientific (Lot No.: 073694).

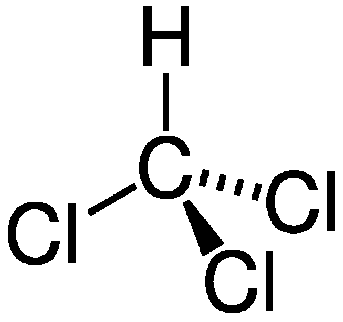

Figure 3.2 Structure of Chloroform

Table 3.1. Physical Properties of Chloroform and Methanol

Solvent	Polarity	Boiling Point	Melting Point	Relative Density to Water	Vapor Pressure (at 20°C)
Chloroform	Nonpolar	62°C	-64°C	1.48	21.2
Methanol	Polar	65°C	-98°C	0.79	12.3

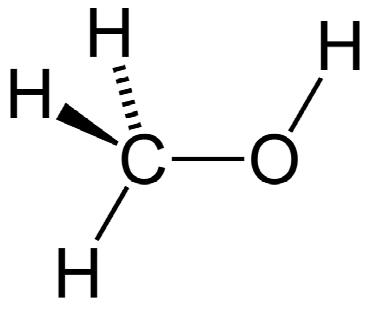

Figure 3.3 Structure of Methanol

3.2.3. Antimicrobial agent

Broad-spectrum antimicrobials with high selectivity are of interest in this study. Ampicillin is an example of such a kind of antimicrobial compounds. It belongs to the beta-lactam antibiotics class, which inhibit bacteria cell wall synthesis by binding to specific penicillin-binding proteins (PBPs) located inside the bacterial cell wall. Ampicillin's chemical structure is shown in Figure 3.4. The ampicillin used in this study was ampicillin sodium salt purchased from Mediatech Inc. (Lot No.: 61238112).

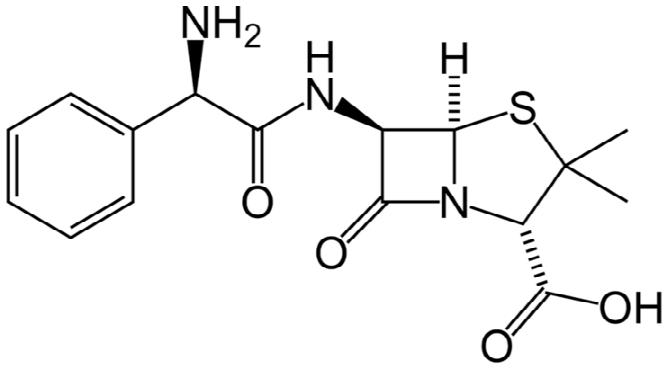

Figure 3.4. Chemical Structure of Ampicillin

3.3 Methods

3.3.1 Polymer solution preparation

I. Solution preparation procedures

The polymer solution was prepared by mixing the PCL polymer pellets as received with the proper solvent and stirring for one hour on a NUOVA Stir Plate with a stirring speed of 2. Chloroform was used as the solvent for the pure PCL. Ampicillin, due to its pure hydrophilic nature, did not dissolve in chloroform. The mixture of chloroform and methanol was used as the solvent for the PCL solution with ampicillin incorporated. A small amount of methanol, a polar solvent, was used to dissolve the ampicillin first, and then the ampicillin methanol solution was mixed with the PCL chloroform solution. The volume ratio of chloroform to methanol was 9:1. Solutions were spun into fibers upon being prepared. The polymer concentration was expressed as the percentage of the weight of the polymer (g) to the volume of the solvent (ml). The concentration of ampicillin was expressed as the percentage of the weight of ampicillin to the weight of the PCL polymer.

II. Viscosity measurement of the polymer solution

The viscosity of the prepared polymer solution was measured using a Brookfield (LV) DV-E 115 Viscometer equipped with a small sample adaptor. The spindle used was #18.

3.3.2 Electrospinning and fiber formation

I. Electrospinning conditions

The electrospinning was carried out under ambient conditions. The setup of the apparatus will be presented in Section 4.1. The rotating speed of the fiber collector was set to approximately 1500 revolutions per minute (rpm) with a surface speed of approximately 7.85 meter/second (m/s). Other spinning conditions, including polymer concentration, ampicillin

concentration, voltage, distance from the needle tip to the collector, and feedrate, varied from test to test. These parameters will be stated before each test result is presented.

II. Fiber collection

The form of the collected samples is critical to the end use and to the successful completion of the following tests. For example, to perform the tensile properties test, a single fiber or yarn is needed. For the test to be described in Section 3.3.3, if not specified, fibers were collected on aluminum foil strips, which were taped on the rotating collector while it was spinning. A sample of the collected fibers is shown in Figure 3.5. Fiber bundles were removed from the aluminum foil strips (as shown in Figure 3.6) after evaporation of the solvent. The fibers or fiber bundles were then tested for various properties. Figure 3.7 (a) shows an example of the fiber samples. The orientation of the fibers in the fiber bundle could be clearly seen along the length of the sample, as shown in Figure 3.7 (b). The amount of fibers being collected was controlled by the amount of polymer solution fed to the needle tip.

Figure 3.5 A Sample of Collected Fibers on Aluminum Foil Strip

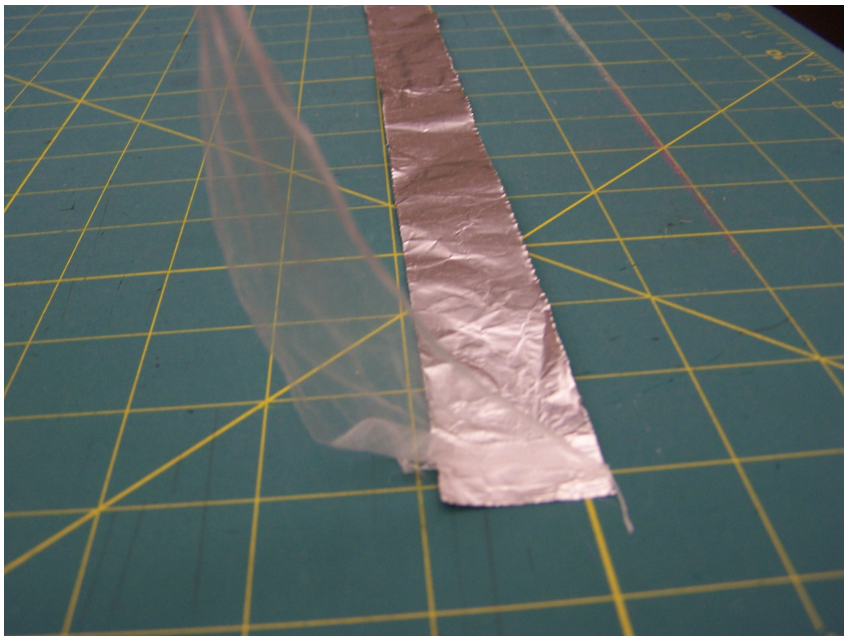

Figure 3.6 Fibers Being Removed from the Substrate

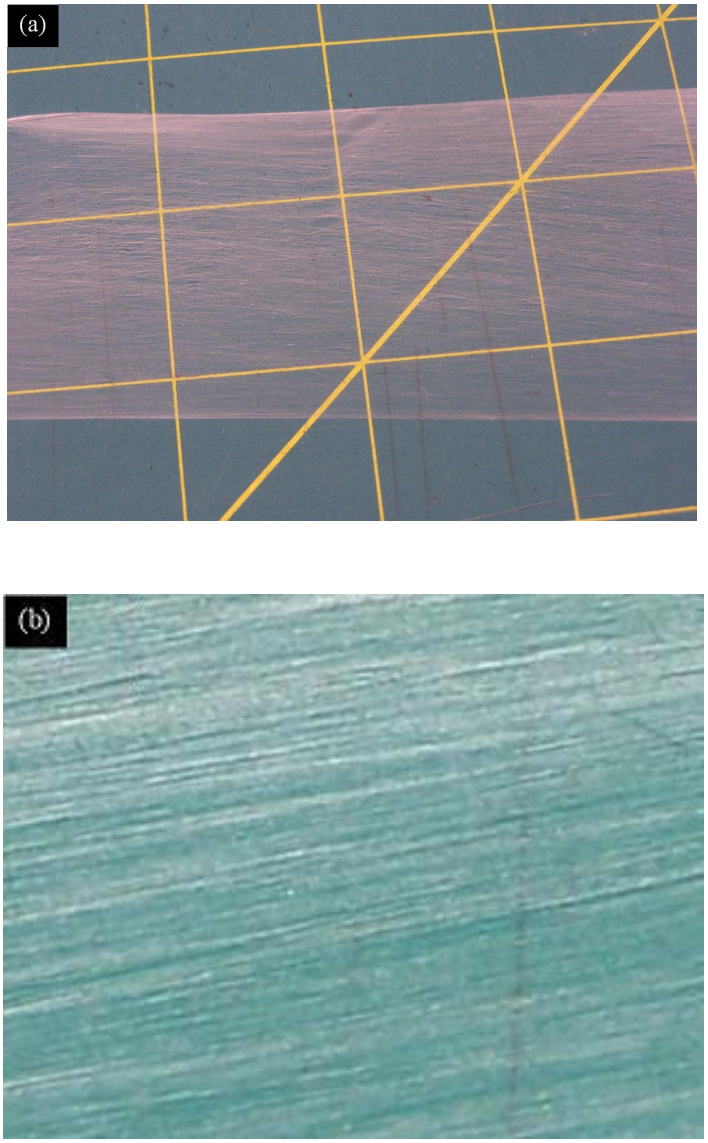

Figure 3.7 Fiber Samples (a) A Fiber Sample Removed from Aluminum Foil; (b) Close-up of the Fiber Sample Showing the Alignment of Fibers

III. Residual solvent detection

The solvents used in this study, including chloroform and methanol, are volatile and have low vapor pressure. The solvents begin to evaporate upon the accumulation of the polymer solution on the tip of the needle. The evaporation continues when the fibers are ejected and fly toward the collector as well as after being deposited on the collector. Complete evaporation of the solvents is critical since they are both considered toxic to human beings. Therefore,

throughout this research, all fibers were kept in a fume hood with ventilation for a minimum of 12 hours (overnight) before any testing was preformed. To ensure the solvents were released completely, samples stored for a minimum of 12 hours after spinning were examined using thermogravimetry analysis (TGA) to detect any residual solvent or other impurities in fibers. The TGA used was Mettler Toledo TGA/SDTA851[e]. The temperature ranged from room temperature to 100°C with a heating rate of 5°C/min.

3.3.3 Evaluation of fiber properties

I. Physical and mechanical properties

Fiber diameter analysis

Fiber samples for diameter analysis were collected using silicon wafer chips, which were taped to the surface of the rotating collector. Images of the fibers were taken using the Zeiss 1450EP Scanning Electron Microscopy (SEM). Samples were sputtering coated with gold for 60 seconds using a SPI – Module™ Sputter Coater to minimize the influence of the charges. The thickness of the gold coating was 153 Å. The diameters of the fibers were analyzed using ImageTool 3.0. For each sample, the diameters of 30 fibers were measured to calculate the mean and standard deviation.

Crystallinity measurement

The crystallinity of fibers is critical to their mechanical and degradation properties. The percentage o crystallinity of the electrospun fibers with and without the antimicrobial agent was measured using Differential Scanning Calorimetry (DSC) (Mettler Toledo DSC821[e]). To prepare samples, the fibers were chopped into fine pieces. Since the glass transition temperature and melting point of PCL are –60°C and 60°C, respectively, the measurement was started from –

60°C and ended at 100°C. The heating rate was 10°C/min. Ambient air was used. The percentage of crystallinity ($C_{rystal}\%$) was calculated using Equation 3.1:

$$C_{rystal}\% = \Delta H/\Delta H_f \times 100 \quad (3.1)$$

Where ΔH was the enthalpy per gram (J/g) of the sample. It was measured by integrating the area under the melting peak and normalizing to the sample weight. ΔH_f was the theoretical enthalpy of fusion (J/g) of PCL, i.e., the enthalpy of 100% crystalline PCL. The value of ΔH_f of PCL was 139.5 J/g [143, 144].

Tensile properties test

The tensile properties of nanofiber yarns were measured using Instron 4400R. Fibers were first twisted into yarns using a twist tester (Alfred Suter Co. Inc.). The amount of twist was five tpi (twists per inch). Each specimen (yarn) was made of fibers spun from 0.1 ml of polymer solution. Figure 3.8 shows an example of a twisted yarn clamped on the twister. Only the straight tensile properties of dry samples were tested. The samples were conditioned for two hours before testing at standard atmosphere for testing textiles, which was 21 ± 1°C (70 ± 2°F) and 65 ± 2% relative humidity. The gage length was 150 mm, and the rate of operation was 300 mm/minute. The load cell used was 500 N. Pneumatic Captan jaws were applied to clamp samples. Ten specimens for each type of sample were measured. The maximum load and percentage of elongation at break were reported.

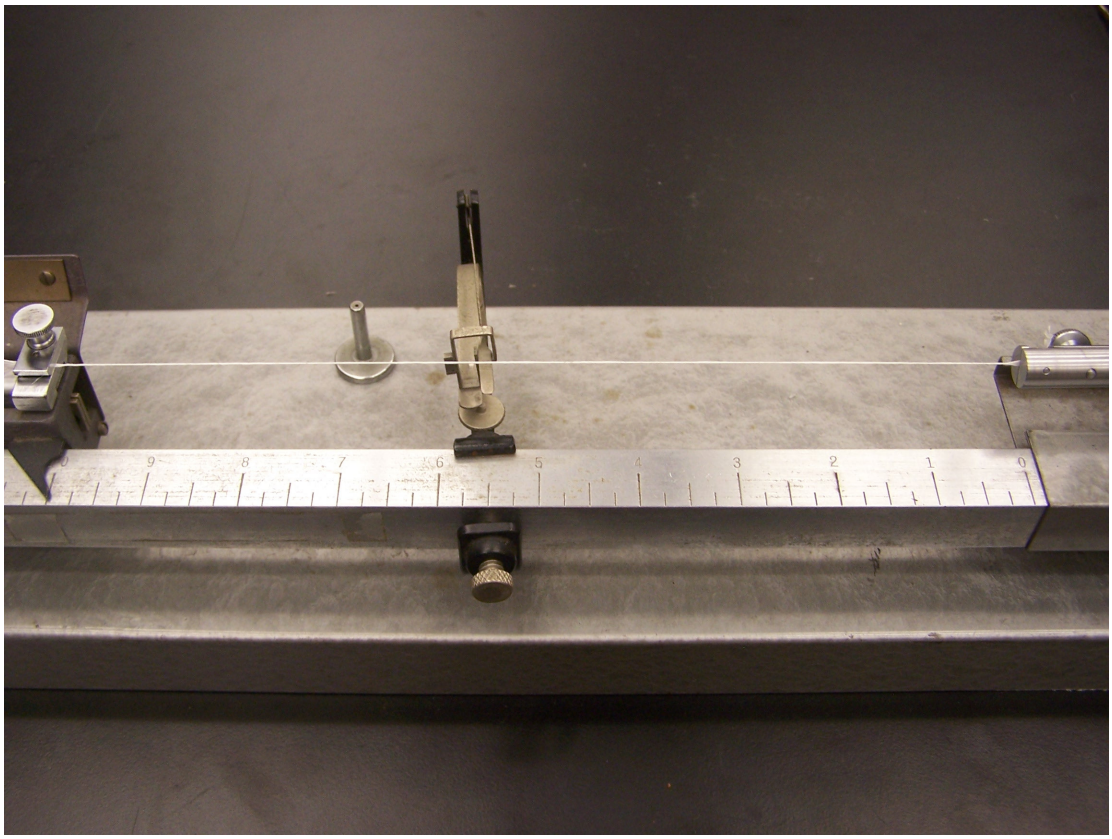

Figure 3.8 A Sample of Twisted Yarns

II. Antimicrobial properties

Zone of inhibition test

Fibers spun with the antimicrobial agent included were evaluated for their antimicrobial properties using the quantitative method of the zone of inhibition. The microorganisms were gram-negative *Klebsiella pneumoniae* (American Type Culture Collection No. 4352) and gram-positive *Staphylococcus aureus* (American Type Culture Collection No. 6538). Both bacteria are potential human pathogens. *Staphylococcus aureus* is a major cause of soft tissue infections, toxic shock syndrome, and scalded skin syndrome. *Klebsiella pneumoniae* causes pneumonia and urinary tract infections in catheterized patients as well as wound infections. *Klebsiella*

pneumoniae possesses polysaccharide capsule. Test samples were fibers spun from 0.1 ml of polymer solution with various concentrations of ampicillin incorporated. The fibers were twisted into yarns and folded into lengths approximately 30 mm long. The mean of the zone of inhibition was reported based on three replications for each sample. The test procedures were as follows.

1. Twenty-four-hour cultures of the microorganisms were diluted to around 10^5 CFU/ml to be used as inoculums.
2. A sterile cotton-tipped applicator (Puritan, MDCI Ltd.) was dipped into the inoculum and pressed gently on the wall of the tube to remove excess inoculum.
3. The entire surface of a Nutrient Agar (Difco™ Nutrient Agar, Lot #: 6264282) plate was wiped evenly with the inoculated applicator three times with a 60° rotation of the wiping direction in between to ensure complete coverage of the plate (as shown in Figure 3.9). (Each liter of the nutrient agar contained approximately 3.0 grams of beef extract, 5.0 grams of peptone, and 15.0 grams of agar.)

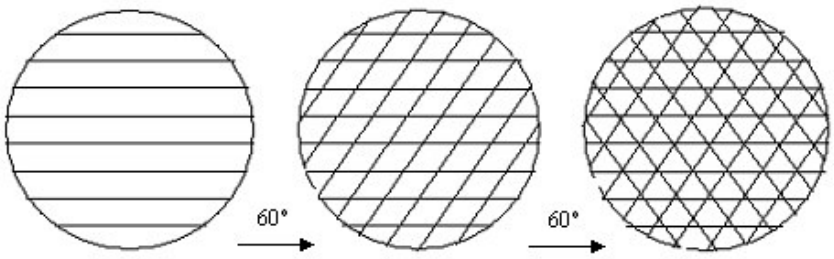

Figure 3.9 Schematic of Preparing the Inoculated Plate

4. Yarns were transferred to the center of the inoculated plate with a pair of sterile forceps. The yarn was gently pressed to the surface of the agar to ensure good contact with the agar.
5. The plates were incubated at 37°C for 24 hours.

6. The clear zones without bacteria growth around the tested sample were measured as shown in the schematic of Figure 3.10.

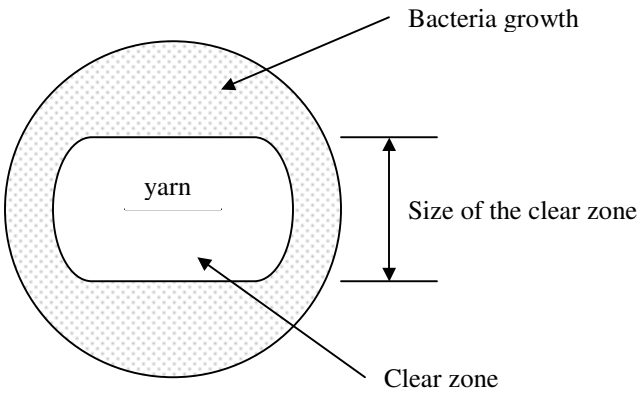

Figure 3.10 Schematic of Measuring the Size of the Zone of Inhibition

Antimicrobial agent release test

The *in vitro* release of the antimicrobial agent from the fibers was investigated by measuring the concentration of the antimicrobial agent released in the phosphate buffer solution (PBS) (with a pH of 7.4), into which the tested fibers were immersed. The samples were prepared the same way as those in the antimicrobial tests. Yarns were immersed into 25 ml of PBS in centrifuge tubes, which were placed in a 37°C shaking bath (Precision Reciprocal Shaking Bath) with a shaking speed of 50 rpm. At specific time intervals, 1.5 ml of PBS was taken out into a sterile cuvette for the concentration determination by a UV-VIS spectrophotometer (Shimadzu UV-2401 PC UV-VIS Recording Spectrophotometer). After the measurement, the PBS was carefully moved back to the centrifuge tube to keep the consistency of the releasing environment. The predetermined time intervals were 10 minutes, 20 minutes, 30 minutes, 40 minutes, 50 minutes, 60 minutes, one hour, two hours, three hours, four hours, eight hours, 12 hours, and 24 hours.

To determine the percentage of released ampicillin in PBS, the amount of ampicillin released in PBS needed to be decided first using the UV-Vis spectrophotometer, and then the percentage released was calculated. To determine the amount of ampicillin released in PBS using the UV-Vis spectrophotometer, the wavelength used needed to be figured out first, and a standard curve needed to be calibrated.

1) Determination of the wavelength

The mechanism of determining the concentration of a solution using a spectrophotometer is to determine the relationship between the absorbance (*Abs*) of a solution and its concentration ($C_{solution}$), which follows Lambert-Beer's law, shown in Equation 3.2.

$$Abs = \varepsilon \, l \, C_{solution} \tag{3.2}$$

Where ε is absorption coefficient, and l is the path length of the incident light.

The absorption coefficient, ε, is a function of the wavelength of the incident light, so that the measurement should be set to a certain wavelength. Usually, the wavelength is chosen around an absorbency peak of the solution to maximize the sensitivity of the measurement.

Figure 3.11 shows the absorbency spectrum of the ampicillin PBS solution from 200 nm to 800 nm. A peak was shown in the ultraviolet region. However, the linear relationship of Lambert-Beer's law between the concentration of the solution and its absorbance is only well obeyed under low concentrations. Therefore, the absorbency peak was shifted with the variation of the solution concentration, as shown in Figure 3.12. Usually, when the absorbance is lower than 1, the chi-square of fitting the linear relationship is small. Studies showed that when the ampicillin solution concentration was 31.25 μg/ml, the peak absorbance was below 1 at around 220 nm. Based on this, 220 nm was set as the wavelength for the measurements in this study.

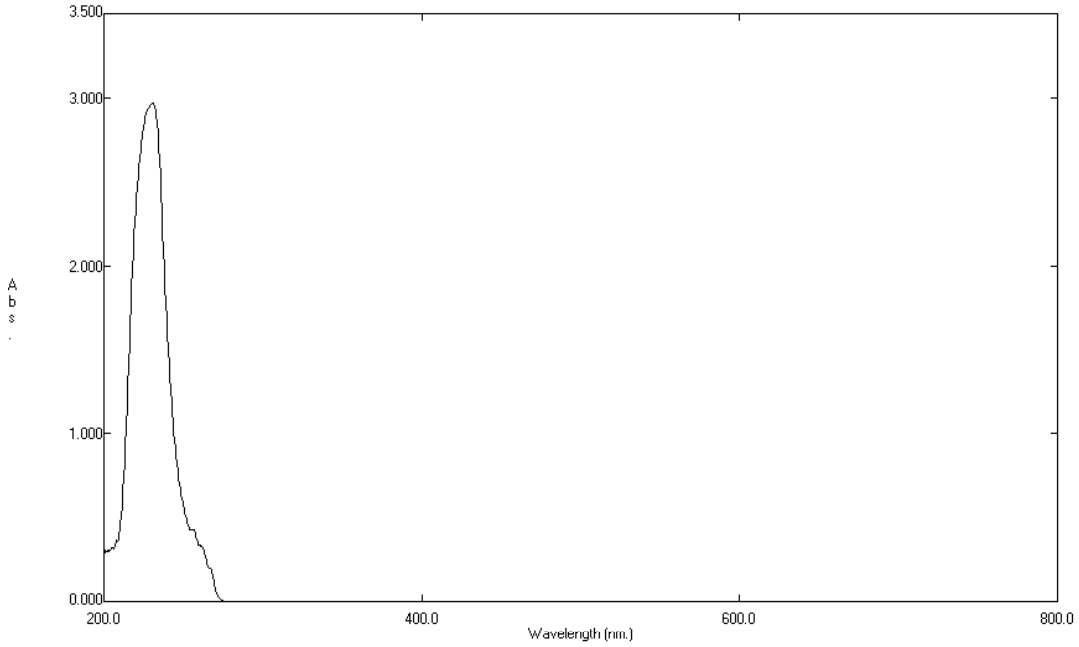

Figure 3.11 Absorbency Spectrum of Ampicillin in PBS

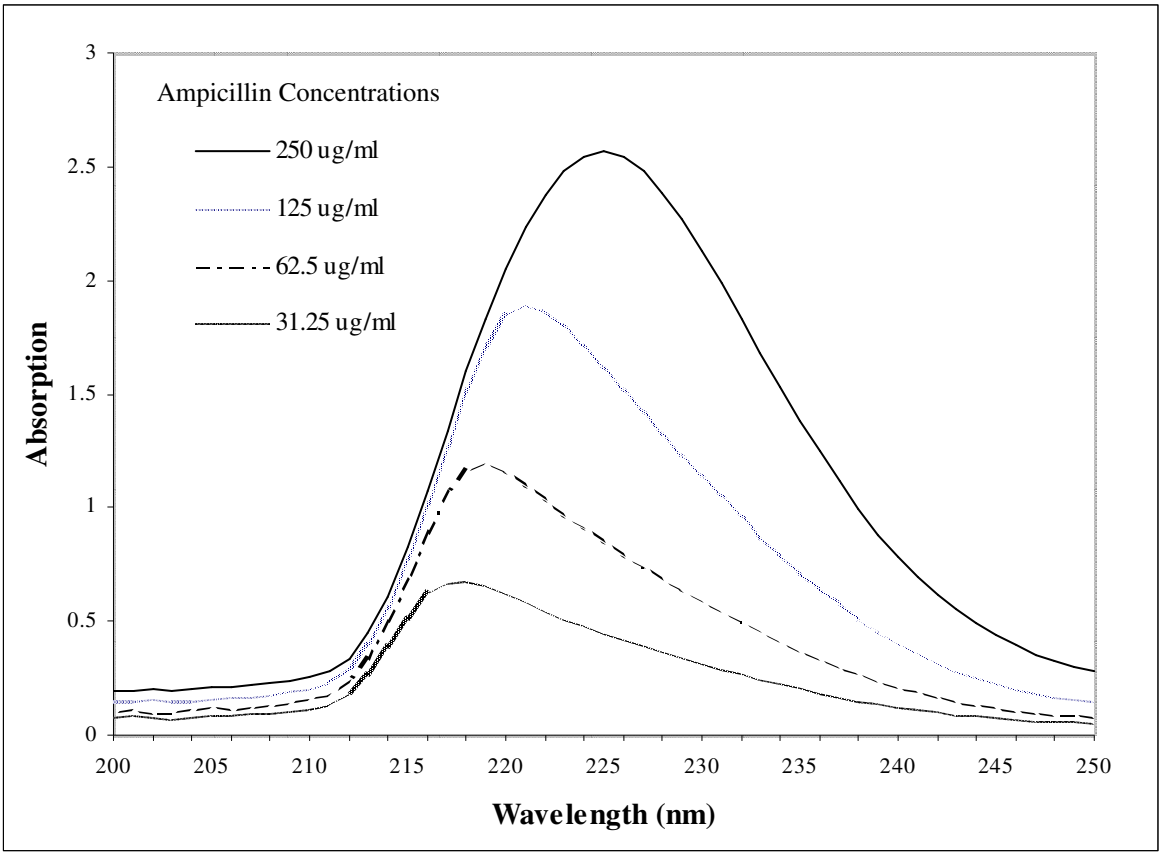

Figure 3.12 Absorbency Spectra of Various Concentrations of Ampicillin in PBS

2) Calibration of the standard curve

In Equation 3.2, ε of a specific solution is a constant with a given wavelength, and l is determined by the width of the sample slot. Therefore, the relationship of $C_{solution}$ and Abs can be expressed as Equation 3.3.

$$C_{solution} = K_0 \times Abs \tag{3.3}$$

Where K_0 = constant.

To determine K_0, the absorbance of a series of ampicillin solutions with known concentrations was measured at the wavelength of 220 nm, and the values were fitted into the above equation. A sample is shown below with six points of measurements in Table 3.2.

Table 3.2 Absorbance of Ampicillin PBS Solutions with Various Concentrations

#	$C_{solution}$	Abs
1	0.0000	0.000
2	41.650	0.727
3	31.250	0.548
4	15.625	0.267
5	7.8125	0.128
6	3.9063	0.067

The obtained equation was

$$C_{solution} = 57.39 \times Abs$$

The chi-square was 0.00063, which indicated a very good fit of the linear relationship, as also shown in Figure 3.13.

Preliminary work found that minor variations to the K_0 were obtained each time due to the precision limitation of the instrument, especially when the spectrophotometer was restarted. To minimize this impact on the accuracy of the measurements, a standard curve was obtained each time the spectrophotometer was turned on.

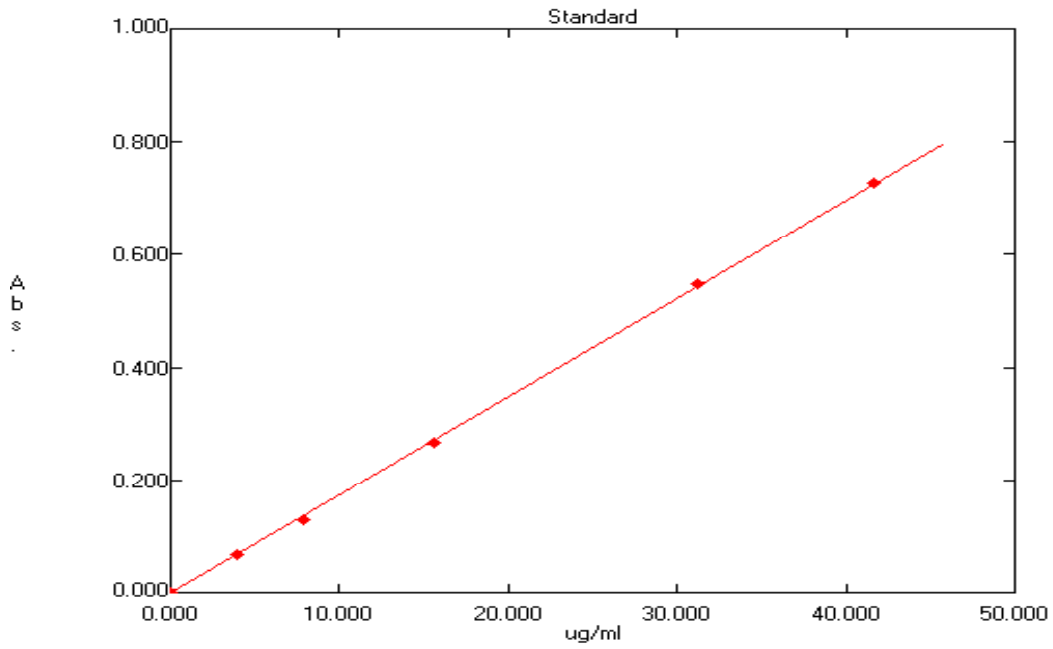

Figure 3.13 Linear Relationship between the Concentration of the Ampicillin PBS Solution and Its Absorbance

3) Calculation of the percentage of released ampicillin

The total amount of the released antimicrobial agent in PBS ($T_{released}$) was calculated by multiplying the concentration ($C_{solution}$) and the total volume of the PBS (25 ml). The percentage of the released antimicrobial agent ($R\%$) to the total amount in the fiber ($T_{contained}$) was reported based on three replications of each sample. $R\%$ was calculated by the equation (Equation 3.4) shown below.

$$R\% = T_{released}/T_{contained} \times 100 \quad (3.4)$$

$T_{contained}$ was calculated based on the concentration of the antimicrobial agent in the fibers (C_{fiber}). C_{fiber} was expressed as the weight ratio of the antimicrobial agent to the polymer (Equation 3.5).

$$T_{contained} = W_{yarn} \times C_{fiber} / (1 + C_{fiber}) \quad (3.5)$$

Where W_{yarn} = weight of the yarn being tested.

III. Biodegradation properties

Mass change measurement

When in the physiological environment, the polyester biodegradable polymers are expected to degrade by hydrolysis of the ester bonds. To investigate the *in vitro* degradation rate of polycaprolactone, the mass change in fibers in PBS was studied. Samples were prepared as those in the antimicrobial tests. Yarns were stored in standard atmosphere for two hours before the initial weight (W_0) measurement. (Preliminary work showed that the weight of the yarns came to equilibrium after being stored in the standard atmosphere for one hour.) Then, the yarns were immersed in PBS. After predetermined time intervals, the yarns were taken out and rinsed with deionized water, then stored in standard atmosphere for two hours before the weight (W) was measured. The percentage of weight loss ($WL\%$) was calculated by Equation 3.6:

$$WL\% = (W_0 - W) / W_0 \times 100 \tag{3.6}$$

The samples were transferred back to PBS after the weight measurement was completed. During the entire process, care was taken to minimize handling of the samples and to minimize potential contamination, which would influence the fiber weight. The PBS was discarded and replaced with fresh PBS every day for the first three days and every seven days thereafter. To provide a consistent degradation environment for all samples, the amount of PBS in milliliters was the same as the weight of the sample in milligrams.

The predetermined time intervals were one day, two days, three days, five days, seven days, 10 days, 14 days, 21 days, 28 days, and 35 days. The balance used to measure the weight of the fibers was a Sartorius MC 5 Ultra Micro Balance with readability of 0.1 μg. Three replications were made for each sample.

Morphology change

As the degradation proceeded, it was expected that the surface morphology of fibers would be altered. The surface morphology of the fibers was examined by SEM (LEO 982 Field Emission Scanning Electron Microscopy). Images of fiber surfaces were taken before and after immersion in PBS.

3.3.4 Data analysis

Initially, Analysis of Variance (ANOVA) tests were to be used to determine the significance of the difference among the properties of fibers produced under different spinning parameters. There are three assumptions that underlie the ANOVA: 1) The samples are independent, 2) The populations being sampled are normally distributed, and 3) The variances of the populations are equal. After testing the validity of these assumptions, it was found that ANOVA was not an appropriate method for this study. Therefore, a nonparametric test, the Wilcoxon Singed-Ranks Test, was used rather than ANOVA. A significance level of 0.05 was used.

Chapter 4. Results and Discussion

The results from this study are presented in the following five sections.

Section 1. Apparatus design and preliminary experiments

Section 2. The impact of spinning parameters on fiber properties

Section 3. Physical and mechanical properties of fibers

Section 4. Antimicrobial properties of fibers and the release of ampicillin from fibers

Section 5. Biodegradation of fibers

4.1 Apparatus Design and Preliminary Experiment

4.1.1 Design of the fiber collector

The electrospinning apparatus is composed of three main components: a high-voltage supply, a syringe pump, and a fiber collector. Both the high-voltage supply and the syringe pump are standard parts. However, the design of the fiber collector is determined by the type of electrospun products to be collected. In this study, the collector needed to fulfill several requirements. First, since the final product of interest is surgical sutures or other textile biomaterials, the fibers are required to have a certain degree of orientation in the collected samples, or the collected fibers must have the potential to be processed to align themselves as in the traditional carding process. Hence, a fiber collector that can collect continuous individual fibers, or well-aligned filament fiber bundles, is desirable. Secondly, the length of the fiber samples needed be adequate to perform various tests to evaluate the properties of interest. Third, the fibers collected must be able to be easily removed from the collector intact. Fourth, the amount of fiber material collected must be controllable.

A sketch of the initial design for the apparatus is shown in Figure 4.1. A cylinder is connected through a shaft to a motor, which drives the cylinder to spin. Fibers are collected on the surface of the cylinder. One pole of the high-voltage supply is connected to the cylinder by an electric brush. The other pole is clipped on the needle.

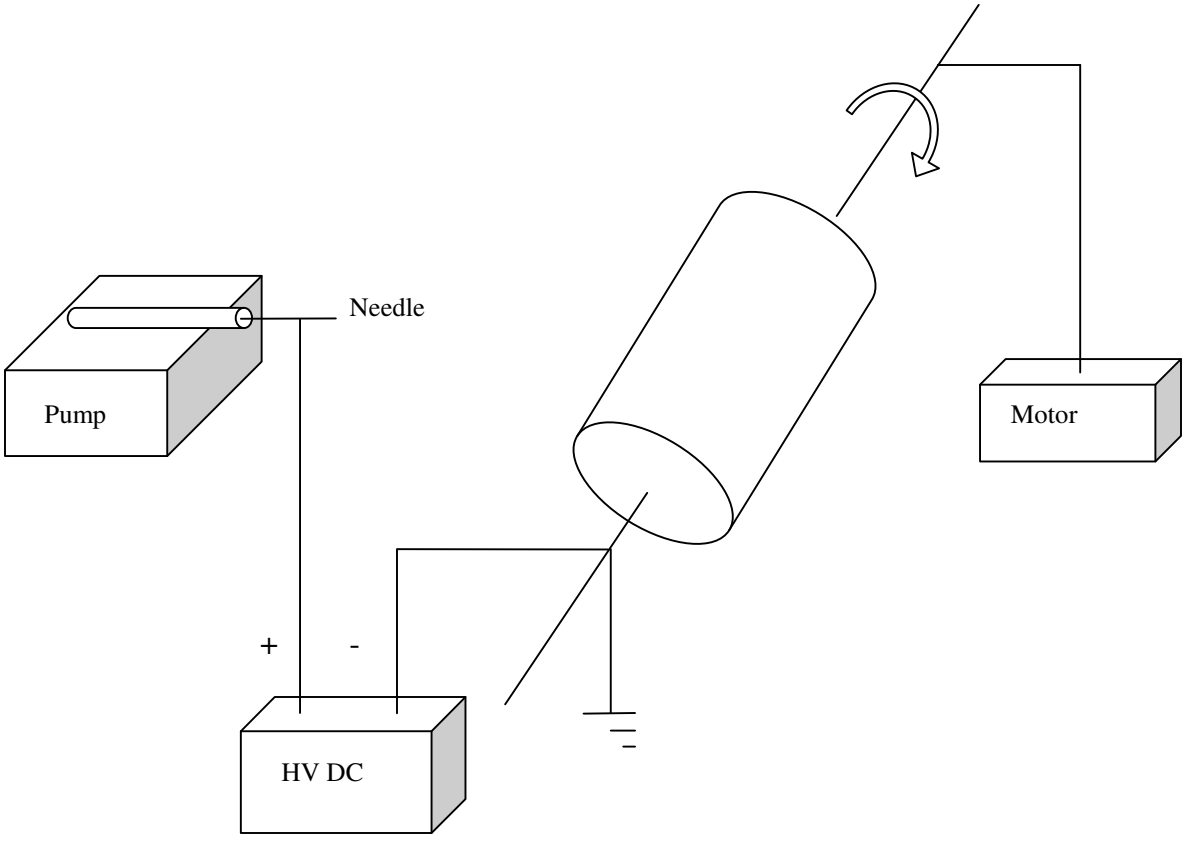

Figure 4.1 Schemetic of the Initial Design of the Electrospinning Apparatus

A prototype of the collector was constructed to verify its feasibility. This prototype is shown in Figure 4.2. The radius of the cylinder was 5 cm, and the width was 8 cm. The speed shifts of the motor used in this prototype were low-medium-high. Fibers spun and collected with this system had observable alignment along the rotating direction of the collector although they were not perfectly aligned. After collection, fibers were removed from the drum and observed

using an optical microscope. It was found that the fiber alignment was improved when the rotating speed increased from low to high. The image in Figure 4.3 shows an example of the collected fibers under high rotating speed. However, the fibers spread over the entire surface of the cylinder. This spread was due to the wide electric field distribution.

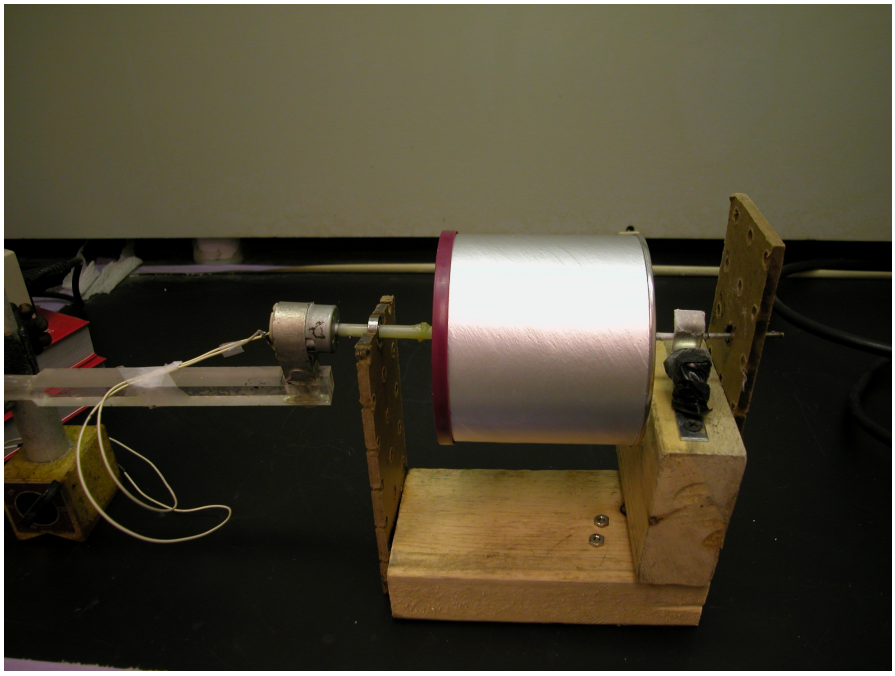

Figure 4.2 Prototype of the Fiber Collector Using a Cylinder

To increase the degree of alignment and reduce the spread of the collected fibers, a thin disk was adopted to replace the cylinder, as shown in Figure 4.4. By reducing the width of the collector, the electric field distribution was reduced. Figure 4.5 shows the simulated electric field distribution from the needle tip to the collector. The width of the collector in Figure 4.5 (a) is larger than in Figure 4.5 (b). The small circle stands for the needle tip, to which an electric potential is applied. The rectangle stands for the collector, which is grounded. Figure 4.6 shows a fiber sample collected using the thin disk. The fibers had good alignment. Moreover, the spread

of fibers was limited to the width of the disk. Thus, using a thin disk as the collector was feasible and met all the requirements proposed. First, using the collector, aligned fiber bundles could be obtained. Second, the length of the samples was the circumference of the disk, so that the length was controllable. Third, by attaching a strip of aluminum foil to the collector, the samples collected could be easily removed from the collector and then be removed from the aluminum foil after the solvent(s) were completely evaporated. Fourth, the amount of collected fibers could be controlled by setting the amount of polymer supplied from the syringe pump. As a result, the design of using a thin disk as the collector was finalized, and the schematic was sent to the Instrument Shop at the University of Georgia to be constructed.

The fabricated collector is shown in Figure 4.7. The diameter of the disk is 10 cm, and the width is 1 cm. A whole setup of the apparatus, including the three main parts, is shown in Figure 4.8.

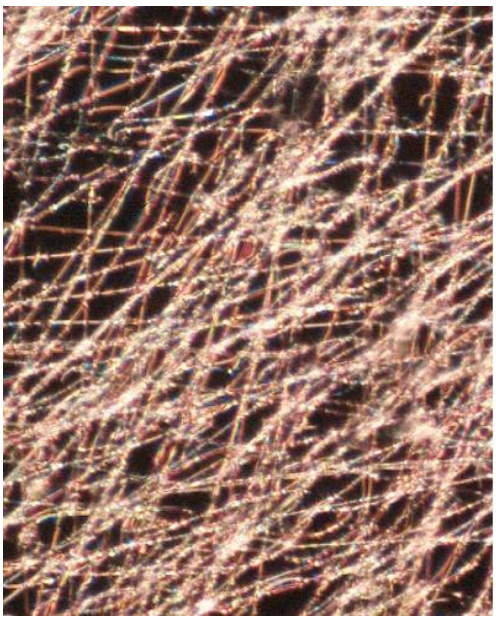

Figure 4.3 A Fiber Sample Collected on the Drum Collector as Observed Using an Optical Microscope at Magnification 100x.

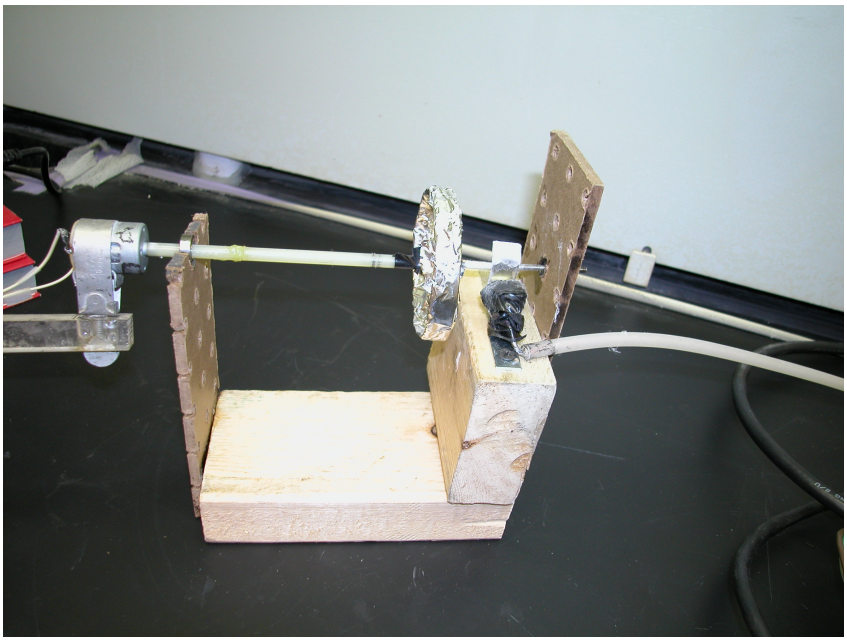

Figure 4.4 Prototype of the Fiber Collector Using a Thin Disk

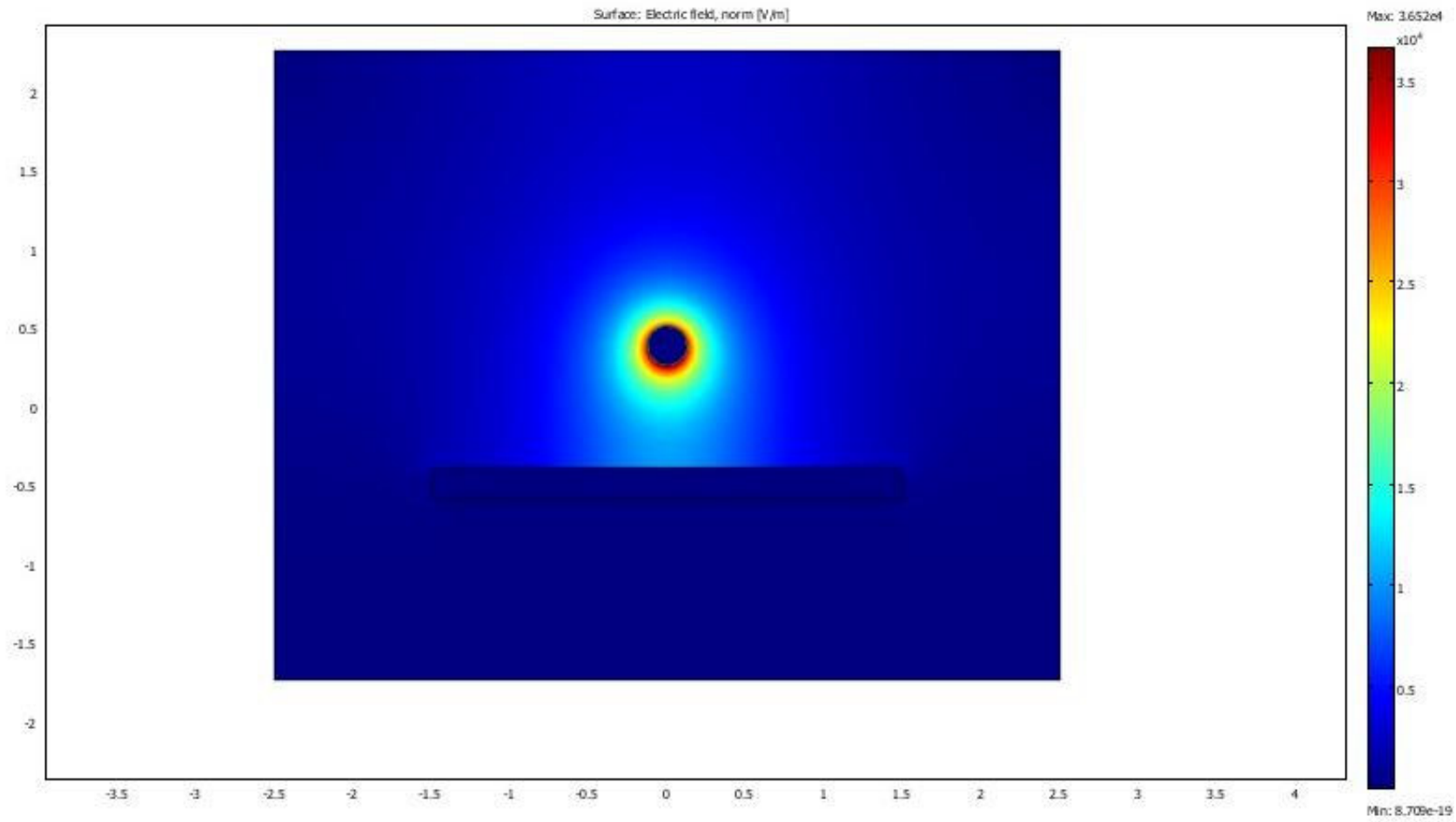

Figure 4.5 (a) Simulated Electric Field Distribution of Electrospinning Using a Cylinder as the Collector

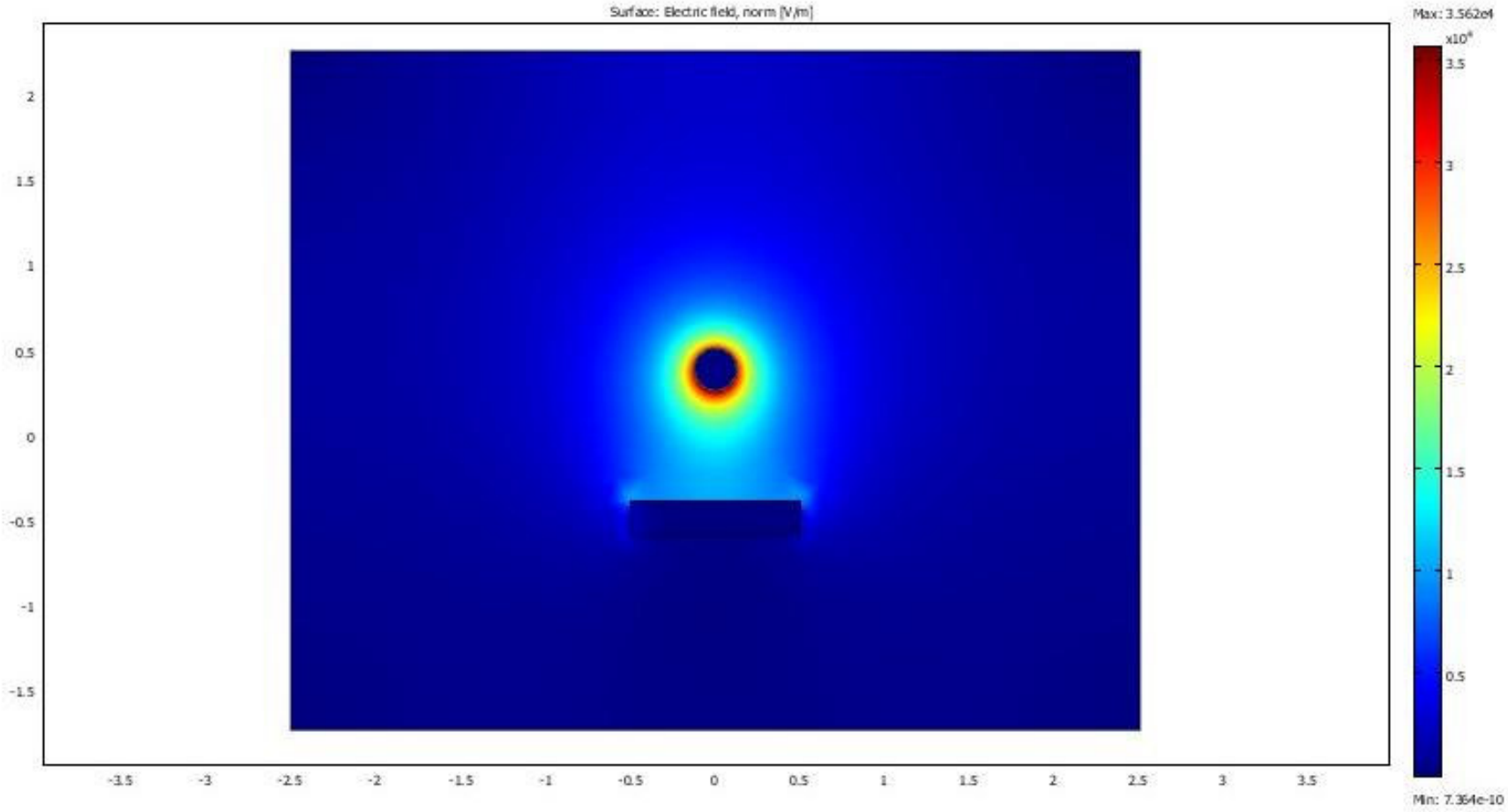

Figure 4.5 (b) Simulated Electric Field Distribution of Electrospinning Using a Thin Disk as the Collector

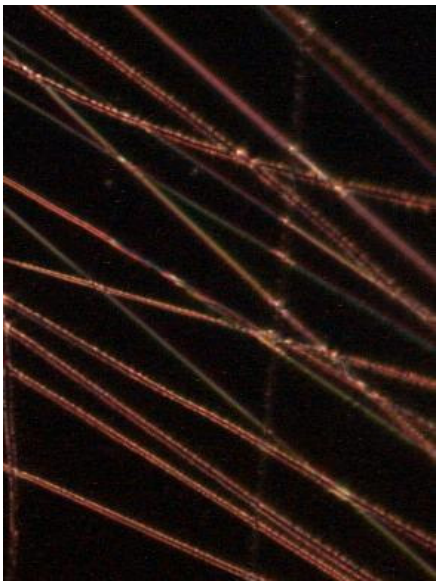

Figure 4.6 Fiber Sample Collected on the Thin Disk Collector as Observed Using an Optical Microscope at Magnification 100x

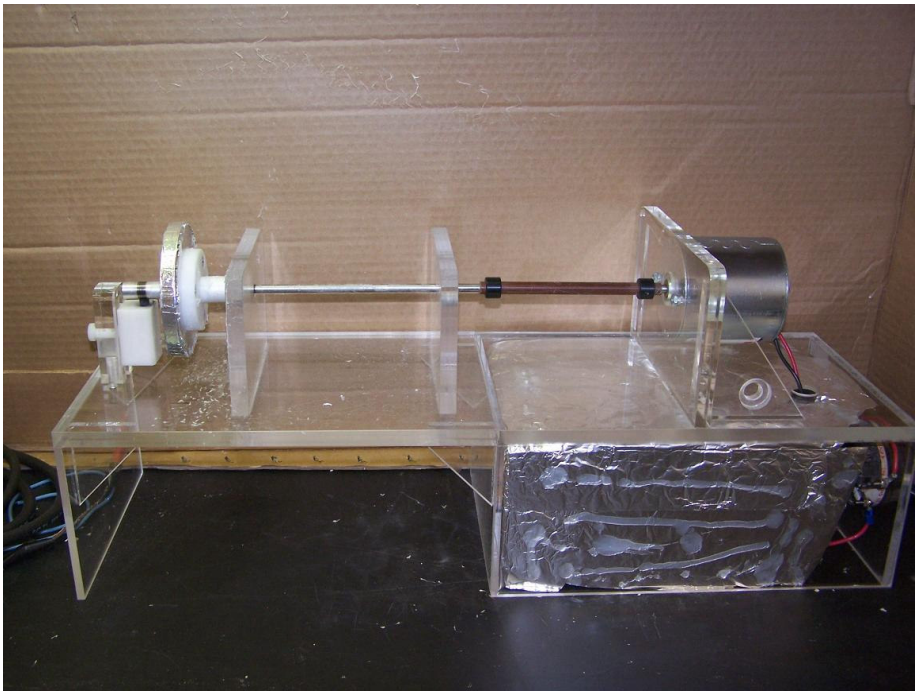

Figure 4.7 The Collector Used in the Study

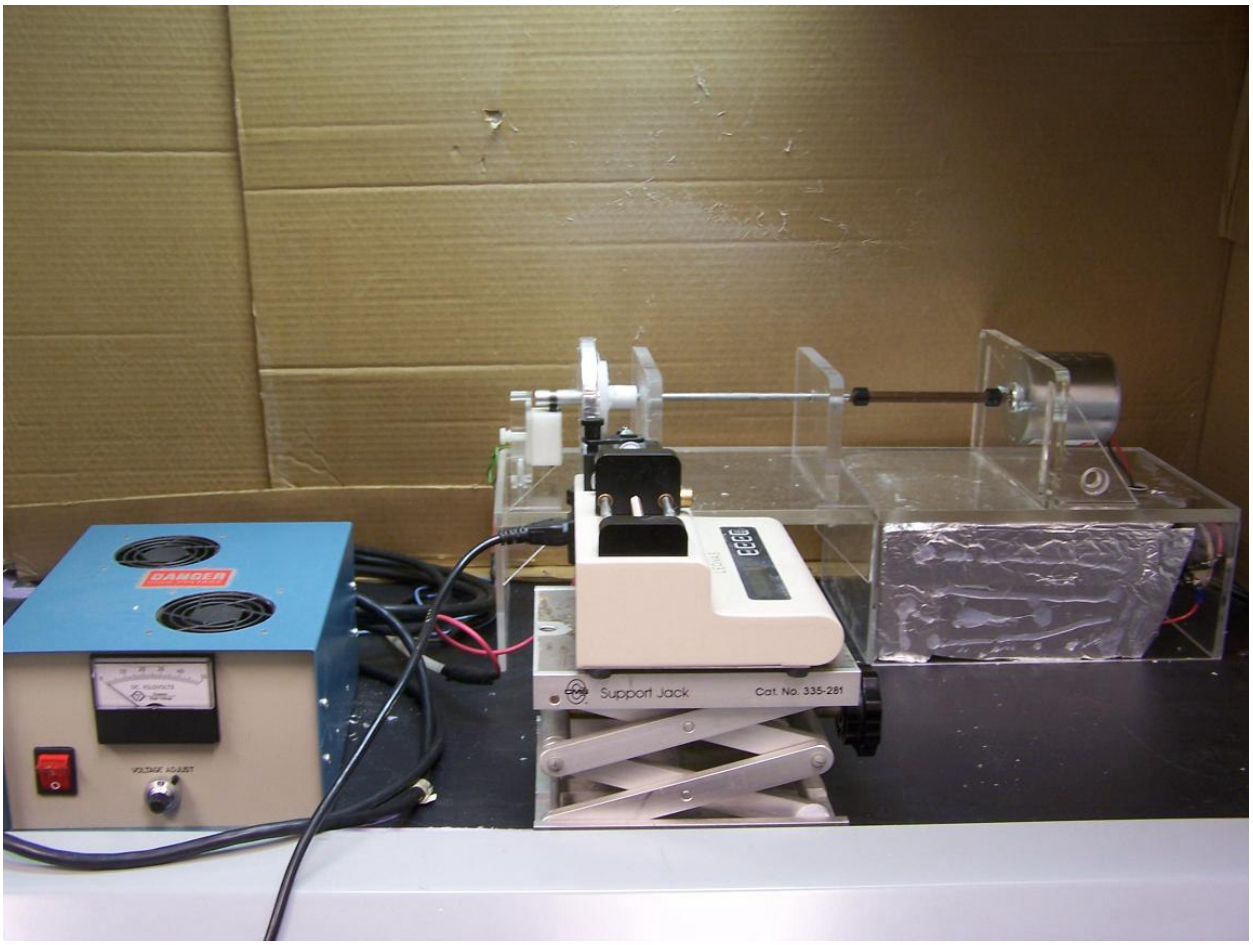

Figure 4.8 The Electrospinning Apparatus

4.1.2 Preliminary experiments

Electrospinning is a versatile spinning method. Both the spinning setup and the spinning processing parameters can be adjusted to obtain the desired products. This also means that small changes in the spinning setup or in the spinning parameters may result in dramatic modifications of the properties of the electrospun products, even when the same polymer type and solvent are used. Previous work reported in the literature provides some information on the effect of spinning parameters, but this has not been thoroughly studied. Therefore, for the electrospinning setup and the polymer to be used in this study, some preliminary studies to establish a baseline were necessary. This included the procedures to prepare the polymer solution, the practical ranges of the polymer solution concentration, the voltage, the feedrate, the distance from the needle tip to the collector, and the time required for the solvent to evaporate completely from fiber samples after formation.

I. Preparation of the polymer solution

An appropriate degree of molecular chain entanglement of the polymer solution is a critical factor in electrospinning to produce a continuous polymer jet from the tip of the needle to the collector (other than noncontinuous polymer beads). Viscosity is a parameter that reflects the degree of this entanglement. When the viscosity of the polymer solution is very low, polymer beads, instead of a continuous polymer jet that forms fibers, are produced. When the viscosity is too high, the polymer jet cannot be initiated before the polymer drop coagulates at the needle tip. In this study, the polymer concentration and the procedures of preparing the solution influenced the viscosity of the polymer solutions.

Preliminary studies showed that the viscosity of the PCL chloroform solution depended on the PCL concentration, the stirring time as well as the stirring speed of the polymer solution.

When the stirring speed was set to speed 2 using a NUOVA Stir Plate, the relationship of the solution viscosity and the stirring time is shown in Figure 4.9. It is clear that the viscosity increased with increasing PCL concentration as well as longer stirring time. The relationship between the increase in the viscosity and increased stirring time was especially evident at higher concentrations. For consistency, all the solutions were stirred for one hour at speed 2.

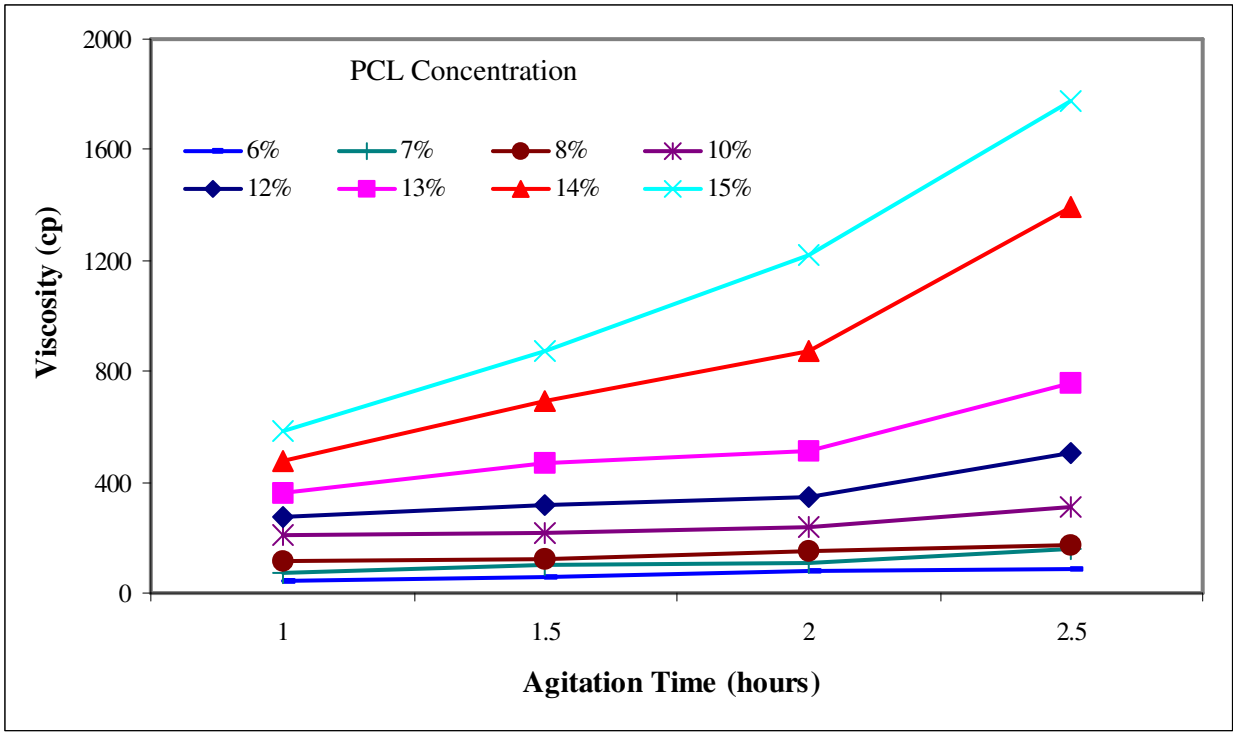

Figure 4.9 Influence of PCL Concentration and Stirring Time on Polymer Solution Viscosity

Since chloroform dissolves PCL, pure chloroform was used as the solvent to achieve a uniform PCL solution. However, when ampicillin was added, it did not dissolve in chloroform. Even though the ampicillin was in a fine powder form and the solution was agitated for one hour, the ampicillin particles were still too large when compared to the fiber diameter. Beads formed along the fibers due to the aggregated ampicillin particles, as shown in Figure 4.10. Therefore, to

improve fiber evenness, methanol was used to dissolve the ampicillin. Then the ampicillin methanol solution was mixed with the PCL chloroform solution. The ratio of methanol to chloroform was 1:9 in volume.

Figure 4.10 Picture of Beads Formed on Fibers under Optical Microscope at Magnification 500x

II. Spinning parameters

Polymer concentration

The viscosity of the polymer solution is crucial to the morphology of the fibers produced. The polymer concentration is a dominating factor that influences the solution viscosity when the molecular weights of the polymer and the solvent are given. The polymer concentration range in which continuous fibers could be produced was investigated.

For pure PCL chloroform solutions, when the concentration was less than 14%, no continuous uniform fibers could be made. When the concentration of the solution was larger than 17%, although continuous fibers could be produced initially, no continuous spinning jet could be maintained due to the rapid evaporation of the solvent, which resulted in a coagulated needle tip.

With the incorporation of ampicillin in the PCL polymer solution, the viscosity increased compared to the same concentration of pure PCL. Figure 4.11 shows the viscosity of PCL solutions with concentrations from 12% to 15% with and without the addition of 5% ampicillin. The increased viscosity with the addition of ampicillin resulted in a PCL concentration range, within which continuous fibers could be produced, that was lower than that without ampicillin. In addition, the conductivity of the polymer solution was improved when ampicillin was added because of the ampicillin salt ions. As a result, continuous uniform fibers could be produced with a PCL concentration as low as 12% and no higher than 16% when 2% or more ampicillin was included.

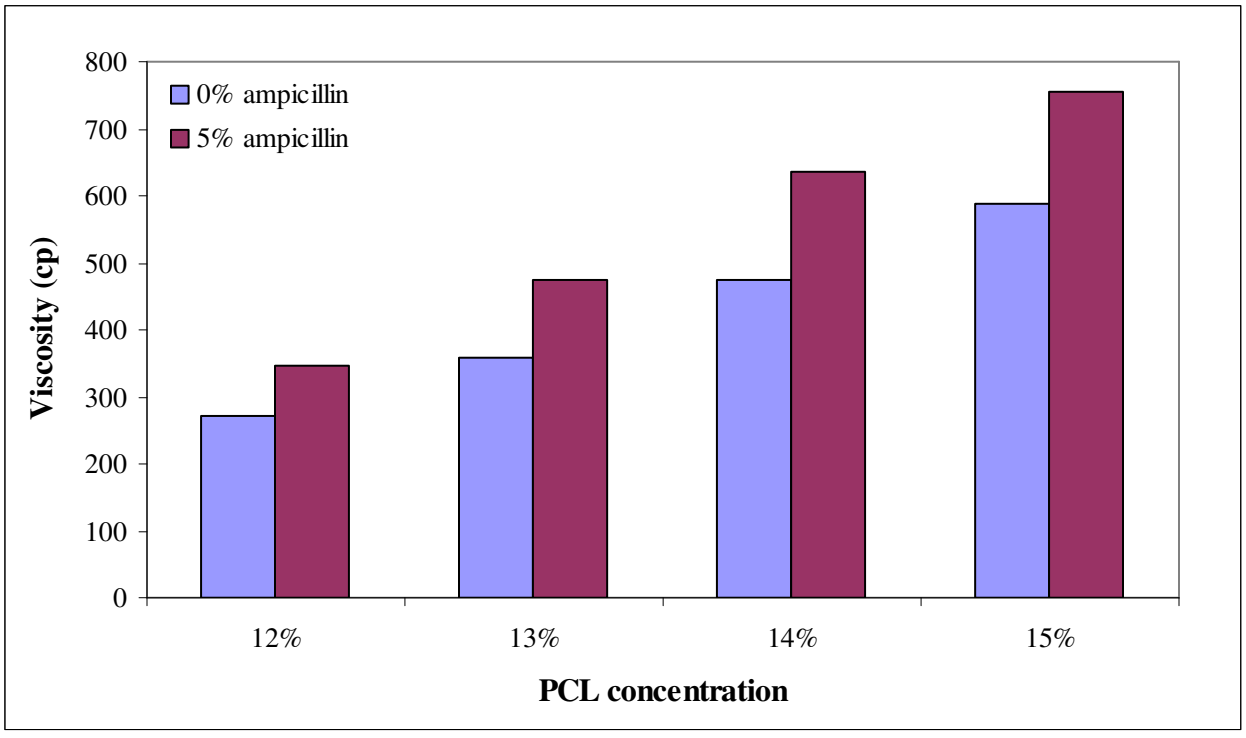

Figure 4.11 Influence of Ampicillin on Polymer Solution Viscosity

Voltage

The voltage applied to the electrospinning system determines the amount of charge accumulated on the polymer drop at the tip of the needle. When the repulsive force of the charges overcomes the surface tension of the polymer, a polymer jet is ejected. There is a minimum requirement for the voltage. In the early stages of this study, when the anode of the high voltage supply was connected to the collector, while the needle was grounded, the minimum voltage required to initiate and maintain a continuous polymer jet was approximately 20 kV. After the electrodes were reversed, i.e., the anode was applied to the needle and the collector was grounded, the minimum voltage dropped to approximately 6 kV. As for the maximum voltage, it should be much lower than the breakdown voltage of air for safety concerns. But experimental results showed that with an increase in voltage, the path of the polymer jet from the needle tip to the collector changed from a straight line to a curve; with an additional increase in the voltage, the polymer jet would not deposit on the collector. Therefore, the voltage applied in this study was in the range of 6 kV to 10 kV.

Feedrate

The feedrate range, within which continuous fibers could be produced, was from several milliliters to several tenths of a millimeter per hour. With a higher feedrate, it was common to obtain samples in which the fibers stuck together. This is the result of the increasing fiber diameter with the increasing feedrate. The time for the solvent to evaporate to form solidified fibers became longer when the fiber diameter increased. Without hardening of the fiber surface, fibers fused together when they were deposited on the collector and formed fiber webs instead of individual fibers. Fibers spun with a feedrate of 5 ml/h (PCL concentration: 15%; Distance: 8 cm; voltage: 6 kV) are shown in Figure 4.12. The adjacent fibers are stuck together and with or

without the visible fibers' original boundaries. The feedrate at which most fiber samples produced in this study was less than 1 ml/h.

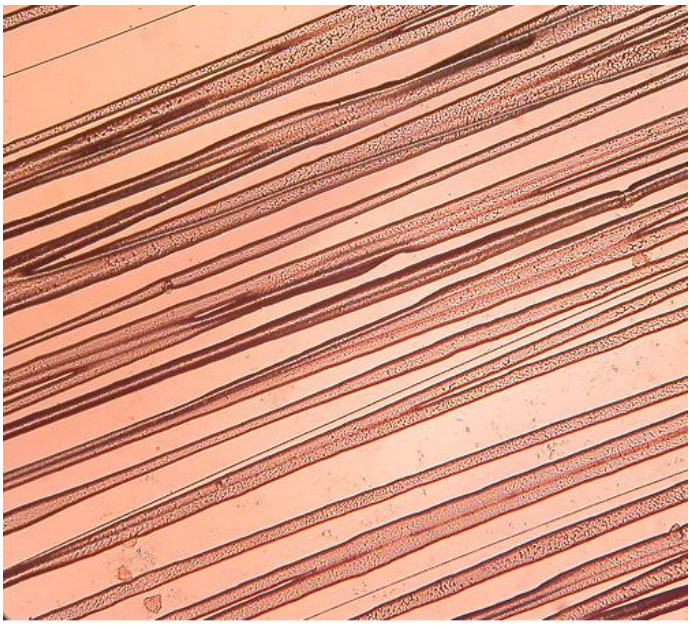

Figure 4.12 A Fiber Sample Showing Fibers Fused Together under Optical Microscope at Magnification 500x

Distance

The distance from the needle tip to the collector influenced both the flying time of the polymer jet and the strength of the electric field. When the distance was increased, the flying time was increased, and the electric force was weakened. The influences of these two factors on the polymer jet were opposite. To balance these two factors, the distance was set to 5 cm to 12 cm in this study.

III. Detection of residue solvent in fiber samples

All fiber samples were left in the fume hood with ventilation for a minimum of 12 hours before other tests were performed. Residual solvent was detected using TGA. Less than 2% weight loss was detected from 20°C to 100°C. At least part of the weight loss was due to the

evaporation of the moisture in fibers. The boiling points for chloroform and methanol were 62°C and 65°C, respectively. The results gave sufficient evidence to expect that most of the solvent, if not all, had evaporated within 12 hours.

4.2 Influence of the Spinning Parameters on Fiber Properties

The spinning parameters and polymer solution properties in electrospinning can be adjusted to obtain fibers with various properties. In this section, the influence of adjustable parameters on fiber properties was studied. Fiber diameter and fiber alignment were the fiber properties of interest. The adjustable parameters included polymer concentration, feedrate (FR), voltage (V), distance (D), and the addition of ampicillin.

4.2.1 Fiber diameter

The fiber diameters produced from pure PCL and PCL plus 5% ampicillin under various spinning conditions are shown in Table 4.1 and Table 4.2, respectively. The polymer concentrations used were 14% and 15%. The feedrates were 0.3 ml/h and 0.4 ml/h, and the distances were 5 cm and 8 cm. The voltages applied to the needle were 7 kV, 8 kV, and 9 kV. Not all the combinations of these parameters were practical for producing continuous fibers. However, continuous fibers could be produced with all the combinations listed in the tables. The diameter of fibers spun under all the conditions listed here was between 1.59 μm and 0.33 μm. The influence of each spinning parameter is discussed.

I. Polymer concentration

Figure 4.13 and Figure 4.14 show the diameters of fibers produced with different polymer concentrations and with and without the incorporation of ampicillin. Fibers spun with higher polymer concentrations had larger diameters, as expected. The reasons for this are three-fold. First, the polymer solution with the higher polymer concentration had a higher viscosity due

to the increased entanglement of the polymer molecular chains. The increased entanglement resulted in greater resistance to stretching from the electric force, so the polymer jet was less drawn when flying from the needle tip to the collector, resulting in a larger fiber diameter. When the entanglement force exceeded the electric stretching force, no polymer jet could even be initiated. Therefore, the polymer concentration should be under a certain value.

The second reason for the larger polymer concentration resulting in a larger fiber diameter was that the faster solidification of the polymer jet made the stretching more difficult. The solvent in the solution served as a lubricant when the polymer jet was being drawn. The polymer solution solidified with the evaporation of solvent. The relative amount of solvent to the polymer in a given volume of polymer solution decreased with the increased polymer concentration. Therefore, with the same solvent evaporation rate, higher-concentration polymer solutions solidified faster than lower-concentration polymer solutions.

Third, the higher surface tension of a larger-concentration polymer solution contributed to the increase in the diameter. The polymer jet was ejected with an initial charge accumulating stage, during which the polymer drop at the needle tip changed its shape from a roughly round shape to a cone shape, which is referred to as a Taylor cone, as shown in Figure 4.15. When the repulsive force of the charges overcame the surface tension, a polymer jet was ejected. The amount of ejected polymer affected the fiber diameter. The larger the amount of polymer being ejected, the larger the diameter of the resulting fibers. Compared to a lower surface tension solution, the polymer jet of a solution with higher surface tension was larger. This could be explained by simulating a scenario of pulling a rod out of a polymer solution, as shown in Figure 4.16. Larger amounts of solution were pulled from the solution surface by the rod from a solution with a higher surface tension than from a solution with lower surface tension.

Although all fibers spun from 14% PCL had smaller diameters than those spun with 15% PCL, the Wilcoxon Signed-Ranks test results showed that the difference was not statistically significant. The p value was 0.0595 (>0.05). The SAS program and output are shown in Appendix A.

Table 4.1 *Diameter of Fibers Spun with Pure PCL

Polymer concentration	Spinning conditions			Diameter	
	FR[a] (ml/h)	D[b] (cm)	V[c] (kV)	Mean (μm)	Standard deviation
14%	0.3	8	7	0.53	0.26
			8	0.43	0.16
			9	0.33	0.25
		5	7	0.69	0.34
			8	0.52	0.25
			9	0.48	0.19
	0.4	8	7	0.79	0.17
			8	0.60	0.16
			9	0.50	0.15
15%	0.3	8	7	0.64	0.31
			8	0.47	0.17
			9	0.37	0.12
		5	7	0.79	0.18
			8	0.63	0.20
			9	0.50	0.16
	0.4	8	7	1.59	1.79
			8	1.11	0.36
			9	0.55	0.18

Note: [a]FR = Feedrate; [b]D = Distance; and [c]V = voltage

*The means and standard deviations were calculated based on 30 measurements.

Table 4.2 *Diameter of Fibers Spun with PCL Plus 5% Ampicillin

Polymer concentration	Spinning conditions			Diameter	
	FR[a] (ml/h)	D[b] (cm)	V[c] (kV)	Mean (μm)	Standard deviation
14%	0.3	8	7	0.47	0.20
			8	0.40	0.07
			9	0.33	0.12
		5	7	0.52	0.20
			8	0.46	0.14
			9	0.40	0.08
	0.4	8	7	0.60	0.12
			8	0.51	0.13
			9	0.40	0.07
15%	0.3	8	7	0.56	0.20
			8	0.44	0.13
			9	0.35	0.12
		5	7	0.61	0.20
			8	0.56	0.22
			9	0.53	0.14
	0.4	8	7	0.76	0.14
			8	0.60	0.12
			9	0.44	0.17

Note: [a]FR = Feedrate; [b]D = Distance; and [c]V = voltage

*The means and standard deviations were calculated based on 30 measurements.

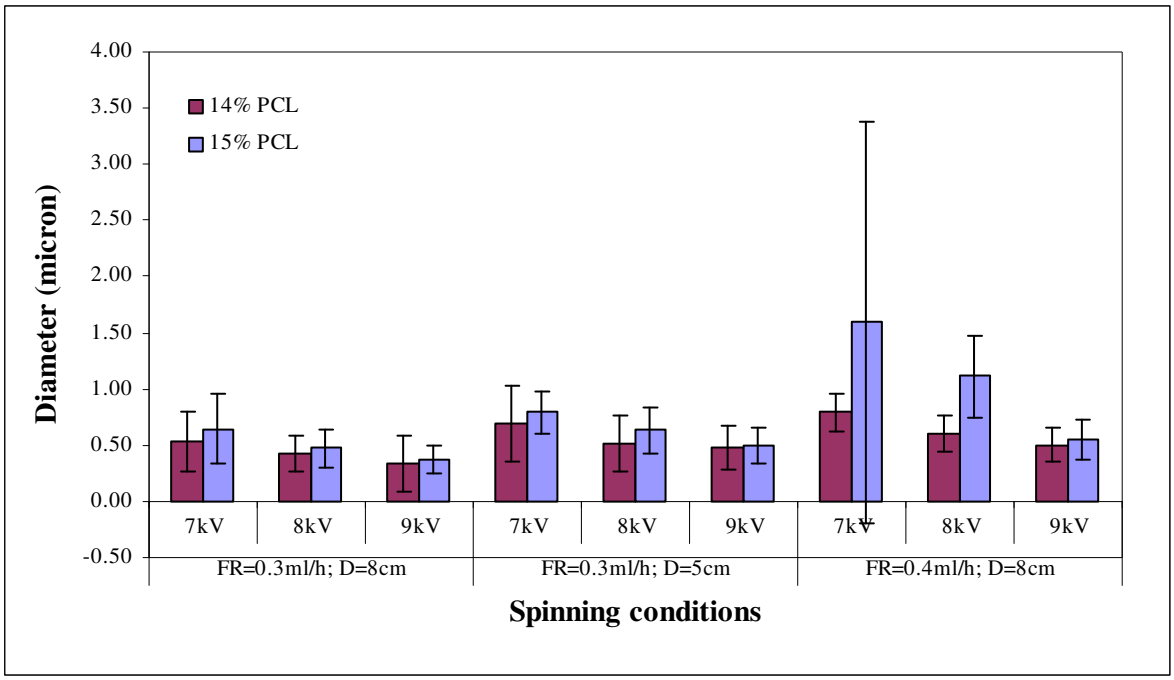

Note: FR = Feedrate and D = Distance;
The means and standard deviations were calculated based on 30 measurements.

Figure 4.13 Influence of Polymer Concentration on Fiber Diameter (pure PCL)

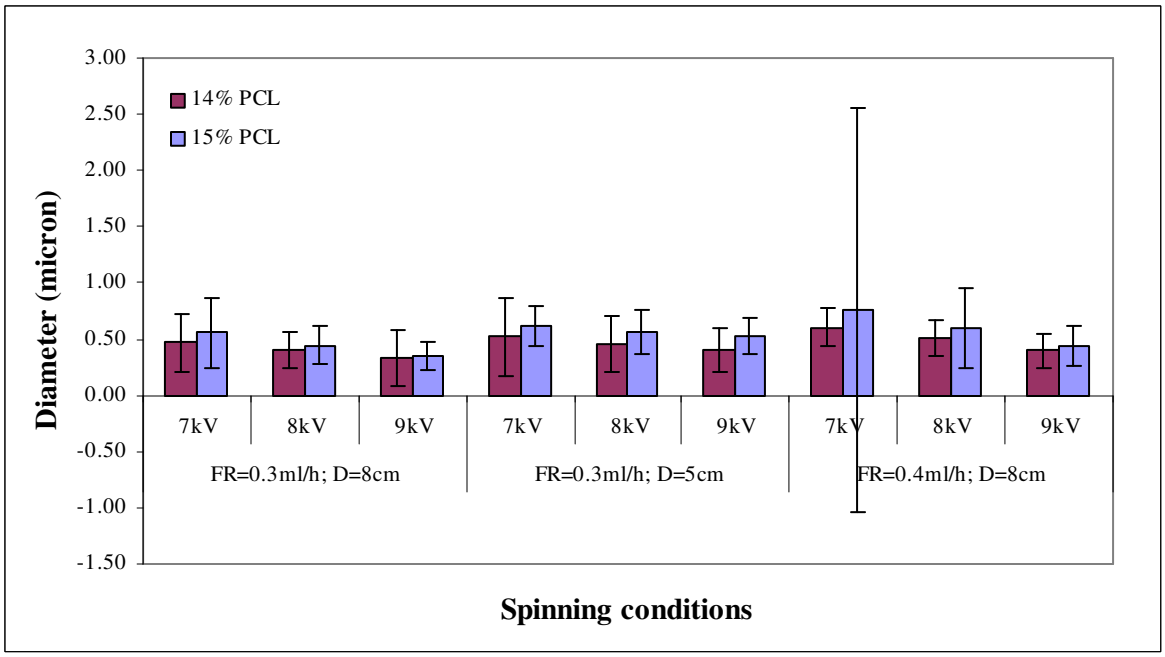

Note: FR = Feedrate and D = Distance;
The means and standard deviations were calculated based on 30 measurements.

Figure 4.14 Influence of Polymer Concentration on Fiber Diameter (5% ampicillin)

Figure 4.15 Cone Shape (Taylor Cone) of a Polymer Drop at the Tip of the Needle

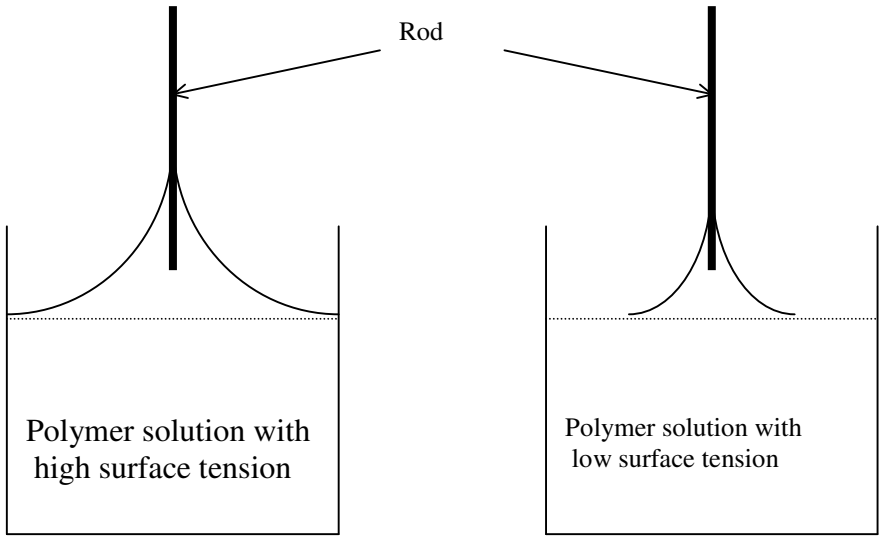

Figure 4.16 Rod-pulling Experiment to Study the Influence of Polymer Surface Tension on the Amount of Polymer Being Taken out

II. Feedrate

Figure 4.17 shows the fiber diameters produced when different feedrates were used in spinning. The feedrate determines the amount of solution that is available for the electrospinning jet at the tip of the needle. It was apparent that the higher feedrate yielded larger fiber diameters. When a higher feedrate was used, there was more polymer available at the tip of the needle than when a smaller feedrate was used. Therefore, there was more polymer carried by the polymer jet, resulting in fibers with larger diameters being produced. Figure 4.18 simulates the scenario using the rod-pulling experiment. A greater amount of polymer is pulled out from a larger solution pool than from a small pool. The difference in fiber diameter, as a result of spinning with two different feedrates, 0.3 ml/h and 0.4 ml/h, was significant with a *p* value of 0.0060. The SAS program and output are shown in Appendix A.

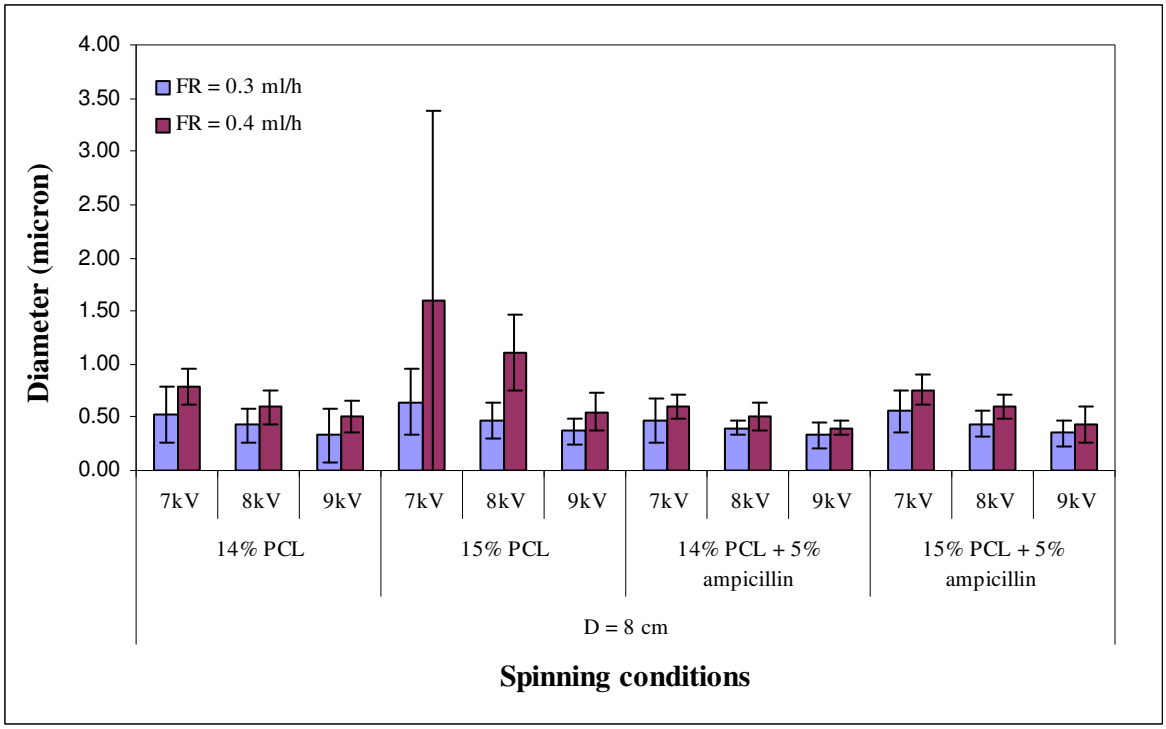

Note: FR = Feedrate and D = Distance;
The means and standard deviations were calculated based on 30 measurements.

Figure 4.17 Influence of Feedrate on Fiber Diameter

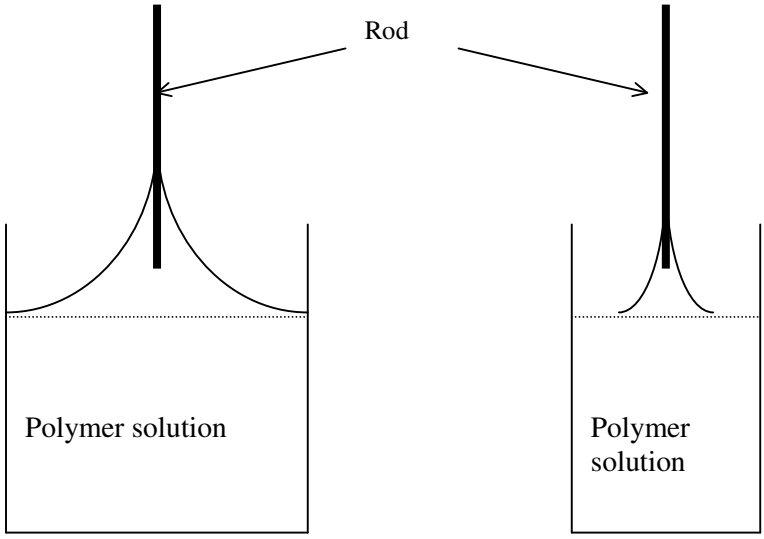

Figure 4.18 Rod-pulling Experiment to Study the Influence of the Amount of Available Polymer on the Amount of Polymer Being Taken out

III. Voltage

The electric potential difference between the needle and the fiber collector produces an electric field, the intensity of which is determined by the voltage applied when the distance is given. The intensity of the electric field increases as the voltage increases. Therefore, the higher the voltage, the larger the electric force applied to the polymer jet. Not considering the frictional force of air on the polymer jet, its acceleration is directly proportional to the voltage. Higher voltage produces larger acceleration. The acceleration causes the stretching of the polymer jet. Hence, theoretically the diameter of fibers decreases when the voltage is raised, which was confirmed by this study. The diameter of fibers spun under various conditions decreased when the voltage increased from 7 kV to 8 kV and then to 9 kV in the cases of pure PCL solution and PCL plus 5% ampicillin (Figure 4.19). Statistically, the differences in fiber diameters between 7 kV and 8 kV, between 7kV and 9kV, and between 8kV and 9kV were all significant with *p*

values of 0.0241, 0.0003, and 0.0241, respectively. The SAS programs and outputs are shown in Appendix A.

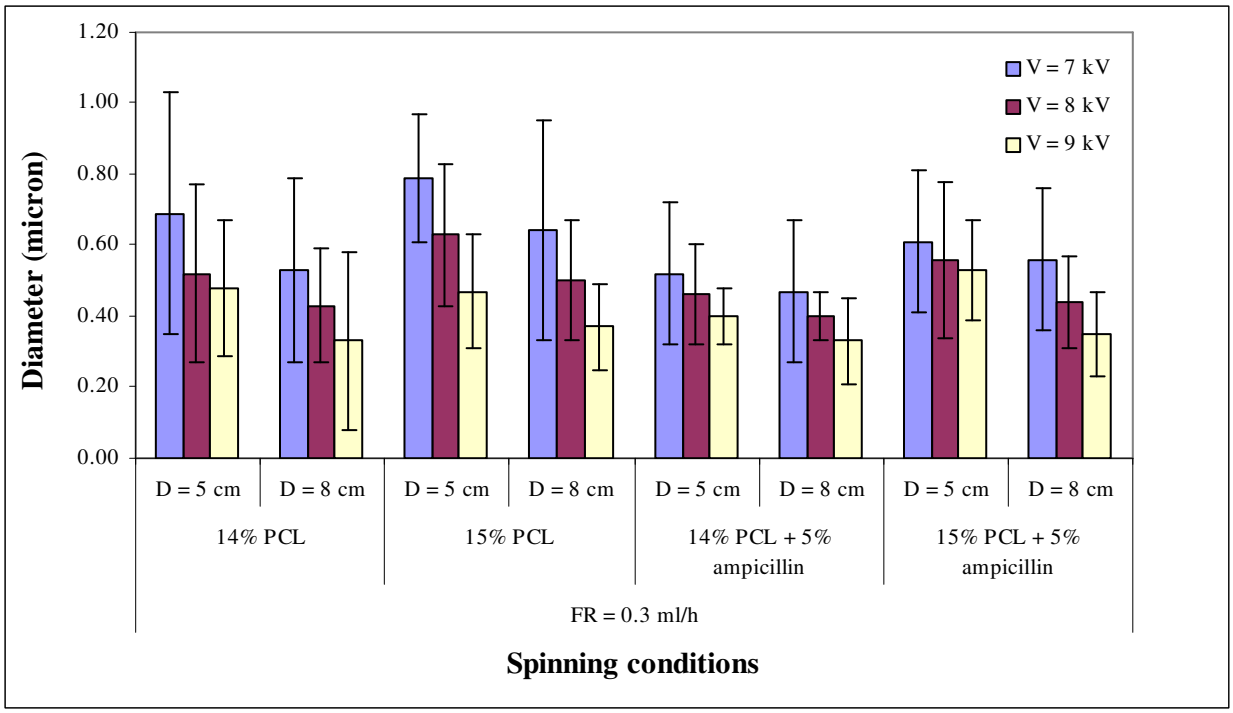

Note: FR = Feedrate, V = Voltage and D = Distance;
The means and standard deviations were calculated based on 30 measurements.

Figure 4.19 Influence of Voltage on Fiber Diameter

IV. Distance

The influence of the distance from the needle tip to the collector on fiber diameter is shown in Figure 4.20. Fiber diameter decreased when the distance became larger. The effect of a greater distance on fiber diameter was two-fold. First, with a greater distance, more time was allowed for the polymer jet to be stretched as longer flying time from the needle tip to the collector was needed. Second, with the same applied voltage, the electric field strength was reduced with greater distance, leading to smaller acceleration of the polymer jet. These two effects counteracted each other. The decreased fiber diameter corresponding to the increased

distance indicated that the effect of more stretch time dominated over the effect of weakened electric field strength. This result was in accordance with the study by Rutledge et al. with a glycerol solution [145]. Figure 4.21 shows the shape of the glycerol jets near the needle tip at different electric field strengths. The radius of the jet was thinned with the intensification of the electric field. However, after the jet proceeded further from the needle tip, the diameters of the three jets became similar. According to Rutledge et al., the diameter of the polymer jet that distance from the Taylor cone followed the principle of

$$r \propto z^{-1/4}$$

where r was the radius of the jet and z was the distance from the needle tip [146]. Hence, the fiber diameter increased with distance.

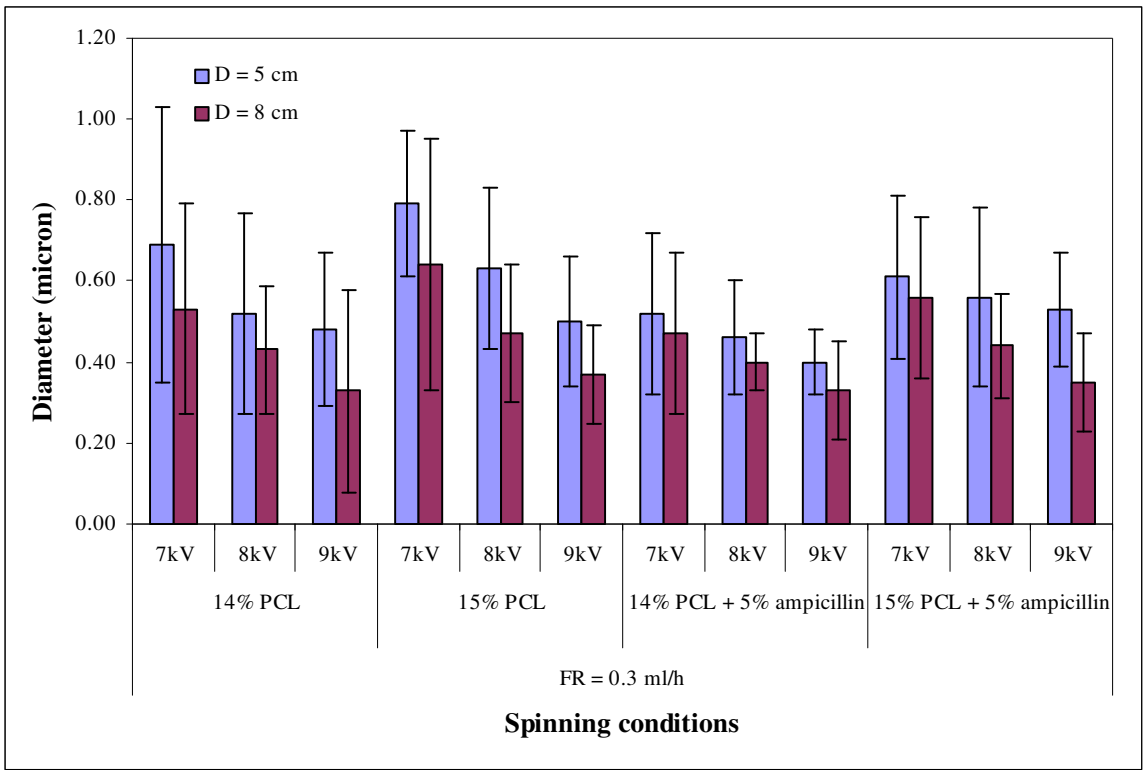

Note: FR = Feedrate and D = Distance;
The means and standard deviations were calculated based on 30 measurements.

Figure 4.20 Influence of Distance on Fiber Diameter

The Wilcoxon Signed-Ranks test results indicated that the diameter difference between the two different distances was significant with a *p* value of 0.0178. The SAS program and output are shown in Appendix A.

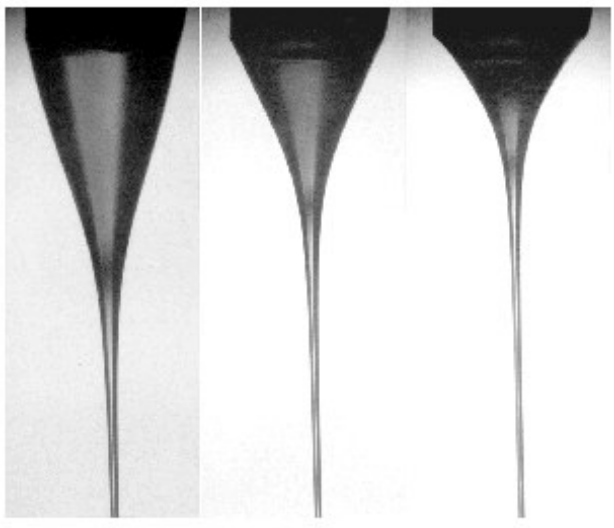

Figure 4.21 Glycerol Jets at 0.5 ml/min. Left to right: 3.67 kV/cm, 4.33 kV/cm, 5. 0 kV/cm [145]

V. Addition of ampicillin

Figure 4.22 and Figure 4.23 show the diameters of fibers produced with and without ampicillin. The addition of ampicillin sodium salt to the polymer solution resulted in reduced fiber diameters. The viscosity of the polymer solution with 5% ampicillin included was higher than the polymer solution without ampicillin. Thus, it was expected that the diameter of fibers containing ampicillin would be larger than those without. However, in this study the fibers containing 5% ampicillin had smaller diameters than those without ampicillin when all of the other spinning conditions remained the same. This is thought to be due to the ionic nature of the ampicillin salt. The ions in the solution contributed to the charge building at the tip of the needle,

which magnified the effect of the electric field. Furthermore, the conductivity of the solution improved with the salt addition. Both factors contributed to the resulting smaller diameters. The Wilcoxon Signed-Ranks test results showed that the difference was not significant with a *p* value of 0.0964. The SAS program and output are shown in Appendix A. Figure 4.24 shows the diameters of fibers produced with 14% PCL and different concentrations of ampicillin. These results further illustrate the effect of ampicillin resulting in decreasing fiber diameters. Under the same spinning conditions, the higher the concentration of ampicillin, the smaller the fiber diameters.

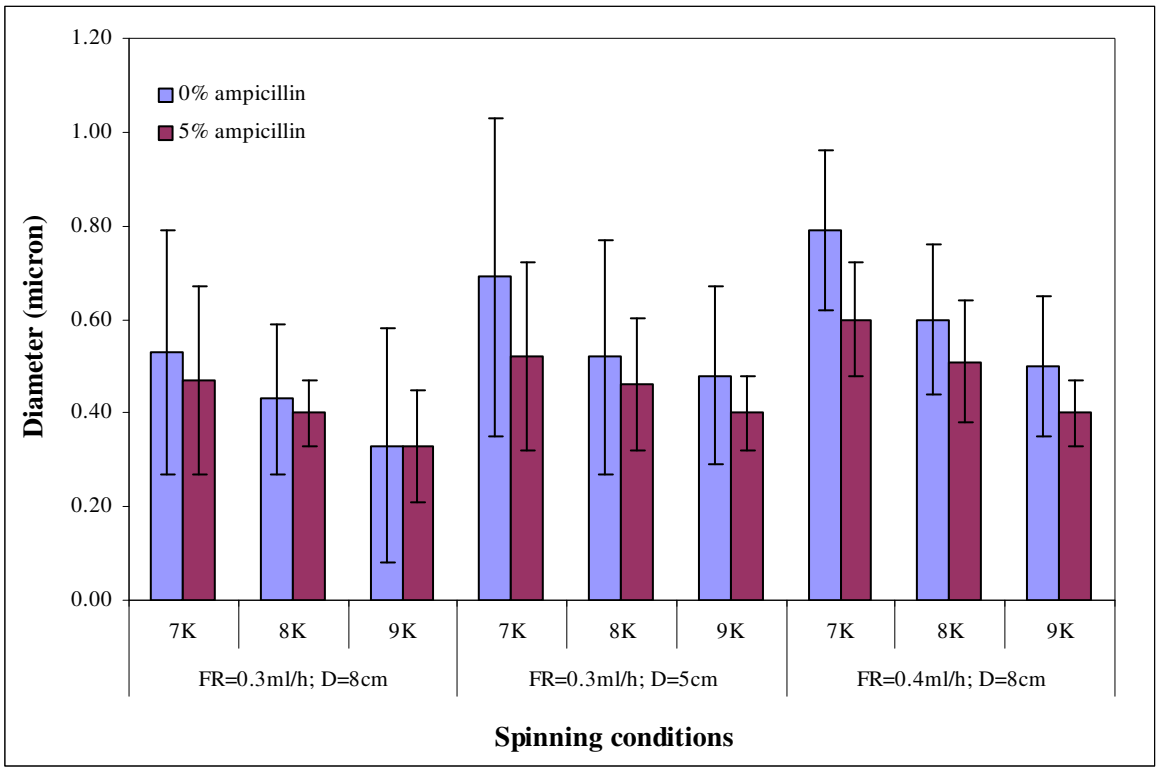

Note: FR = Feedrate and D = Distance;
The means and standard deviations were calculated based on 30 measurements.

Figure 4.22 Influence of Ampicillin on Fiber Diameter (14% PCL)

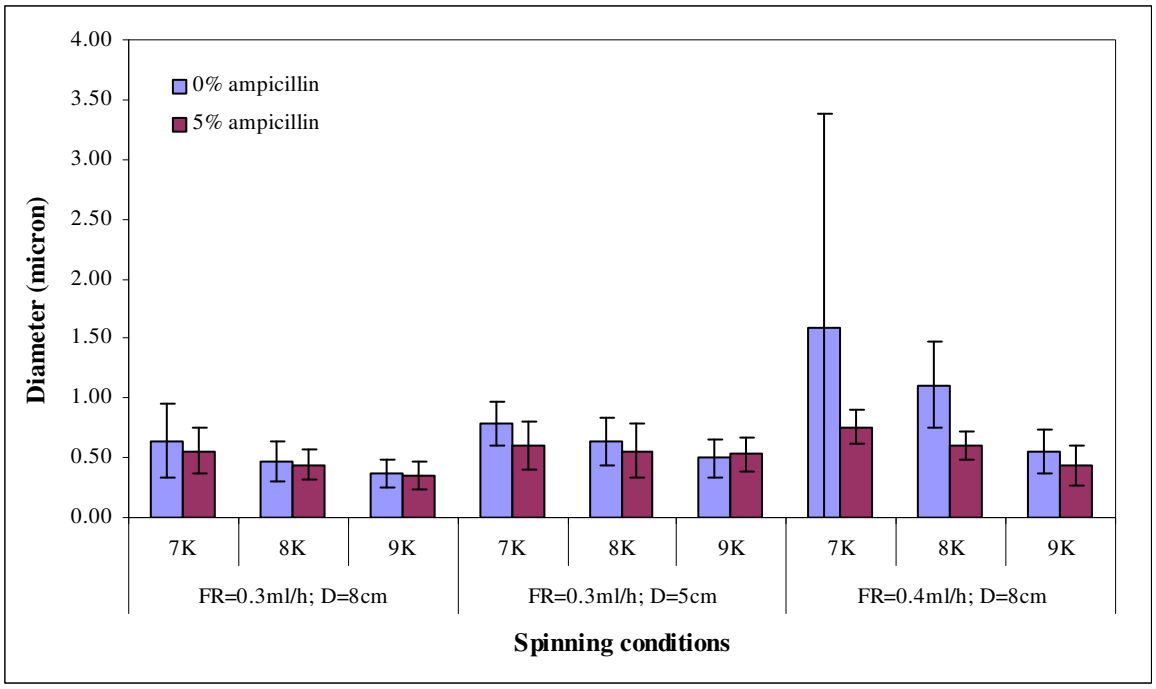

Note: FR = Feedrate and D = Distance;
The means and standard deviations were calculated based on 30 measurements.

Figure 4.23 Influence of Ampicillin on Fiber Diameter (15% PCL)

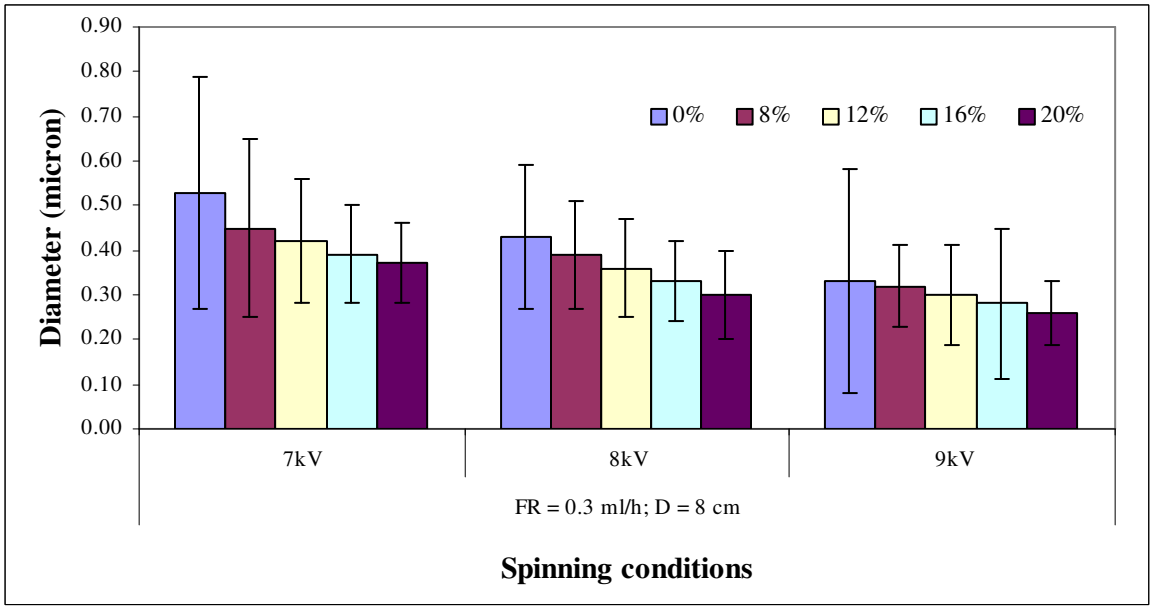

Note: FR = Feedrate and D = Distance;
The means and standard deviations were calculated based on 30 measurements.

Figure 4.24 Diameter of Fibers Spun with 14% PCL plus Various Concentrations of Ampicillin

4.2.2 Alignment

The good alignment of continuous fibers on the collector indicated a correct balance of the winding speed of the collector and the depositing speed of the polymer jet. The velocity at which the polymer jet deposited on the collector was affected by the spinning parameters and polymer solution properties, including the voltage, distance, feedrate, and ions in the polymer solution. To obtain good fiber alignment, the winding speed of the collector needed to be no lower than the velocity of the polymer jet at the point of reaching the collector. Two fiber samples spun with the same conditions but collected at different rotating speeds are presented in Figure 4.25. The collection speed of 1500 rpm used in producing samples was high enough to collect well-aligned fibers under all spinning conditions. Figures 4.26 – 4.29 are SEM images of electrospun PCL with different PCL and ampicillin concentrations and various voltages. For all fibers shown in these figures (4.26 – 4.29), the spinning parameters were a distance of 8 cm and a feedrate of 0.3 ml/h.

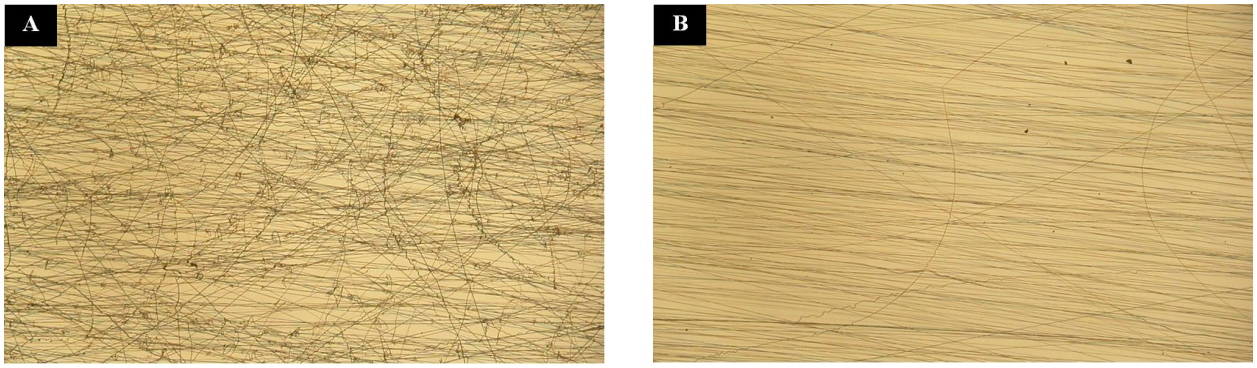

Figure 4.25 Influence of Rotating Speed of the Collector on Fiber Alignment (A) Fibers Collected with Lower Collector Rotating Speed; (B) Fibers Collected with Higher Collector Rotating Speed (Pictures taken under optical microscope at magnification 100x.)

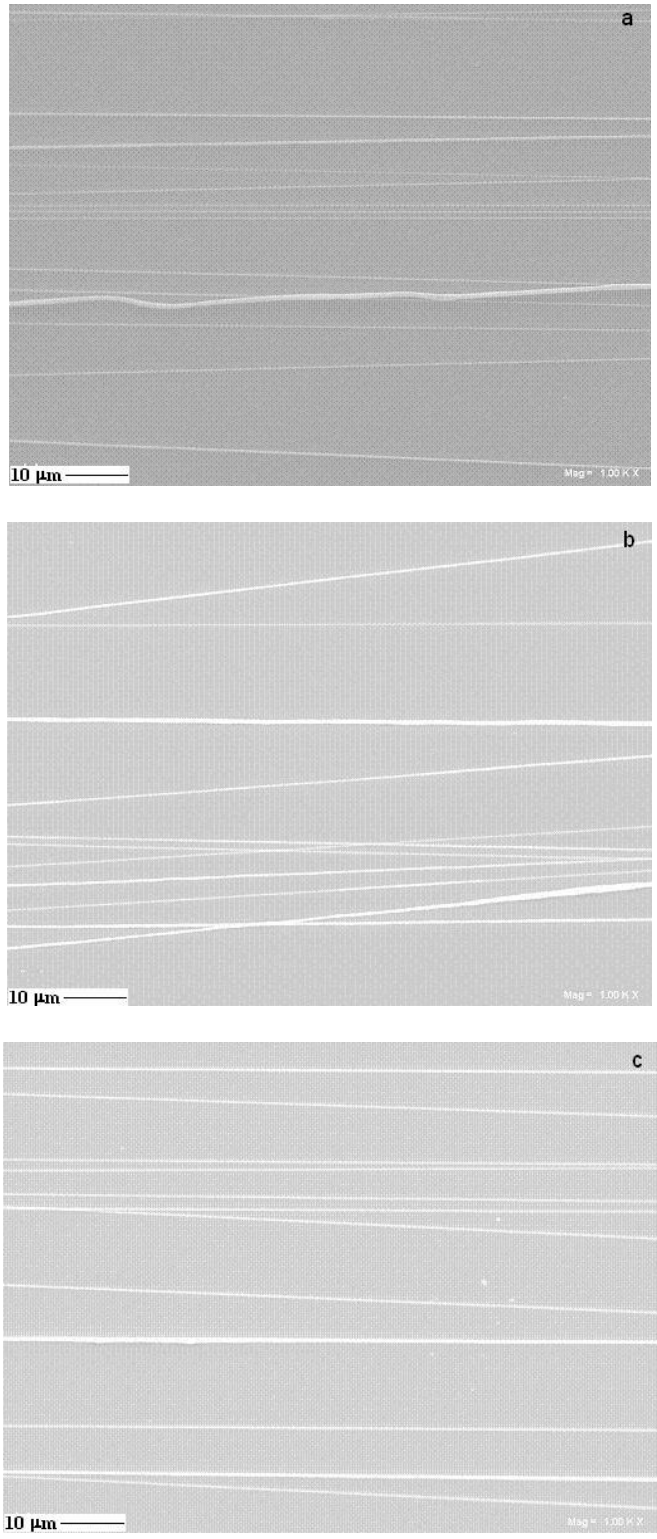

Figure 4.26 Images of Fibers Spun with 14% PCL under Various Voltages (a) 7 kV; (b) 8 kV; and (c) 9 kV

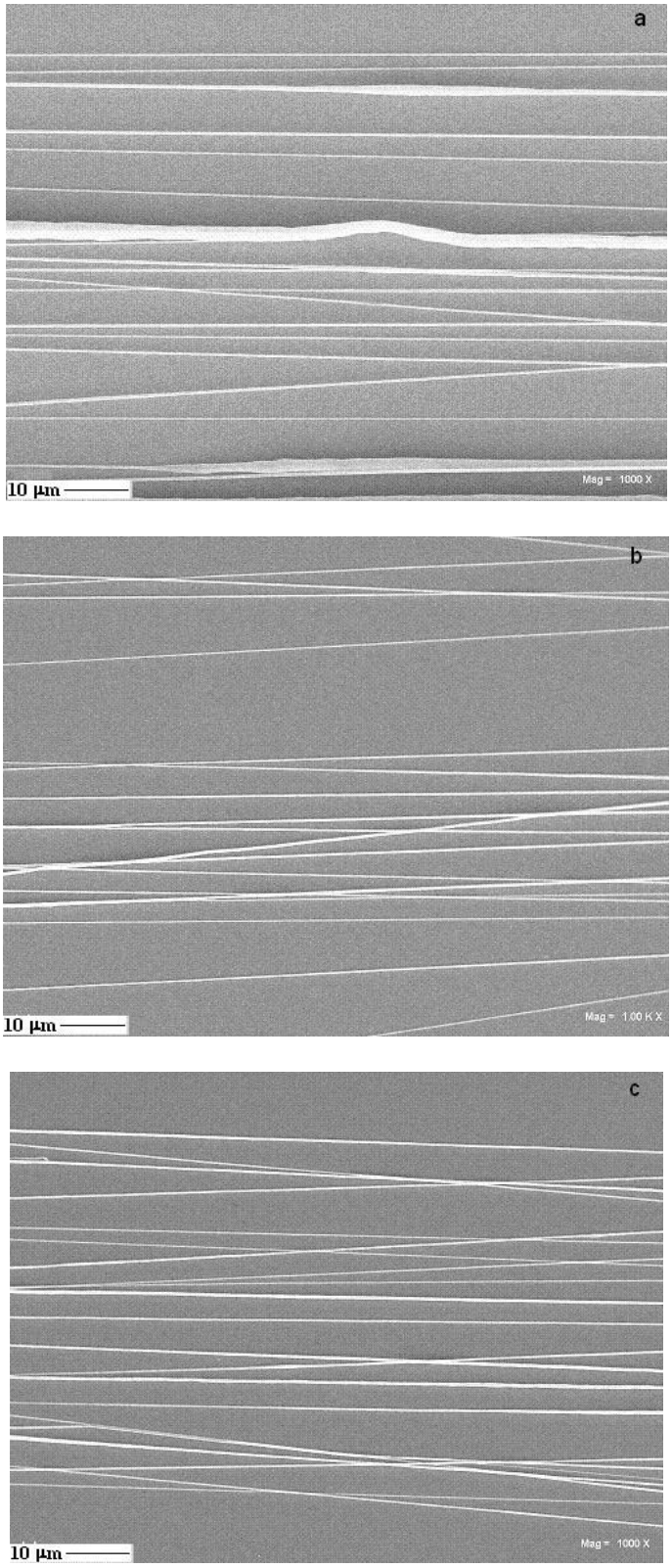

Figure 4.27 Images of Fibers Spun with 15% PCL under Various Voltages (a) 7 kV; (b) 8 kV; and (c) 9 kV

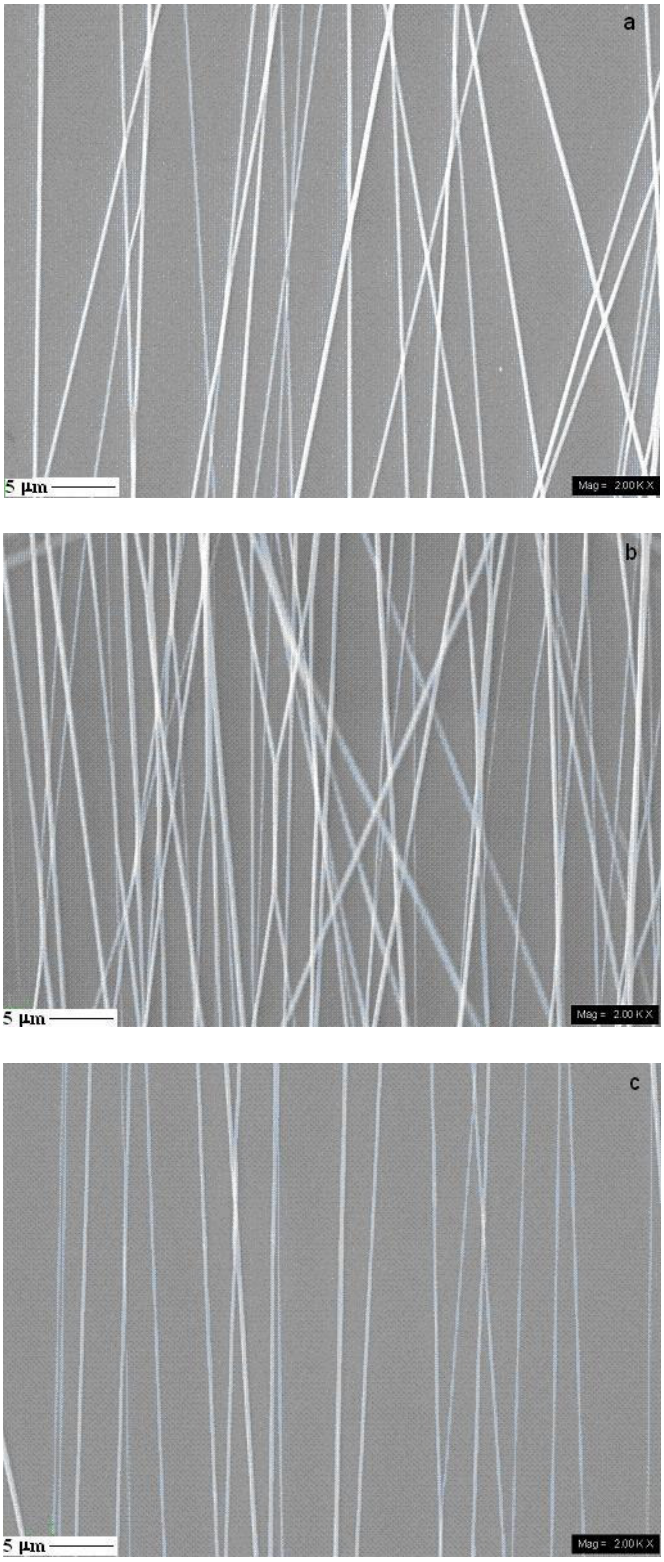

Figure 4.28 Images of Fibers Spun with Various PCL Concentrations plus 5% Ampicillin (a) 12%; (b) 13%; and (C) 14%

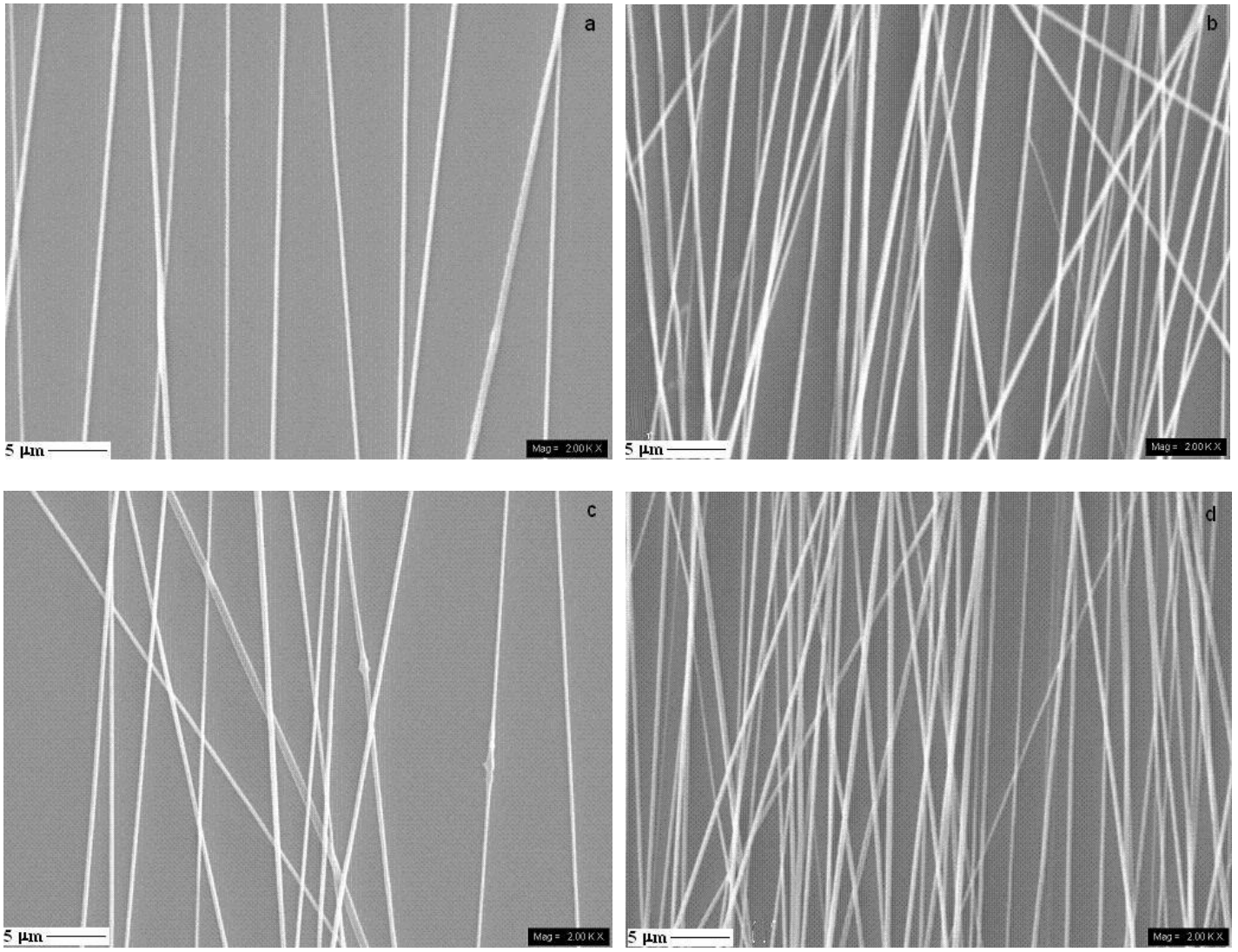

Figure 4.29 Images of Fibers Spun with 14% PCL and Various Ampicillin Concentrations (a) 8%; (b) 12%; (c) 16%; and (d) 20%

4.3 Physical and Mechanical Properties of Fibers

The percentage of crystallinity and tensile properties of the electrospun PCL fibers with and without ampicillin were evaluated as they are important physical and mechanical properties. Results are presented in this section.

4.3.1 Crystallinity of fibers

Two typical DSC curves of 14% PCL electrospun fibers are shown in Figure 4.30. Figure 4.30(a) represents PCL fibers without ampicillin incorporated, and 4.30(b) was for fibers spun with 20% ampicillin. Two endothermic peaks were observed at –60°C and 60°C, corresponding to the glass transition temperature and melting point of PCL, respectively. The endothermic peaks at the melting point indicated there were crystallites in the fibers. All practical textile fibers are semi-crystalline in structure and have both crystalline and amorphous regions, as shown in Figure 4.31. In the crystalline region, molecular chains are parallel and compacted, and form regular crystallites, which are connected by loosely entangled chains forming amorphous regions. The semi-crystalline structure explains some of the physical and mechanical properties of fibers. For example, the glass transition temperature is attributed to the transition of amorphous regions from the glass state to the rubbery state. The melting point is attributed to the transfer of crystalline regions from an orderly to a disorderly arrangement. Regarding mechanical properties, the elongation of fibers is mainly due to the stretching of the amorphous region. And the crystalline regions contribute more to the fiber strength than the amorphous regions do.

By measuring the heat absorbed at the melting point, the crystallinity of fibers can be calculated (the value of ΔH_f of PCL was 139.5 J/g [143, 144]). Table 4.3 shows the percentage of crystallinity of 14% PCL fibers spun with and without 5% ampicillin under various spinning

conditions. The percentage of crystallinity of 14% PCL fibers was all at approximately 40% or higher under the spinning conditions studied here. With ampicillin, the percentage of crystalline regions was reduced.

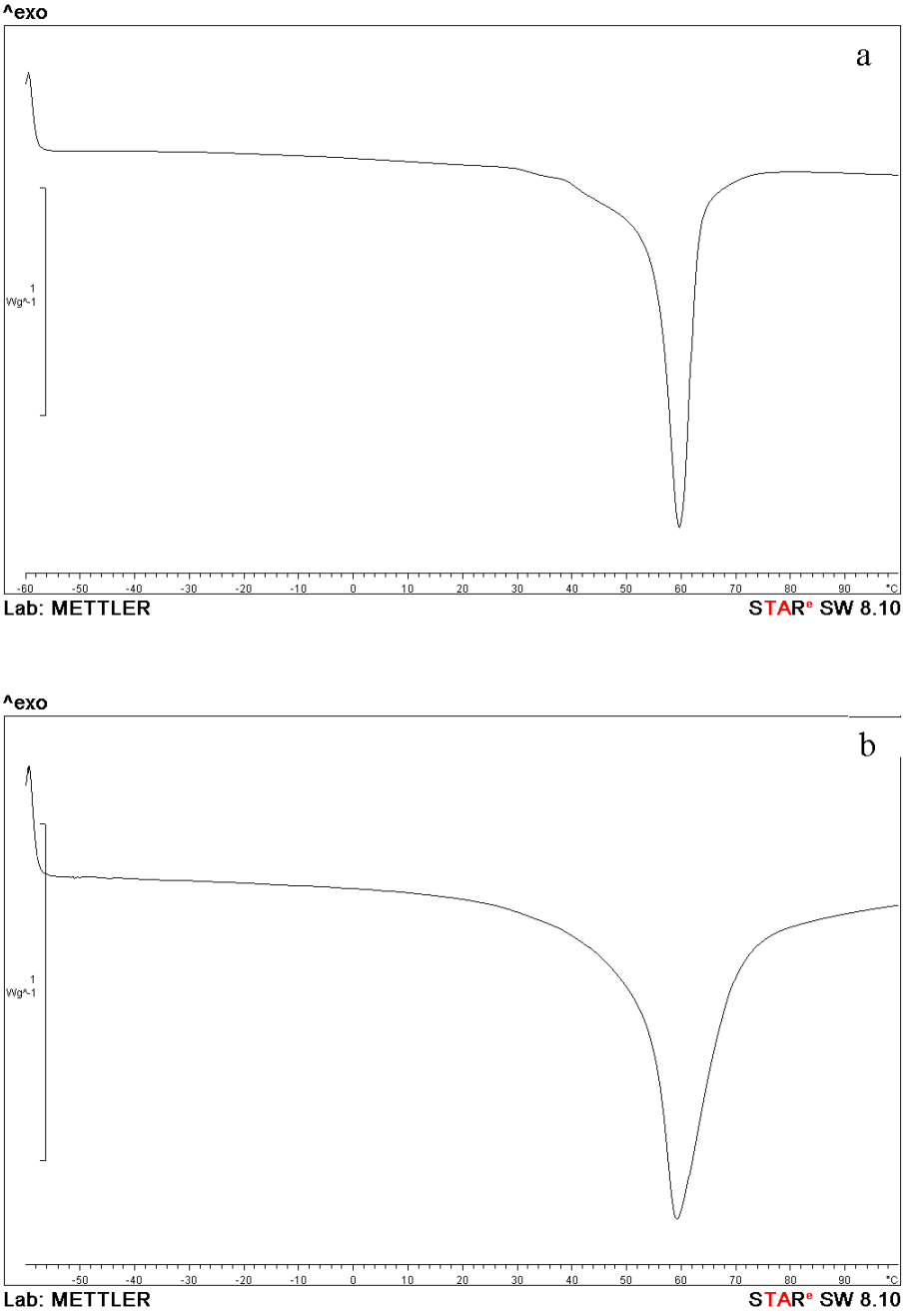

Figure 4.30 DSC Curves of Electrospun Fibers (a) Pure PCL; (b) PCL with 20% Ampicillin

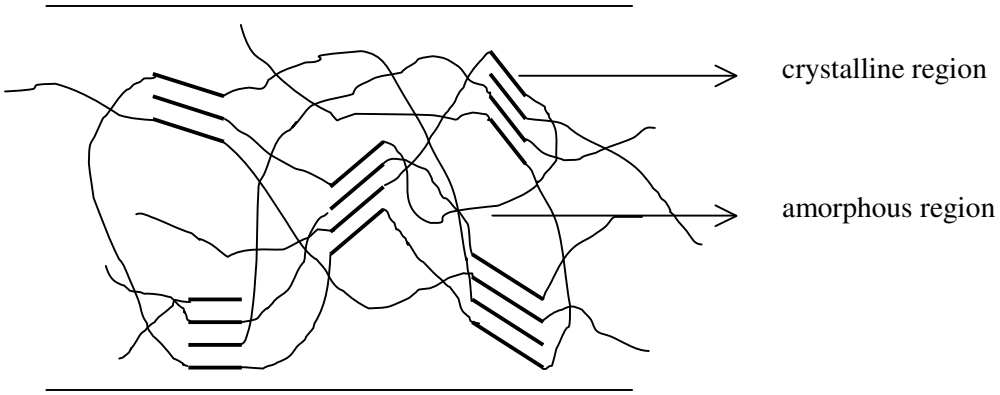

Figure 4.31 Schematic of Semi-crystalline Structure of Fibers

Table 4.3 Percentage of Crystallinity of Fibers Spun with and without Ampicillin

Spinning Conditions			C_{rystal}%	
FR[a] (ml/h)	**D[b] (cm)**	**V[c] (kV)**	**14% PCL**	**14% PCL + 5% Ampicillin**
0.3	8	7	43.21	28.11
		8	47.14	35.00
		9	49.52	41.76
	5	7	39.54	12.66
		8	42.65	14.07
		9	46.44	27.08
0.4	8	7	44.71	34.84
		8	47.98	37.12
		9	56.27	50.43

Note: [a]FR = Feedrate; [b]D = Distance; and [c]V = voltage

From a completely amorphous polymer solution to a semi-crystalline solid fiber, the formation of a crystallite is based on molecular chain movement. For electrospun fibers, the formation of a crystallite begins at the point when the polymer jet is initiated and ends when the solvent has completely evaporated. Therefore, during this period of time, any factor that influences the movement of the molecular chains affects the crystallinity of the fibers. The results indicated that all factors studied here (feedrate, distance, voltage, and the addition of

ampicillin) had some effects on the crystallinity of the fibers. For easy comparison, the data are shown in a bar graph (Figure 4.32). The percentage of crystallinity increased with the increasing feedrate from 0.3 ml/h to 0.4 ml/h, increasing voltage from 7 kV to 8 kV to 9 kV, and increasing distance from 5 cm to 8 cm.

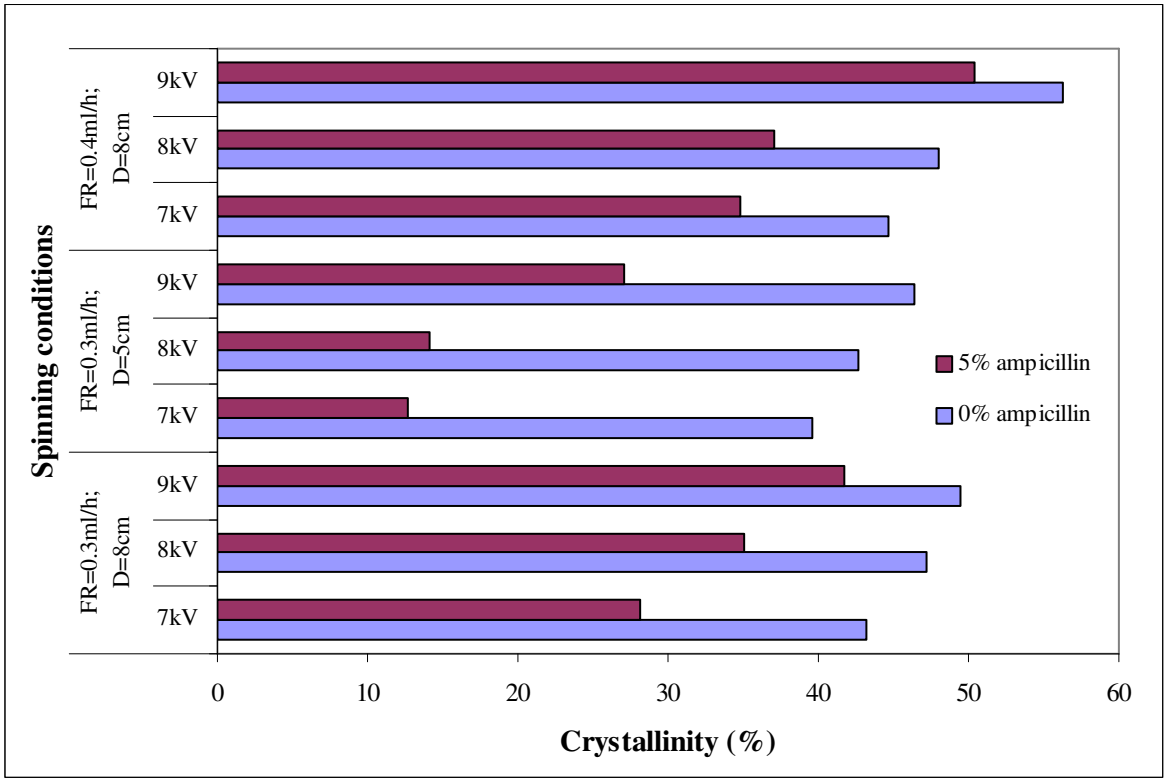

Note: FR = Feedrate and D = Distance

Figure 4.32 Influence of Ampicillin on the Percentage of Crystallinity of the Fibers

The attributes of the crystalline regions include the chain segments in these regions having a high degree of order in that they are parallel to each other and these chains being more compacted (closer to one another) compared to those in the amorphous regions. Only when adjacent chain segments reach a certain degree of order is there a possibility of forming crystallites. The degree of chain orientation and order are determined by the extent to which the polymer jet is stretched when being removed from the polymer solution. While in solution, the

molecular chains are randomly entangled. In a highly stretched jet, the molecular chains have a higher degree of orientation along the longitudinal direction of the flying jet plus a larger possibility for the chains to come closer to each other with the thinning of the jet. As discussed in the fiber diameter section, higher voltage and longer distance led to an elevated degree of stretching; therefore, it is not difficult to understand the effects of these two factors on the crystallinity. As to the corresponding increase in crystallinity with respect to the feedrate, the increase might be due to the higher stretching power, which was a result of the larger accumulation of charges on the polymer drop at the tip of the needle with the higher feedrate. The addition of ampicillin had a negative effect on the formation of crystallites. There were multiple reasons for this, which might offset or magnify the effect of each other. First, the addition of ampicillin increased the charge accumulation, thus raising the stretching power and increasing the potential for an increase in crystallinity. Next, the higher stretching power led to a shorter flying time of the polymer jet, which allowed less time for the molecular chains to reorganize themselves to form crystallites. Third, the existence of ampicillin molecules among the PCL molecular chains might hinder the PCL chains from coming close to each other, preventing the formation of crystallites. The molecular mass of ampicillin sodium salt used in the study was 371.19 g/mol, and that of the caprolactone (the monomer of the PCL polymer) was 114.14 g/mol. Comparatively speaking, the ampicillin sodium salt was large and actually disrupted the formation of crystallites by preventing close packing of the polymer chains, thereby reducing crystallite formation. Fourth, since the polymer jet was further stretched by the rotating collector as it deposited on the surface, the comparative speed of the polymer jet to that of the collector determined the drawing ratio. The rotating speed of the collector was consistent throughout this study, i.e., 1500 rpm. However, the velocity of the polymer jets with ampicillin

was higher than those without ampicillin. As a result, the drawing ratio of the polymer jet with ampicillin was smaller than that of the polymer jet without ampicillin, which accounted for the lower crystallinity. As the results indicated, the last three effects offset and exceeded the first effect. The fact that the addition of ampicillin decreased the crystallinity of fibers was most prominent when the distance was 5 cm. The Wilcoxon Signed-Ranks test results showed that the crystallinity of fibers with ampicillin was significantly lower than that of without ampicillin. The *p* value was 0.0062. The SAS program and output are shown in Appendix B.

Table 4.4 shows the crystallinity of 14% PCL fibers spun with different ampicillin concentrations. The spinning conditions were FR = 0.3 ml/h, D = 8 cm, and V = 9 kV.

Table 4.4 Crystallinity of Fibers Spun with 14% PCL and Various Ampicillin Concentrations

Ampicillin Concentration	0%	8%	12%	16%	20%
Percent Crystallinity	49.52	43.83	41.04	43.05	43.52

The influence of ampicillin on the morphology of fibers was not only the percentage of crystallinity but also the size of the crystallites. Figure 4.33 shows five DSC curves of fibers with different concentrations of ampicillin from 0%, 8%, 12%, and 16% to 20%. The peak of 0% ampicillin at around 60°C was slightly narrower than the others. This might be attributed to the influence of ampicillin on the sizes of the crystallites. The narrow peak indicated more even size distribution than if the peak had been broader. The presence of ampicillin led to a larger size distribution of crystallites.

Considering the percentage of crystallinity of both pure PCL fibers and fibers with ampicillin, in the studies of tensile properties, antimicrobial properties, and degradation properties, the following polymer and spinning parameters were adopted to produce fiber

samples: 1) polymer concentration: 14%; 2) feedrate: 0.3 ml/h; 3) distance: 8 cm; 4) voltage: 9 kV; and 5) ampicillin concentration: lower than 20%. The percentage of crystallinity of the fibers produced under these conditions was between 40% and 50%; the range was acceptable for textile fibers.

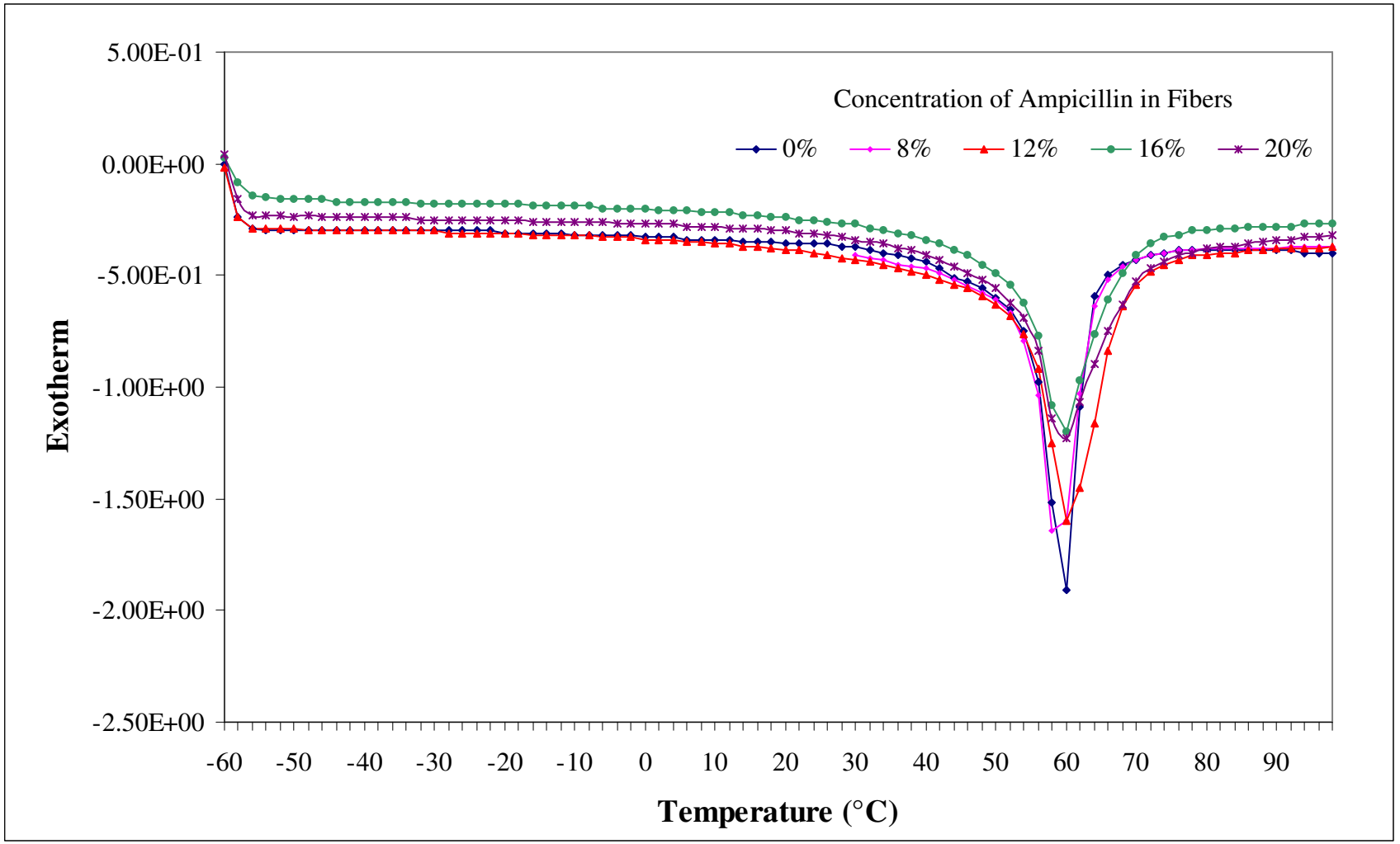

Figure 4.33 DSC Curves of Fibers Spun with 14% PCL and Various Ampicillin Concentrations

4.3.2 Tensile properties: Load and elongation

The two morphological regions in fibers, the crystalline and amorphous, have some effect on the tensile properties of fibers although these properties are not the only influencing factors. The load and the percentage of elongation at break of electrospun yarns were studied. Figure 4.34 shows the load and elongation of fibers spun with 14% PCL with and without ampicillin. The means and standard deviations were calculated based on 10 measurements for each sample.

Since the currently available test methods for measuring yarn size could not be applied to the samples in this study, the yarn size of the samples was unknown. Therefore, load instead of stress was reported. The values varied from 2.12 N to 3.96 N. The load of pure PCL fiber yarn was the lowest, while the yarn with 16% ampicillin had the highest load. All yarns composed of fibers containing ampicillin were stronger than those without ampicillin. The percentage of elongation at break was between 58% and 70%. Fibers containing 16% ampicillin had the highest percentage of elongation at 70%, and fibers with 12% ampicillin had the lowest percentage at 58%.

The Wilcoxon Signed-Ranks test results indicated that the load of the pure PCL yarns was significantly lower than the loads of all yarns with ampicillin. The load of yarns with 16% ampicillin was significantly higher than all other yarns but those with 20% ampicillin. Only the difference of elongation between 12% and 16% ampicillin yarns was significant. The loads of yarns with 8%, 12%, and 20% ampicillin were at the same level. The SAS program and output are shown in Appendix C. Since the load was not normalized to yarn size and based on the author's observation that the size of the yarn samples varied, a direct comparison of load values could not reflect the strength of the yarns. As the length of the yarns is the same (the circumference of the collector before twisting), the yarn size is directly proportional to the yarn

weight. In the future, the weight of samples should be measured before the tensile tests, so that the load can be normalized and compared between different samples.

The tensile properties of yarns are a complex issue. There are many factors influencing yarn tensile properties, including the properties of fibers composing the yarn, the interaction between fibers within the yarn, and the yarn structure. In terms of fiber properties, the molecular chain orientation and the percentage of crystallinity are important. Regarding the interaction between fibers and the yarn structure, the smoothness of the fiber surface, yarn twist, and fiber length are all influencing factors. Warner pointed out that it was difficult to treat analytically the rupture behavior of twisted yarns because of the following three complications: 1) the migration behavior of fibers in yarns, 2) the local strains resulted from twisting, and 3) the local recovery and buckling behavior of fibers in yarns [147]. Figure 4.35 show the load-elongation curve examples of PCL fibers with various ampicillin concentrations. The load-elongation curves of the electrospun yarns were typical of stress-strain curves of conventional fiber yarns.

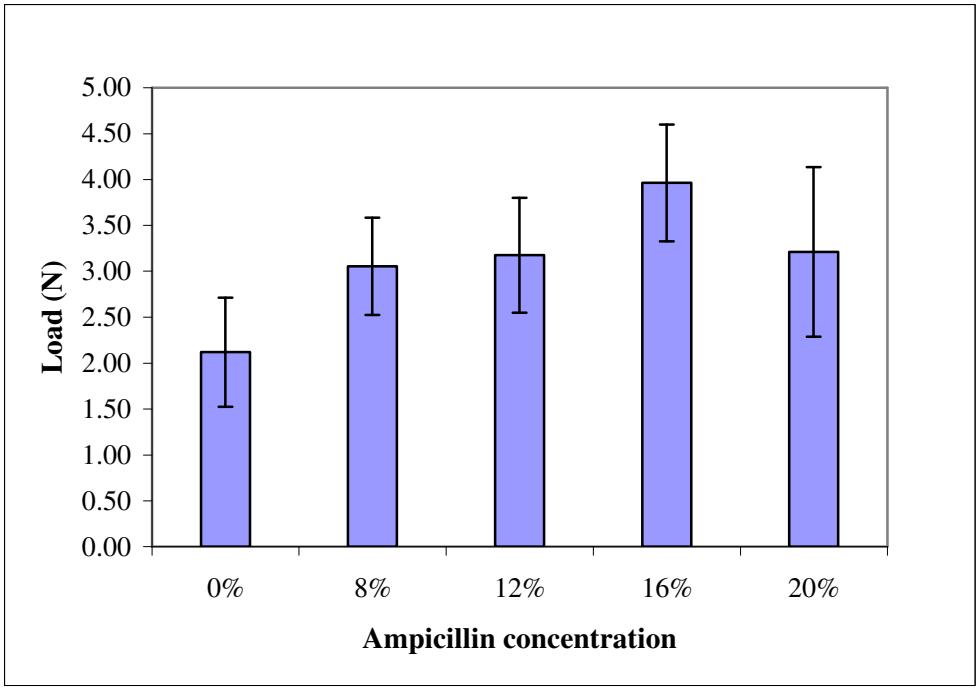

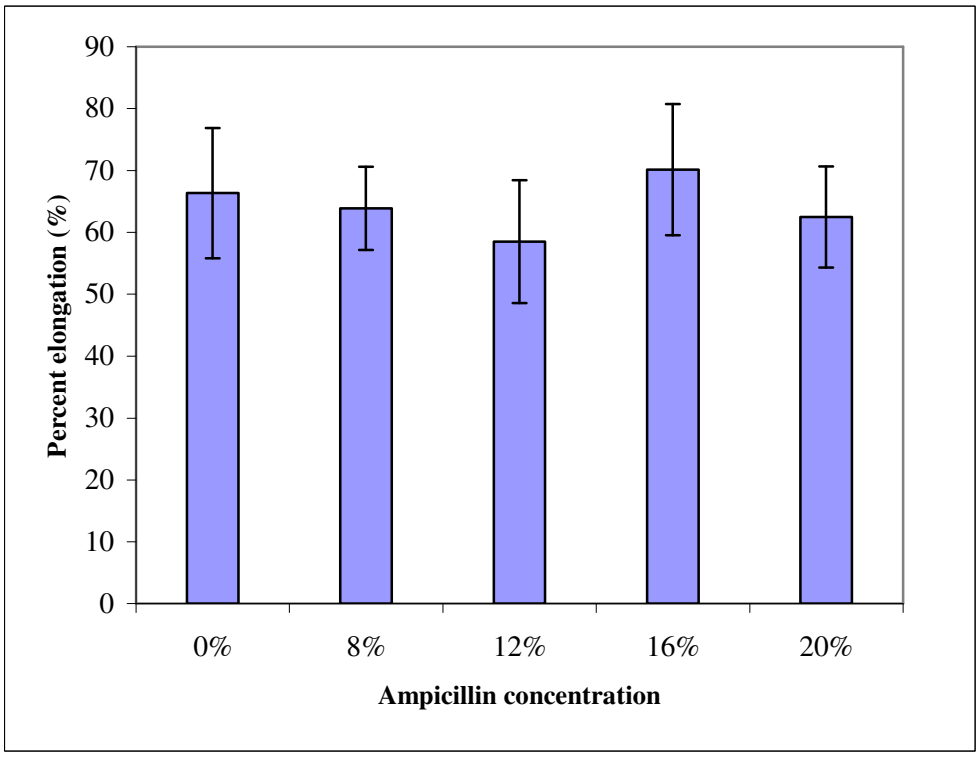

Note: The means and standard deviations were calculated based on 10 measurements.

Figure 4.34 Influence of Ampicillin on Yarn Tensile Properties

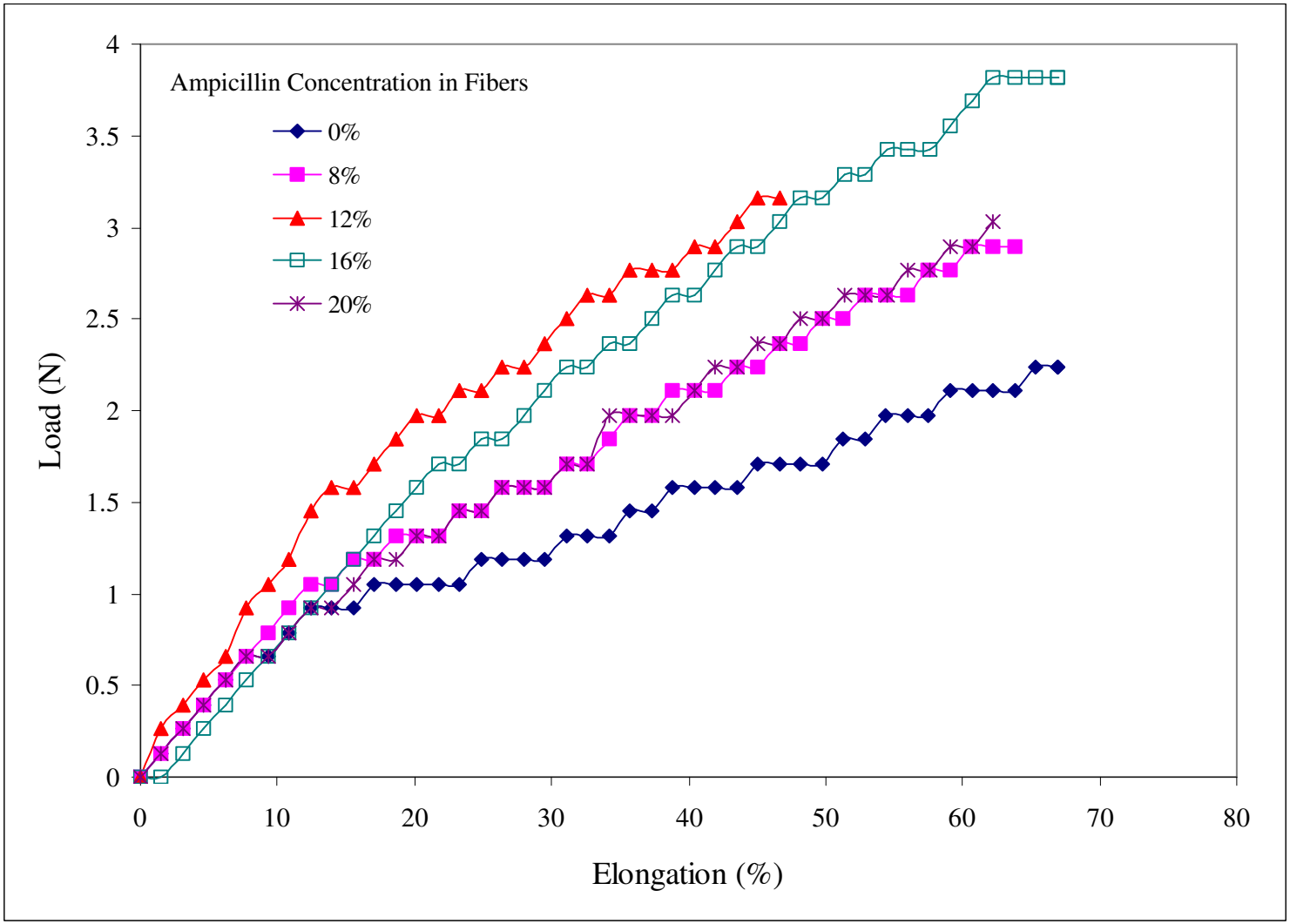

Figure 4.35 Load-elongation Curves of Yarns of Fibers Spun with 14% PCL and Various Ampicillin Concentrations

4.4 Antimicrobial Properties and the Release of Ampicillin from Fibers

As ampicillin was incorporated in the polymer solution before spinning, it was unknown if the solvent or the polymer and the spinning process had some effect on ampicillin's properties. Moreover, it was uncertain whether or not ampicillin could be released from spun fibers and retain its antimicrobial effectiveness. Therefore, the antimicrobial effectiveness of fibers with ampicillin and the duration of their antimicrobial effectiveness were evaluated *in vitro* by the zone of inhibition and ampicillin release tests.

4.4.1 Antimicrobial test: Zone of inhibition

The antimicrobial properties of fibers spun with 14% PCL and ampicillin concentration of 2%, 5%, 8%, 12%, 16%, and 20% were examined. Pure 14% PCL fibers were used as the control. The results of the antimicrobial tests are presented in Table 4.5 and Figure 4.36. The results demonstrated that the released ampicillin retained its effectiveness after being dissolved in the polymer solution and spun into fibers using the methods in this study. Neither the solvent nor the spinning processes influenced the antimicrobial properties. The zone of inhibition increased when the ampicillin concentration in the fibers increased in the low value range, from 2% to 5%, and then to 8%. But from 8% to 20%, the increase in the zone of inhibition was not that remarkable, especially for *S. aureus*.

Comparing the two bacteria studied here, *S. aureus* and *K. pneumoniae*, it was obvious that *S. aureus* was more sensitive to ampicillin than *K. pneumoniae* because when the ampicillin concentration in fibers was 2% no zone of inhibition existed. When the concentration rose to 20%, the size of the zone where no *K. pneumoniae* grew was less than half the size formed by *S. aureus*. Ampicillin is a broad-spectrum antimicrobial agent. The higher resistance of *K.*

pneumoniae to ampicillin might be due to its polysaccharide capsule, which limited the penetration of ampicillin and prevented it from reaching the bacterial cell wall.

The results demonstrated the effectiveness of ampicillin released from the electrospun fibers and indicated the mobility of ampicillin in an aqueous environment. The ability of antimicrobial agents to migrate in agar was required for the formation of the zone of inhibition. Ampicillin sodium salt, the antimicrobial agent used in this study, is highly soluble in water. The ampicillin released from the fiber diffused through the agar to inhibit microorganism growth. Therefore, a clear zone of no bacteria growth was formed.

Table 4.5 Influence of Ampicillin on the *Zone of Inhibition

	Zone of Inhibition (mm)						
Ampicillin concentration	**0%**	**2%**	**5%**	**8%**	**12%**	**16%**	**20%**
S. aureus	0	38	49	50	52	52	53
K. pneumoniae	0	0	14	18	22	24	26

Note: *The values were the means of three measurements for each sample.

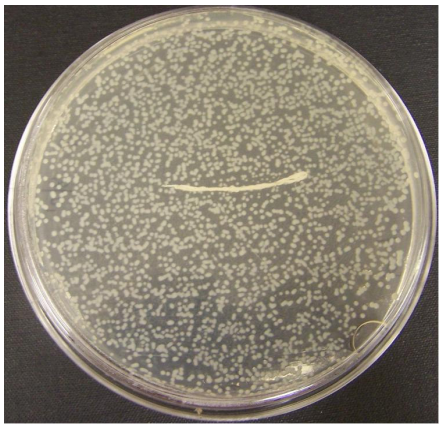

2% ampicillin

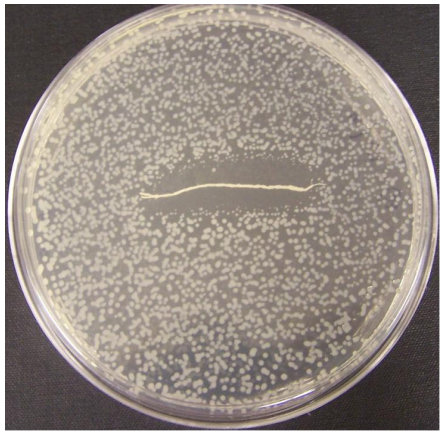

5% ampicillin

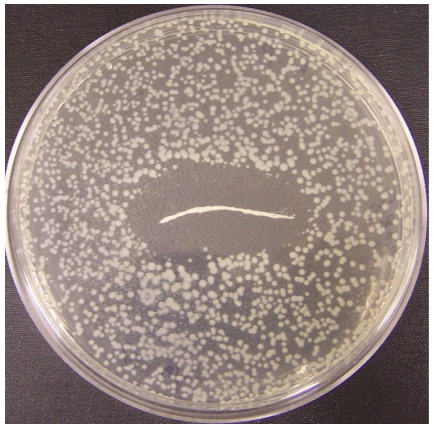

8% ampicillin

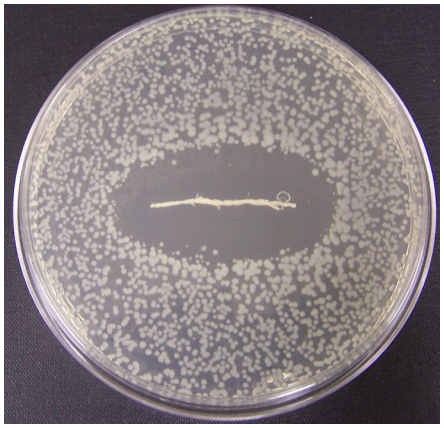

12% ampicillin

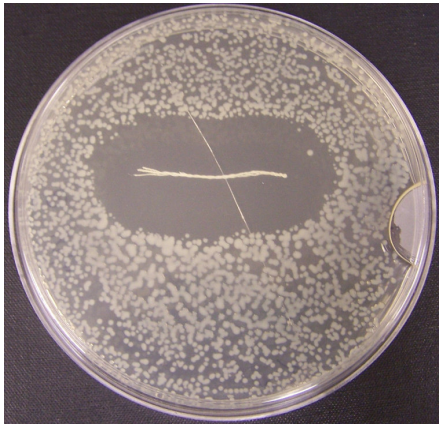

16% ampicillin

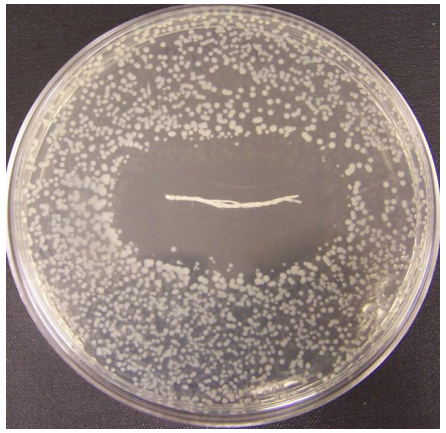

20% ampicillin

Figure 4.36 (a) Zone of Inhibition Formed around Fibers Spun with Various Ampicillin Concentrations (*K. pneumoniae*)

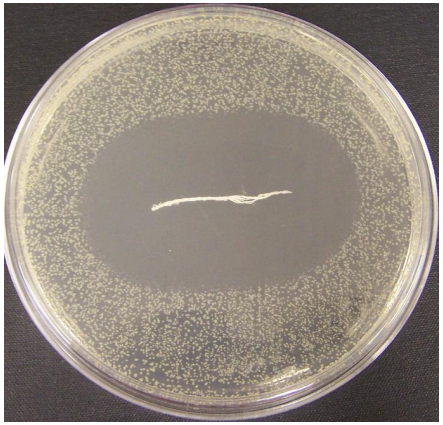

2% ampicillin

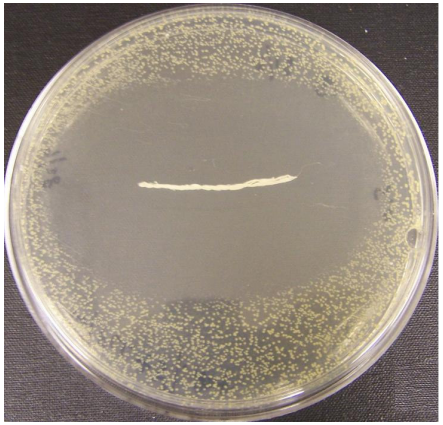

5% ampicillin

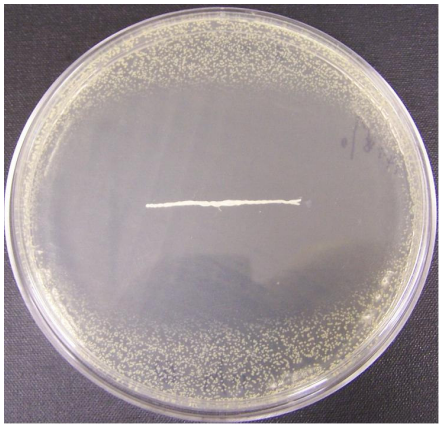

8% ampicillin

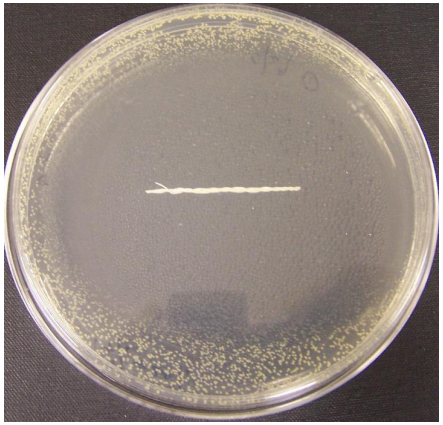

12% ampicillin

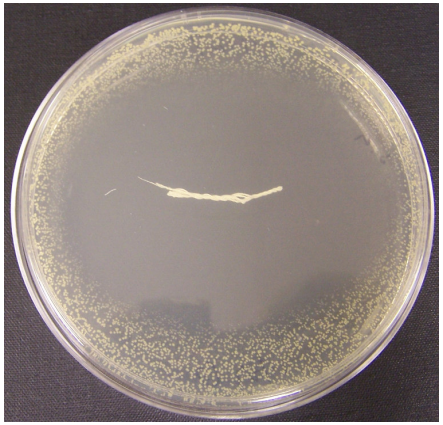

16% ampicillin

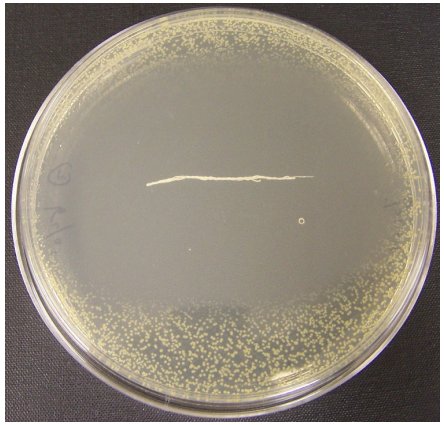

20% ampicillin

Figure 4.36 (b) Zone of Inhibition Formed around Fibers Spun with Various Ampicillin Concentrations (*S. aureus*)

4.4.2 Release of ampicillin in PBS

The ampicillin release results from fibers containing 8%, 12%, 16%, and 20% ampicillin are summarized in Table 4.6 and plotted in Figure 4.37. A burst depletion of more than 75% in the first hour for all the fibers with different ampicillin concentrations was observed. Then the release rate slowed down dramatically. After the initial burst, the remaining ampicillin in the fibers was released gradually, and at 24 hours more than 95% of the ampicillin had diffused from the fiber and was in the PBS solution. The release process was complete for almost all samples within 96 hours.

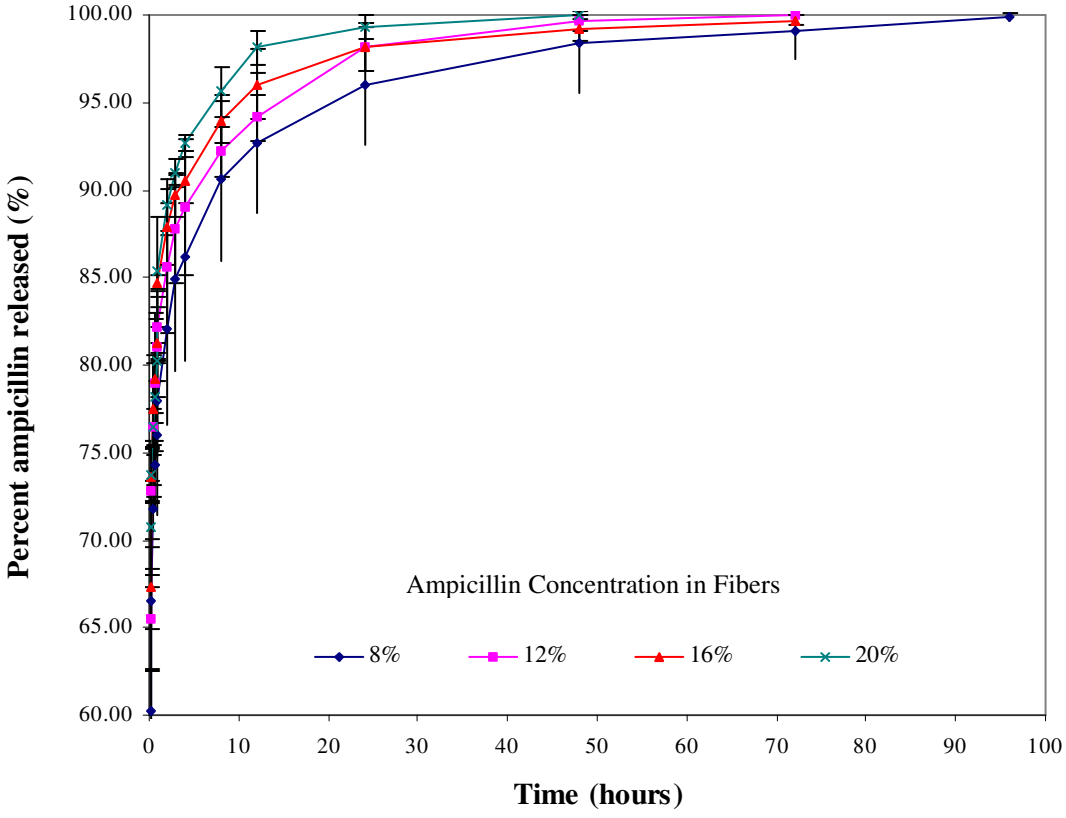

Note: The means and standard deviations were calculated based on three measurements.

Figure 4.37 Release of Ampicillin from Fibers Containing Different Ampicillin Concentrations

Table 4.6 *Percentage of Release of Ampicillin from Fibers Containing Different Ampicillin Concentrations

Ampicillin Concentration	**Percentage of Ampicillin Released (%)**							
	8%		**12%**		**16%**		**20%**	
Time/minutes (hours)	Mean	Standard Deviation	Mean	Standard Deviation	Mean	Standard Deviation	Mean	Standard Deviation
10	60.21	2.37	65.46	2.91	67.29	2.33	70.69	2.69
20	66.48	0.89	72.83	2.78	73.62	1.54	73.77	1.58
30	71.82	1.27	76.51	4.05	77.50	2.64	76.43	1.04
40	74.31	2.40	79.02	3.92	79.16	3.46	78.19	0.89
50	76.05	4.59	81.05	2.86	81.20	2.15	80.21	0.10
60 (1)	77.98	3.27	82.22	2.01	84.74	0.36	85.35	3.13
120 (2)	82.02	5.45	85.58	3.70	87.87	2.15	89.15	1.44
180 (3)	84.95	5.23	87.78	3.08	89.73	1.28	90.99	0.73
240 (4)	86.21	5.97	89.04	3.86	90.55	1.29	92.64	0.46
480 (8)	90.68	4.75	92.21	1.43	93.89	1.16	95.61	1.45
720 (12)	92.70	4.04	94.12	1.27	96.03	2.03	98.12	1.00
1440 (24)	95.97	3.35	98.15	1.40	98.12	1.37	99.31	0.70
2880 (48)	98.37	2.82	99.64	0.62	99.16	0.65	100.00	0.00
4320 (72)	99.06	1.62	100.00	0.00	99.69	0.31		
5760 (96)	99.86	0.24			100.00	0.00		

Note: The means and standard deviations were calculated based on three replications of each sample.

Similar release profiles have been reported by several other studies, such as the release studies of Mefoxin from PDLA electrospun film [148] and Mefoxin from a PLGA nanofibrous scaffold [132]. The overall quick release of ampicillin might be due to the following reasons.

1) The lower compatibility of ampicillin in PCL fibers compared with that in PBS

There are two mechanisms of release of drugs from biodegradable polymers, i.e., small-molecule-diffusion-controlled release and polymer-degradation-driven release [149]. In the diffusion-controlled release process, the aqueous medium first penetrates the polymer and drug matrix, where the drug leaves the polymer, dissolves in the medium, diffuses within the matrix, and finally migrates from the polymer through the pores or capillaries formed by the medium as a result of the concentration gradient. The polarities of drugs and release medium are decisive in the diffusion-controlled release process. Therefore, this release mechanism is applicable only to those drugs that have the same polarity as the aqueous medium. For those drugs that do not

dissolve in the release medium, polymer degradation is the main driving force for drug release. In this study, the ampicillin salt is a hydrophilic drug, while PCL is a lipophilic polymer. The quick release rate confirmed that the diffusion of ampicillin through the PCL fibers was the primary releasing mechanism since degradation of the polymer had not begun in this limited time period. This is discussed in further detail in the degradation study presented in the following section.

There are several factors influencing the rate of diffusion-controlling drug release: 1) dissolvability of the drug in the release medium, 2) ease of the medium penetrating the polymer and drug matrix, and 3) attraction between the polymer and drug. Any factors unfavorable to the dissolution of the drug in the medium and the migration of the dissolved drug from inside the polymer to outside will reduce the release rate. The dissolvability of the ampicillin sodium salt in water is 50 mg/ml. In the ampicillin release tests performed in this study, 25 ml of PBS was used to immerse samples, which were usually no more than 12 mg. Approximately 1250 mg of ampicillin was needed to achieve a saturated ampicillin salt solution in 25 ml of PBS. However, less than 2.0 mg of ampicillin was contained in the samples evaluated here even with the highest ampicillin concentration, i.e., 20%. With all the ampicillin in the fibers dissolved in the 25-ml PBS, the solution is far from saturated. The high solubility of ampicillin salt in water is in favor of its fast release. Theoretically, there are no primary bonds or hydrogen bonds formed between PCL and ampicillin. Therefore, ampicillin is trapped only in the fibers and ready to dissolve in water. The unaffected glass transition temperature of fibers, as shown in Figure 4.33, after the addition of ampicillin is evidence of the absence of physical bonds between PCL and ampicillin. In terms of the migration of ampicillin inside the fiber structure, the unordered amorphous regions provide a larger open space than the crystalline regions; thus, it is easier for water to

penetrate and small molecules to move in the amorphous regions. The crystallinity of electrospun fibers with ampicillin was no more than 50%, leaving more than 50% of the fiber amorphous, which facilitated the release of ampicillin.

2) The accumulation of ampicillin on the surface of the fibers

In addition to the high solubility of ampicillin in water and ampicillin's low compatibility in PCL fibers, the accumulation of ampicillin on the surface or near-surface of PCL fibers led to burst release in the first hour, thereby contributing to the fast release. Approximately 60% to 70% of the ampicillin contained in fibers was depleted in the first 10 minutes in all samples. The only explanation for this quick release during this short time period was the accumulation of ampicillin on the fiber surface. The release speed then decreased, and the rate of decrease was dramatic during the first hour, as shown in Figure 4.38. The release speed was approximated at each data measuring point by dividing the release percentage at a given time period by the period of time, as shown in Equation 4.3.

$$\text{Release speed at time } t_2 = (R_2 - R_1)/ (t_2 - t_1) \tag{4.3}$$

Where R_2 was the released percentage measured at time t_2, and R_1 was the release percentage measured at time t_1, which was the previous time point at which R_2 had been measured.

The understanding of the accumulation of ampicillin on fiber surfaces can be accessed from the physical spinning process point of view. First, the ampicillin ions migrate to the surface of the polymer jet when it flies from the needle tip to the collector due to the ionic strength [132]. Second, since the ampicillin sodium salt and PCL polymer have different polarities, they are incompatible with each other. Therefore, during electrospinning, with the evaporation of methanol, two things may happen at the same time. One is the phase separation of the polymer and the drug. The ampicillin is carried by methanol toward the direction of its evaporation, i.e.,

toward fiber surfaces; the other is the aggregation of adjacent ampicillin molecules into bigger particles. Both processes take place during the jet flying and after the deposition of fibers on the collector until all solvents evaporate. And both processes result in quick release. A study by Zeng et al. demonstrated the influence of the compatibility of drugs in the drug-polymer-solvent system on the distribution of drugs in electrospun fibers [118].

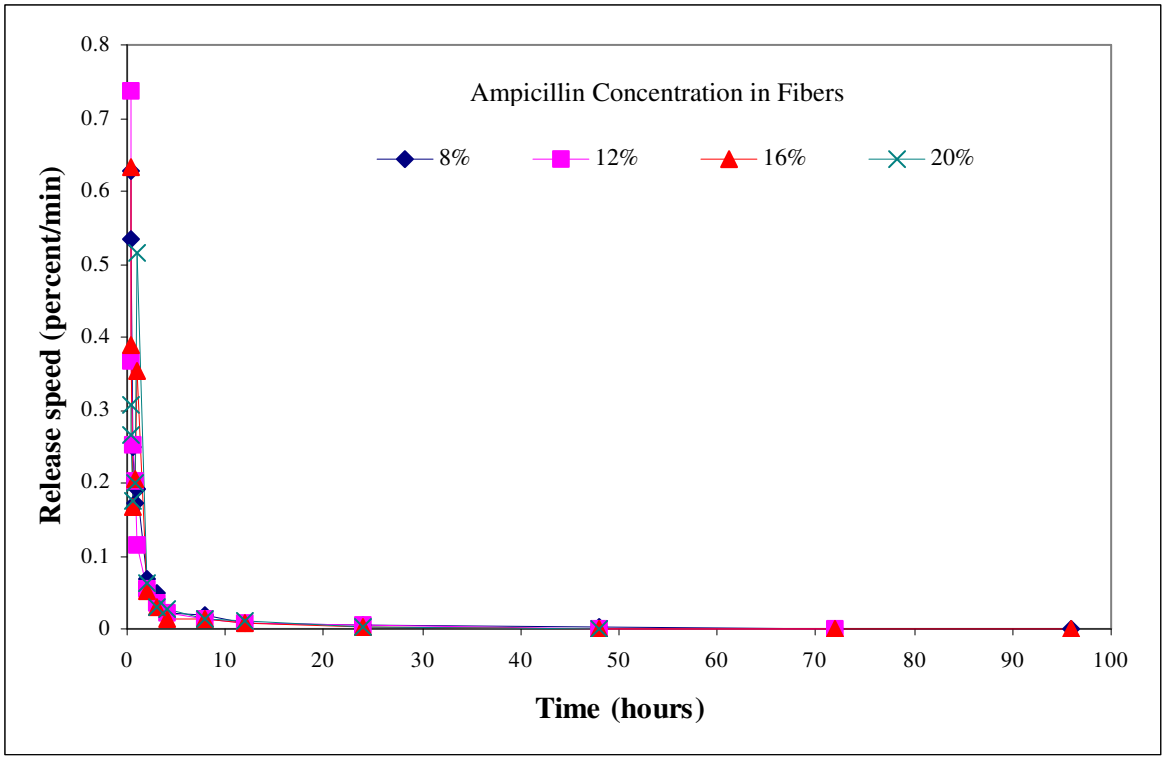

Figure 4.38 Release Speed of Ampicillin from Fibers Containing Different Ampicillin Concentrations

3) The small fiber diameter

The release of ampicillin is associated with the penetration of water in fibers and the dissolution of ampicillin in water. The smaller the fiber diameter, the shorter the time needed for

water to penetrate the fiber. The average fiber diameters used in the release study were between 320 nm and 260 nm. The author believes the fine fiber size contributed to the high release rate.

The influence of ampicillin concentration on its release

From Figure 4.37, it can be seen that in general higher ampicillin concentration led to faster release, due to two reasons: the influence of ampicillin on fiber properties and its distribution in the fibers. Higher ampicillin concentration is associated with smaller fiber size and a higher surface-to-volume ratio of fibers, which accounted for shorter diffusion passage and increased contact area to water when immersed in PBS. As a result, the ampicillin release from fibers spun with the higher ampicillin concentration was faster. Furthermore, with the increasing ampicillin concentration and the decreasing fiber diameter, the probability of forming ampicillin aggregates as well as the size of the aggregates increased when phase separation took place.

Theoretical models for drug release

Modeling of controlled drug release is a subject that has been studied for a couple of decades. Many researchers have used these models to explain their experimental results. The three most popular models are listed here.

1) Fickian diffusion models:

Fickian diffusion equations are the most basic models; most other models were developed based on these equations. There are two models of Fickian diffusion, the zero-order model (Equation 4.4) and the first-order model (Equation 4.5).

Zero-order model:

$$M_t/M_0 = k_0 t \tag{4.4}$$

Where M_t is the amount of drug released at time t, and M_0 is the total amount of drug in the sample. So, M_t/M_0 is the fraction of drug released. K_0 is the zero-order release constant. This

model is derived in steady-state diffusion, i.e., the concentration of the drug in the sample does not change with respect to time. The release rate is constant.

First-order model:

$$\ln (1 - M_t/M_0) = -k_1 t \quad (4.5)$$

Where M_t and M_0 are the same as stated above, and k_1 is the first-order release constant. This first-order model is useful in non-steady diffusion, where the concentration of the drug in the sample changes with time. The release rate is proportional to the residual drug ($1 - M_t/M_0$) left in the sample.

2) Higuchi model:

The Higuchi model is a semi-empirical model describing the drug release from a single face of a non-swelling tablet. Different equations are applied when the drug dissolves or does not dissolve in the aqueous medium. The equation (Equation 4.6) for the release of drugs with high solubility in medium from a cylinder sample is shown below:

$$M_t/M_0 = k_H t^{1/2} \quad (4.6)$$

k_H is the Higuchi release constant. $K_H = 4(D/\pi r^2)^{1/2}$, where D is the diffusion coefficient of the drug [150-152]. Based on this model, the friction of the drug released is proportional to the square root of the time. But the model is valid only at the early stage of release. Different studies provided different values below which the model was valid. Zurita et al. reported that M_t/M_0 should be smaller than 0.6 [153]. Ritger and Peppas said that M_t/M_0 should be no larger than 0.15 to 0.20 [152].

3) Roseman and Higuchi model:

A theoretical model was established by Roseman and Higuchi describing the release of the drug from a cylindrical polymer matrix. The model was based on the assumption that the

drug contained in the sample far exceeded the solubility of the drug in the polymer. The relationship between the percentage of the drug released and time *t* is described in Equation 4.7 [154, 155].

$$(1 - M_t/M_0) \ln (1 - M_t/M_0) + M_t/M_0 = (4CDt)/(Ar^2) \quad (4.7)$$

Where C is the solubility of the drug in the polymer, D is the drug diffusion coefficient in the polymer, A is the total initial drug content in polymer (mg/cm^3), and *r* is the radius of the cylindrical sample. The assumption of the sample is that the release of the drug is from the surface to the center of the cylinder. During the release, a boundary separates the cylinder into two zones, the outer zone and the inner zone. In the outer zone, the drug is completely depleted; in the inner zone, the drug retains its original concentration [155].

Most of the controlled-release studies have used these three models to fit data and help to elucidate the release mechanisms. However, none of these models was found to fit the data of this study. The assumptions for all the above models include that the drug is evenly distributed in the sample and the sample is homogeneous. For the samples in this study, as was previously discussed, it is unlikely that the concentration of ampicillin throughout the fibers was even. Also, the fiber itself was not homogenous. There are crystalline and amorphous regions. Neither the accessibility of water nor the concentration of ampicillin in these two regions should be the same theoretically. Moreover, the molecular chains have some orientation in the fibers. Hence, the release of drugs from spun fibers is more complicated than those from cast samples (either by solvent evaporation cast, physical cast, or mechanical cast) and from fiber coatings.

Empirical model to predict ampicillin release

By combining the Fickian first-order model and the Higuchi model and making a minor modification, a new model, as shown in Equation 4.8, was obtained.

$$\text{Ln}\ (A_1 - A_2\ Mt/M_0) = -kt^{1/2} \quad (4.8)$$

Where A_1, A_2, and k are constants.

Fitting the percentage of ampicillin released and the square root of the releasing time into the above model, good agreement between the model and the data was obtained. The values of the parameters in the equation, A_1, A_2, k, and R^2 (the square of the correlation coefficient), are listed in Table 4.7. The R^2 was equal to 0.9719 or higher for different ampicillin concentrations. The constant k, which reflected the overall release rate, increased with the increase in ampicillin concentration in fibers from 8% to 12% and 16%. The parameters were valid when the percentage of ampicillin released was higher than approximately 60%. The fitted curves are shown in Figure 4.39.

An even better agreement of the release data to the model was obtained if the percentage of the ampicillin-released data of after one hour was fitted. Table 4.8 shows the parameters. The R^2 was higher than 0.99 for all different ampicillin concentrations. The parameters were valid only when the released ampicillin was higher than approximately 80%.

Although the exact meanings of A_1 and A_2 are not clear, it still could be concluded that the release rate is related to the ampicillin left in fibers. The less ampicillin left in fibers, the slower the release rate.

Table 4.7 Parameters for the Fitting of the Ampicillin Released in the Empirical Model

	Fitting Parameters			
Ampicillin concentration	8%	12%	16%	20%
A_1	2.0756	2.3819	2.2372	2.2807
A_2	2.1156	2.4185	2.2776	2.2881
k	0.7529	0.8237	1.0054	0.9418
R^2	0.9824	0.9719	0.9836	0.9890

Table 4.8 Parameters for the Fitting of the Ampicillin Released after One Hour in the Empirical Model

	Fitting Parameters			
Ampicillin concentration	8%	12%	16%	20%
A_1	2.9211	3.5270	3.9230	3.4072
A_2	2.9248	3.4934	3.9200	3.3924
k	0.4593	0.4338	0.5118	0.6685
R^2	0.9988	0.9971	0.9986	0.9970

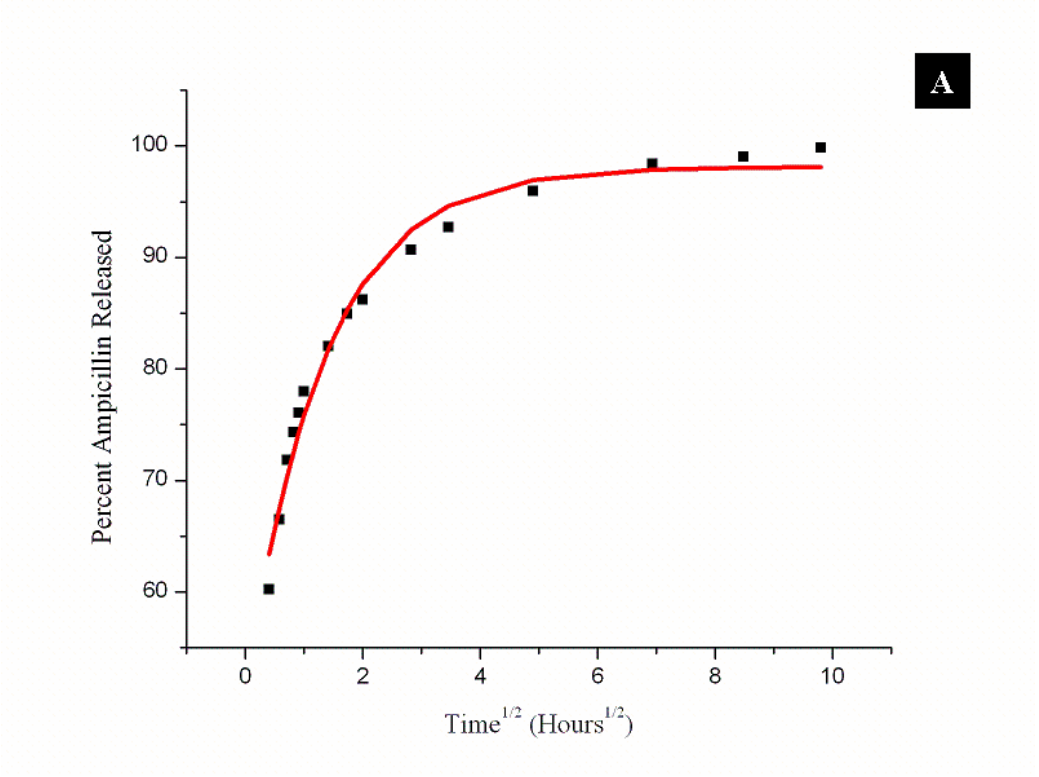
A
Percent Ampicillin Released
100
90
80
70
60
0
2
4
6
8
10
Time^1/2 (Hours^1/2)

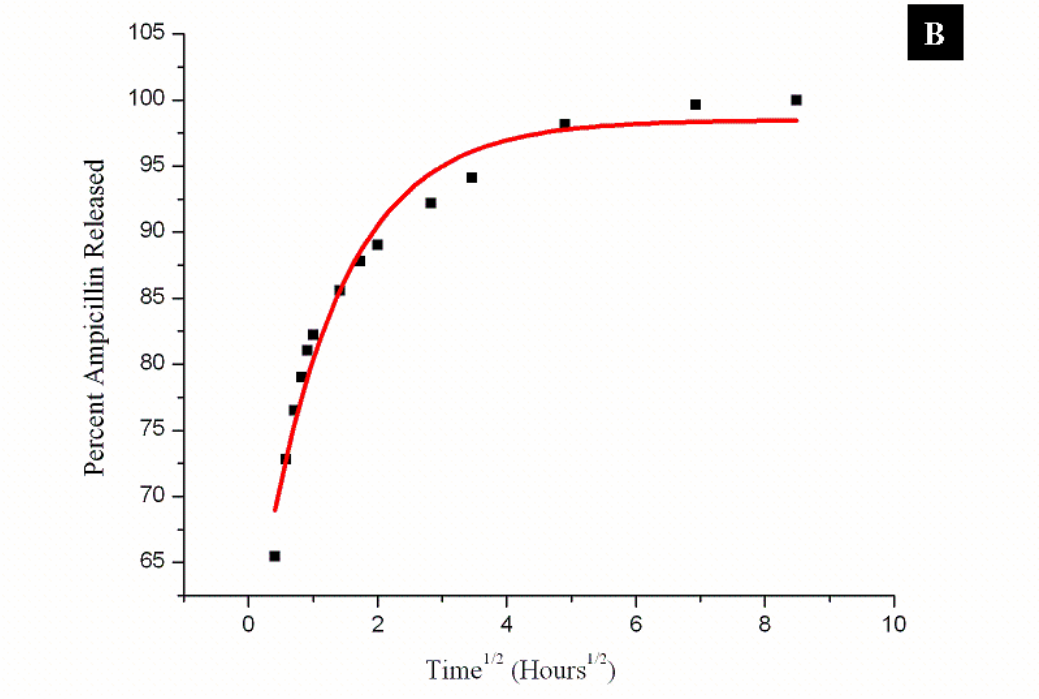
B
Percent Ampicillin Released
105
100
95
90
85
80
75
70
65
0
2
4
6
8
10
Time^1/2 (Hours^1/2)

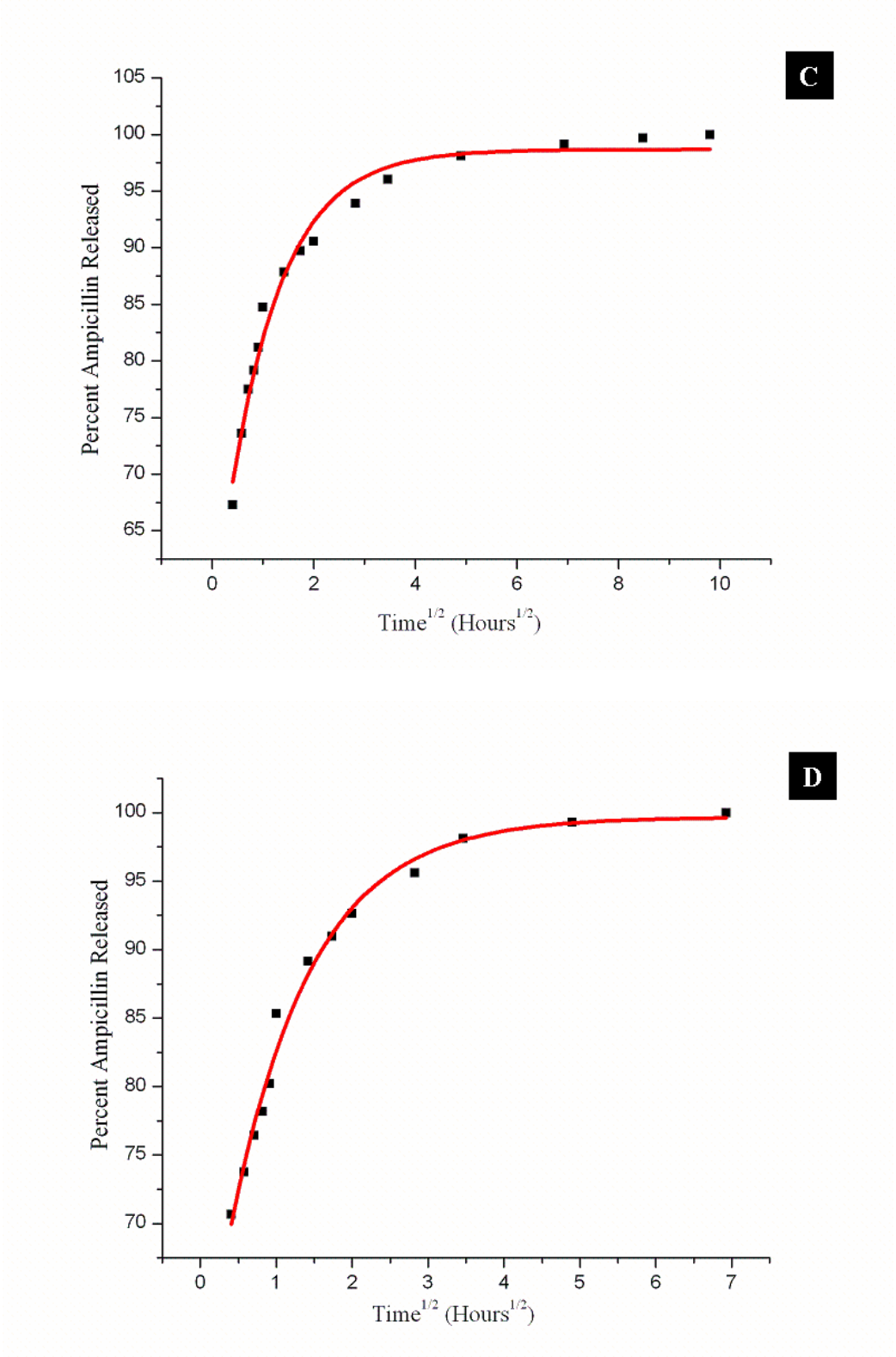

Figure 4.39 Plots of Percentage of Released Ampicillin as a Function of the Square Root of Time from Fiber Samples Containing Different Ampicillin Concentrations (A) 8%; (B) 12%; (C) 16%; and (D) 20%

4.5 Biodegradation Properties of Fibers

The biodegradation properties of the fibers were studied *in vitro* in PBS. Mass loss and fiber morphology change were evaluated.

4.5.1 Mass loss

The biodegradation of PCL is by random scission of the ester bonds by water.

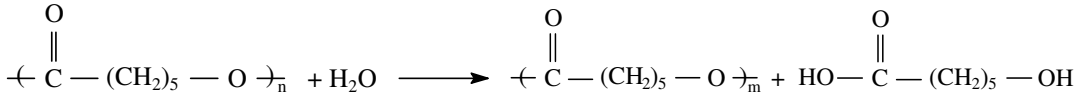

In so-called random scission, the ester linkage being cleaved can be at any of the ester bonds in the molecular chain, in the center or at the ends. If a molecular chain is cleaved in the center, two shorter molecular chains result. If the scission occurs at the chain terminal, a monomer is released, which then will probably leach out of the fiber, hence resulting in mass loss. Compared to other biodegradable polymers commonly used for biomaterials, such as PGA or PLA, the degradation rate of PCL is low. Table 4.9 shows the percentage of the mass loss of PCL fibers electrospun with 14% PCL with various ampicillin concentrations. The mass loss of fibers was the percentage of the weight change of the PCL polymer to the weight of the original PCL polymer contained in the fibers. The weight of the ampicillin in the fibers was deducted from the original fiber weight to get the PCL weight. The assumption here was that all ampicillin was released from fibers completely before the PCL began to degrade.

In 12 weeks (84 days), the percentage of weight loss of all fibers was less than 3%. After comparing the weight loss of the fibers containing ampicillin, it was found that, in general, fibers with higher ampicillin concentration degraded faster than those with less ampicillin. The results were the same as expected and could be explained by the following several aspects. The rate of degradation was related to the accessibility of water penetrating the fibers. Fibers with higher ampicillin concentration had lower crystallinity and a higher percentage of amorphous regions,

resulting in easier penetration of the fiber structure by the water molecules. Studies indicated that the degradation of fibers began from the amorphous regions. In addition, the decreasing fiber diameter, in accordance with the increasing ampicillin concentration, allowed for faster penetration of the fibers by water as well as faster leaching of degradation products from the fibers. Furthermore, for fibers containing ampicillin, with the release of ampicillin, space was left in the fibers to form pores. More pores were formed in the fibers with high ampicillin concentration than in the fibers with lower ampicillin concentration. The pores held water, leading to hydrolysis of the polymer chain.

Table 4.9 *Percentage of Mass Loss of Fibers Containing Different Ampicillin Concentrations over Time

Ampicillin concentration	**Mass Loss (%)**									
	0%		**8%**		**12%**		**16%**		**20%**	
Degradation Time	Mean	Standard Deviation	Mean	Standard Deviation	Mean	Standard Deviation	Mean	Standard Deviation	Mean	Standard Deviation
1d	1.164	0.192								
2d	1.440	0.099			0.163	0.062				
3d	1.519	0.046	0.041	0.157	0.385	0.173	0.374	0.230	0.341	0.727
4d	1.648	0.012	0.367	0.049	0.598	0.378	0.652	0.435	0.738	0.744
5d	1.713	0.053	0.508	0.077	0.712	0.364	0.863	0.266	0.898	0.780
10d	1.855	0.058	0.886	0.299	1.056	0.343	1.310	0.150	1.401	0.594
14d	1.926	0.026	1.122	0.433	1.549	0.553	1.659	0.157	1.732	0.573
21d	2.040	0.056	1.365	0.263	1.907	0.458	1.876	0.419	2.123	0.543
28d	2.005	0.025	1.362	0.423	1.990	0.435	1.969	0.451	2.235	0.507
35d	2.133	0.097	1.521	0.341	2.057	0.374	2.148	0.271	2.306	0.299
42d	2.185	0.041	1.747	0.360	2.279	0.524	2.481	0.489	2.610	0.561
70d	2.182	0.101	1.932	0.338	2.544	0.539	2.682	0.493	2.915	0.497
84d	2.193	0.027	1.971	0.375	2.580	0.552	2.735	0.462	2.948	0.564

Note: The means and standard deviations were calculated based on three replications of each sample.

The percentage of ampicillin released as a function of the release time is presented in Figure 4.40. Two interesting findings can be easily seen from the curves. The first is that the degradation profile of the pure PCL fiber was different from that expected. The second is that the degradation of all fibers in the first three weeks was faster than in the following weeks.

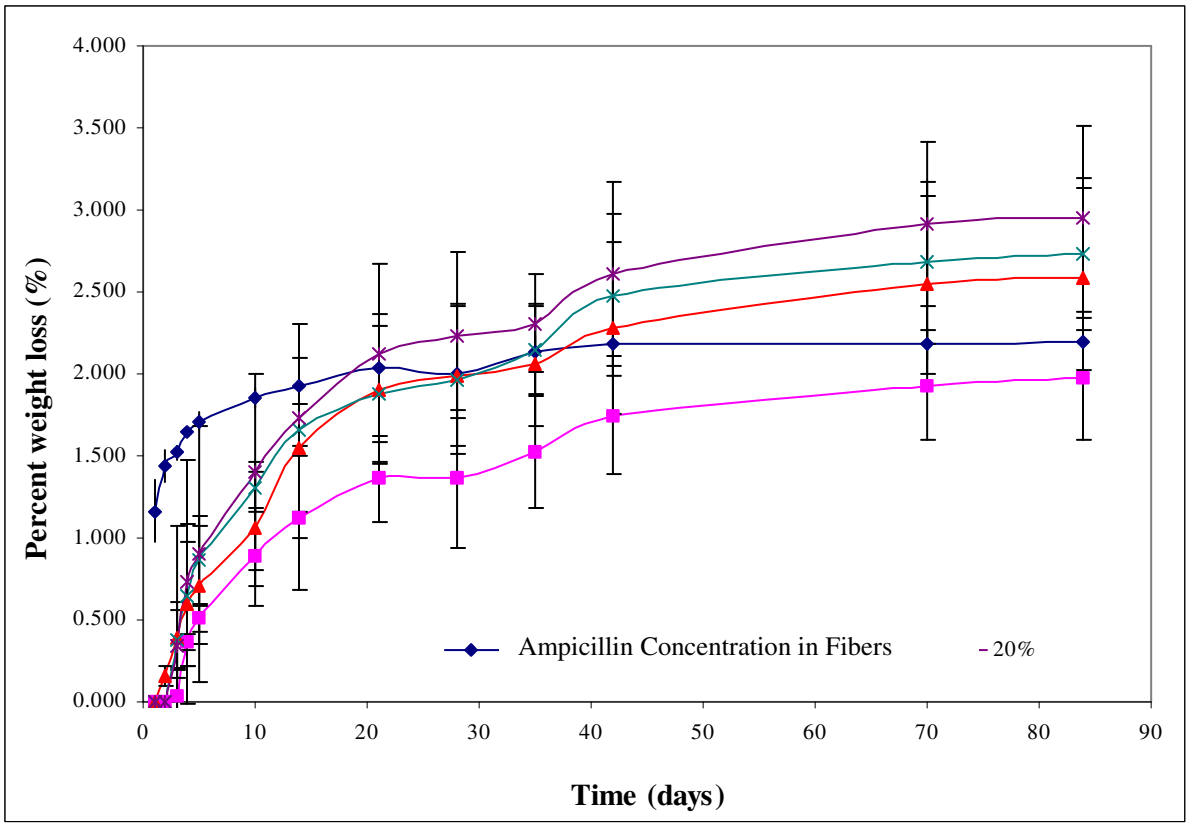

Note: The means and standard deviations were calculated based on three measurements.

Figure 4.40 Plots of Percentage of Mass Loss of Fibers as a Function of Time

The degradation profile of PCL fibers without ampicillin was very different from that of fibers with ampicillin. First, a remarkable weight loss of more than 1% was observed after the fibers had been immersed in PBS for only one day. Second, after the fast degradation in the first five days, the weight loss rate decreased dramatically. From week two to week 12, the total weight loss was less than 0.3%. It was surprising to find that in the first two weeks pure PCL degraded more quickly than any of the fibers with ampicillin, and even until week 12, the pure PCL degraded faster than the fibers with 8% ampicillin. The diameter of the pure PCL fibers was larger and the percentage of crystallinity was higher than the other fibers, so that theoretically the

pure PCL fibers should have degraded more slowly. The results indicated that more complicated degradation mechanisms were involved in these degradation processes, and further studies are needed to learn more about these mechanisms.

Another interesting finding was the high degradation rate for all fibers in the first three weeks compared to the following weeks. This might be due to the presence of some monomers or oligomers in the original PCL polymers, and these small molecules leached out of the fibers at an early stage of the degradation process, resulting in a quick weight loss.

4.5.2 Morphology change

With the degradation of the fibers, the changes in various fiber properties, including physical, mechanical, and morphological properties, took place at the same time. Studies showed that the onset of the loss of mechanical properties was usually earlier than the exhibition of mass degradation and morphological change.

Figure 4.41 shows SEM images of yarn samples after specific time periods of degradation. In the 0 day sample, the fibers were tightly packed in the yarn. But in other samples, the fibers were somewhat less tightly packed within the yarn structure and not as orderly as in the 0 day sample. This was probably due to the relaxation of the fibers after being immersed in PBS. The samples for degradation tests were prepared by twisting the fiber bundles into yarns. The fibers were forced to pack compactly, and some fibers bore larger tension than others, especially those on the yarn's outer surface. After being immersed in PBS, with the assistance of water lubrication reducing friction between fibers, the fibers rearranged themselves to relieve the tension. Plus, with the mechanical agitation of the shaking bath, water flow fluxed into the yarns, thereby destroying their integrity.

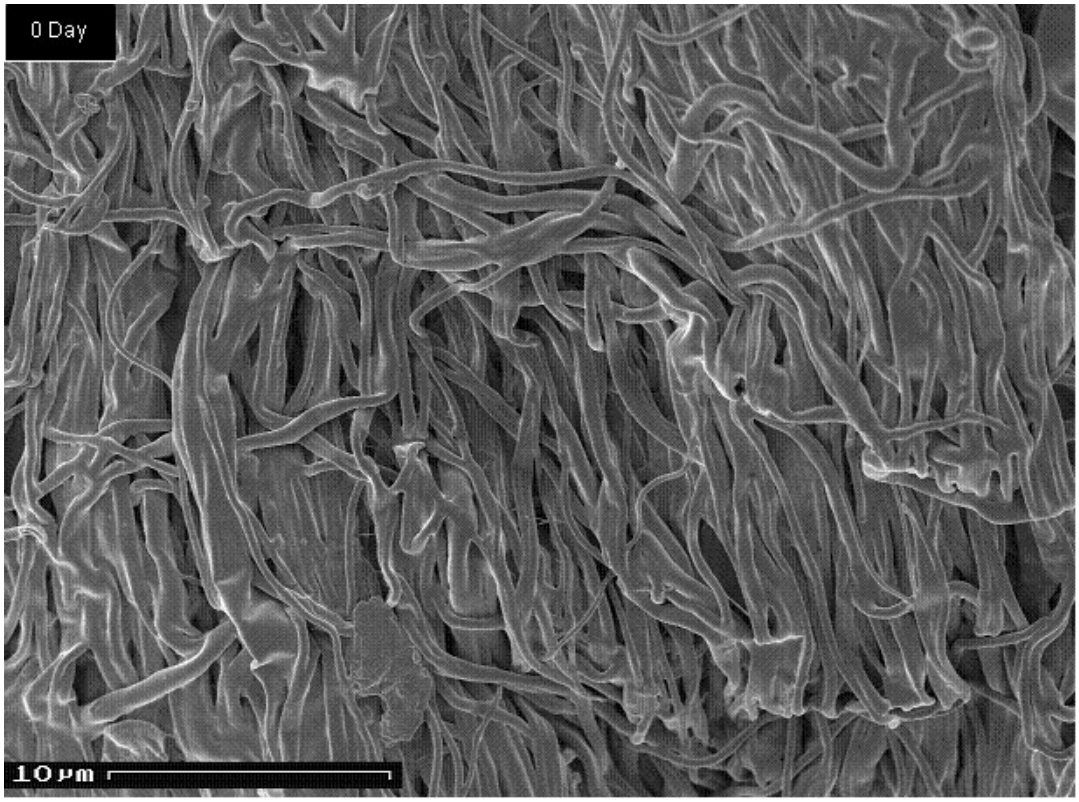
0 Day
10 µm

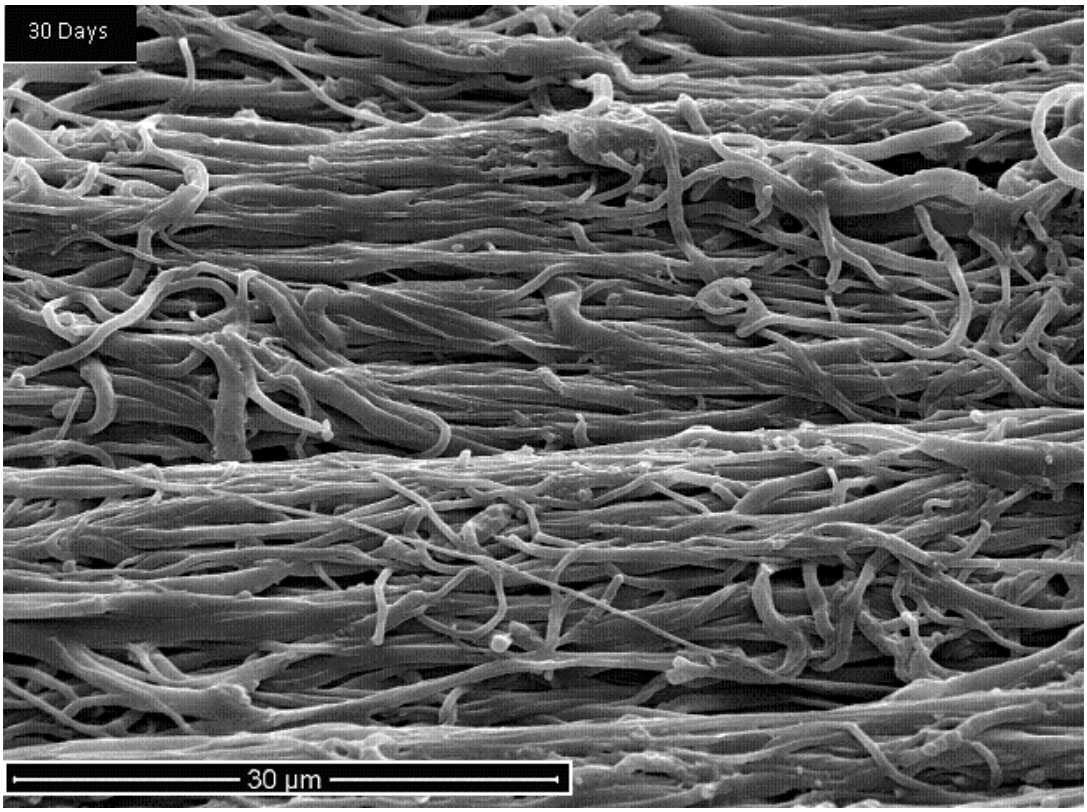
30 Days
30 µm

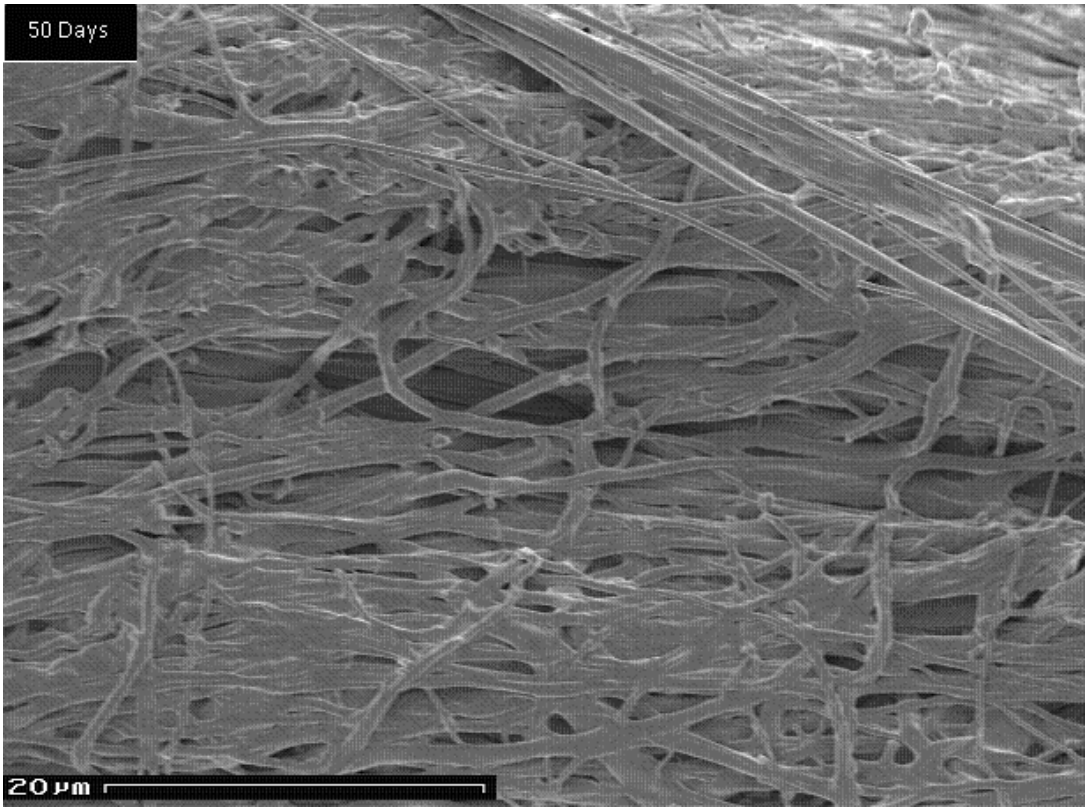
50 Days
20 µm

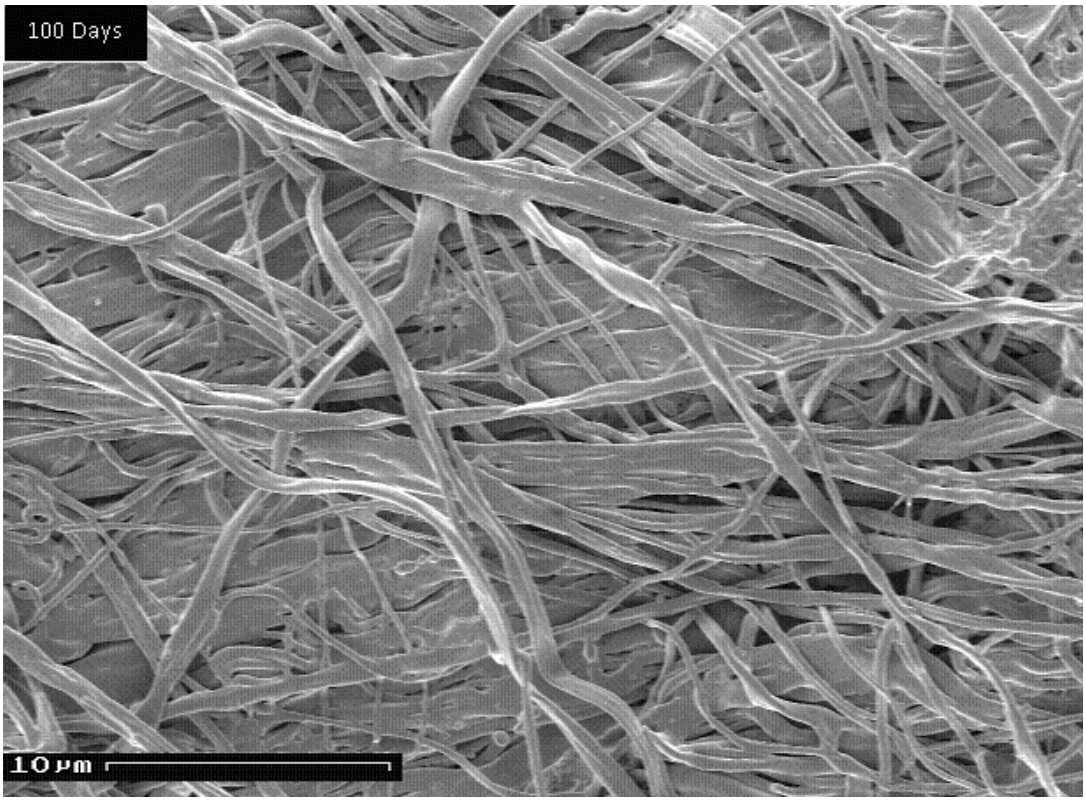
100 Days
10 µm

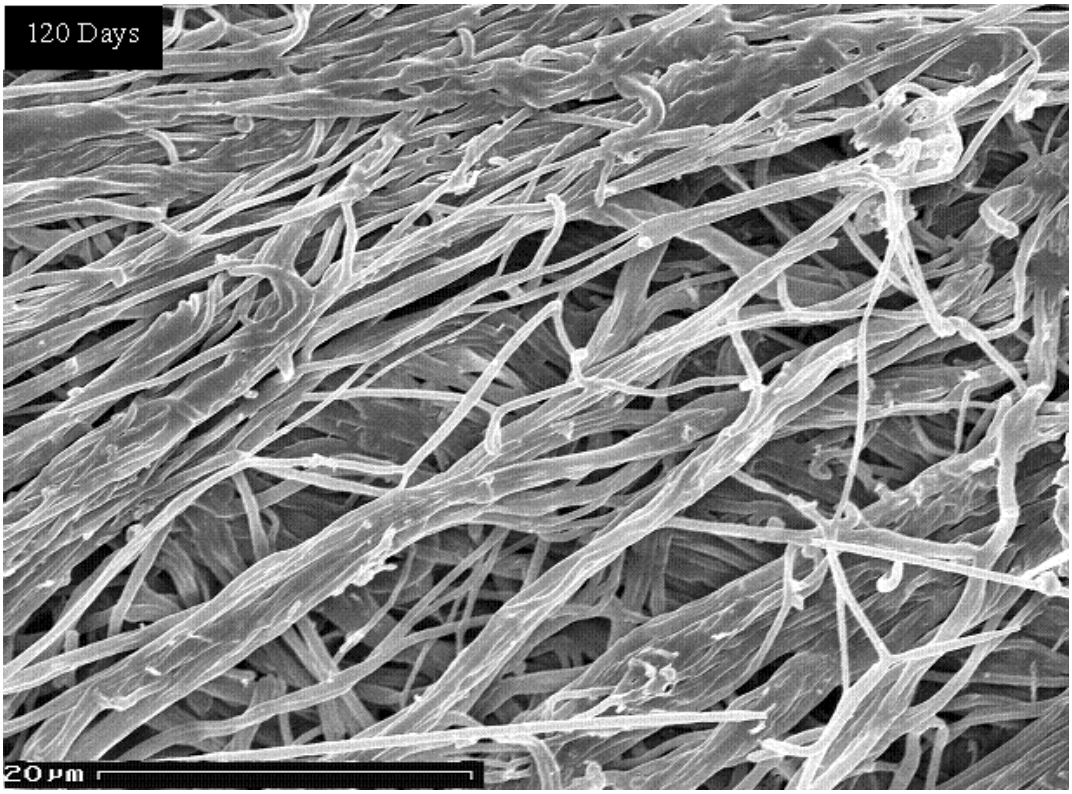

Figure 4.41 Degraded Fiber Images under SEM

Observing the surface of the fibers, after 45 days, localized morphological changes were first observed. Figure 4.42 shows a fiber sample after 100 days of exposure to PBS. Two locations, A and B, were found to exhibit apparent morphological transformations induced by degradation. At area A, numerous microcracks were observed along small segments of several adjacent fibers. Some cracks were barely observable and are seen as the tiny concaves. The small pinholes appeared to have just initiated and were about to propagate to the surrounding areas. There were also several cracks that had already deepened into fibers. At area B, one fiber had been cleaved into two shorter fibers as connected by the red line. Another fiber had almost been completely cleaved, as shown in the red rectangle.

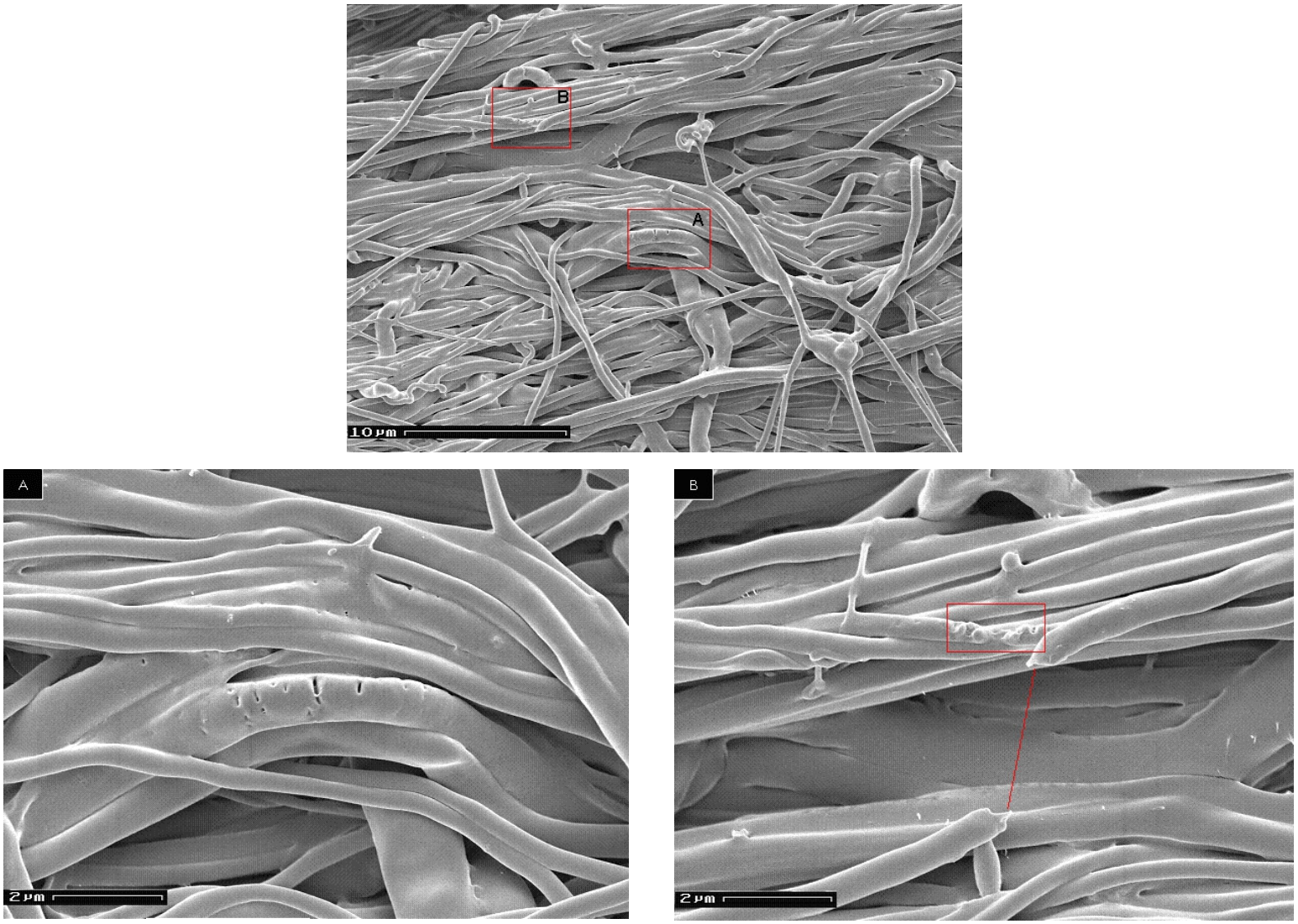

Figure 4.42 SEM Images of Degraded Fiber Samples Showing Morphology Changes

The morphological transformations of the fibers are very informative. Not only do they provide information about the fiber degradation mechanisms, but the transformations also give hints about the microstructure of the fibers.

First of all, the degradation was not of the surface erosion mode. Degradation started from some points on the fiber surfaces and then propagated to the inside of the fiber. When a microcrack appeared on the fiber surface, the microcrack spread both circumferentially and transversely at the same time. Limited longitudinal propagation of the microcrack was observed at a later stage as well. The emergence of the microcracks seemed random among the fibers as well as along a single fiber. The sites of the initial microcracks must have had some "defects," where water molecules easily penetrated and attacked the ester bonds, not seen at other sites.

Second, the degradation had an attribute of localization. When one microcrack was located, it was very likely to find others in close proximity on the same fiber or on other adjacent fibers.

Third, the morphological transformation revealed the microstructure of fibers, i.e., the fibers were not homogeneously structured. Some regions were easy to degrade, and other regions were more difficult to degrade. In the SEM images of Figure 4.43, two adjacent fiber blocks, which were cleaved, were connected by microfibrils, and the surrounding area was already hydrolyzed away by water. The phenomena can be well explained using the fringed fibril model of fiber structure [156]. According to this model, fibers are composed of fibrils, which are clusters of molecular chains with a certain degree of orientation. Fibrils are made up of microfibrils, the most elementary component of fibrils. Microfibrils have both crystalline regions and amorphous regions. A schematic of the fringed fibril model is shown in Figure 4.44. The semi-crystalline structure of microfibrils accounts for the different degradation rate. In

amorphous regions, the polymer chains are loosely entangled, so that water molecules can easily penetrate. In crystalline regions, the polymer chains are tightly packed with order; therefore, it is not as easy for the water molecules to penetrate, compared with the amorphous regions.

Fourth, the microfibrils connecting the fiber segments suggested that the polymer molecular chains had orientation along the fiber length. This verified the reorganization of the molecular chains under the stretching power of the electric field during spinning.

Although the tensile properties of the degraded fibers were not evaluated, it could be concluded that with the presence of microcracks, especially the localized and gathered microcracks, fiber tensile strength would be greatly impaired. The strength of a fiber is the strength of the weakest point along the fiber's length. With the microcracks, even the smallest cracks, under tension, would propagate very quickly, and fibers would rupture immediately.

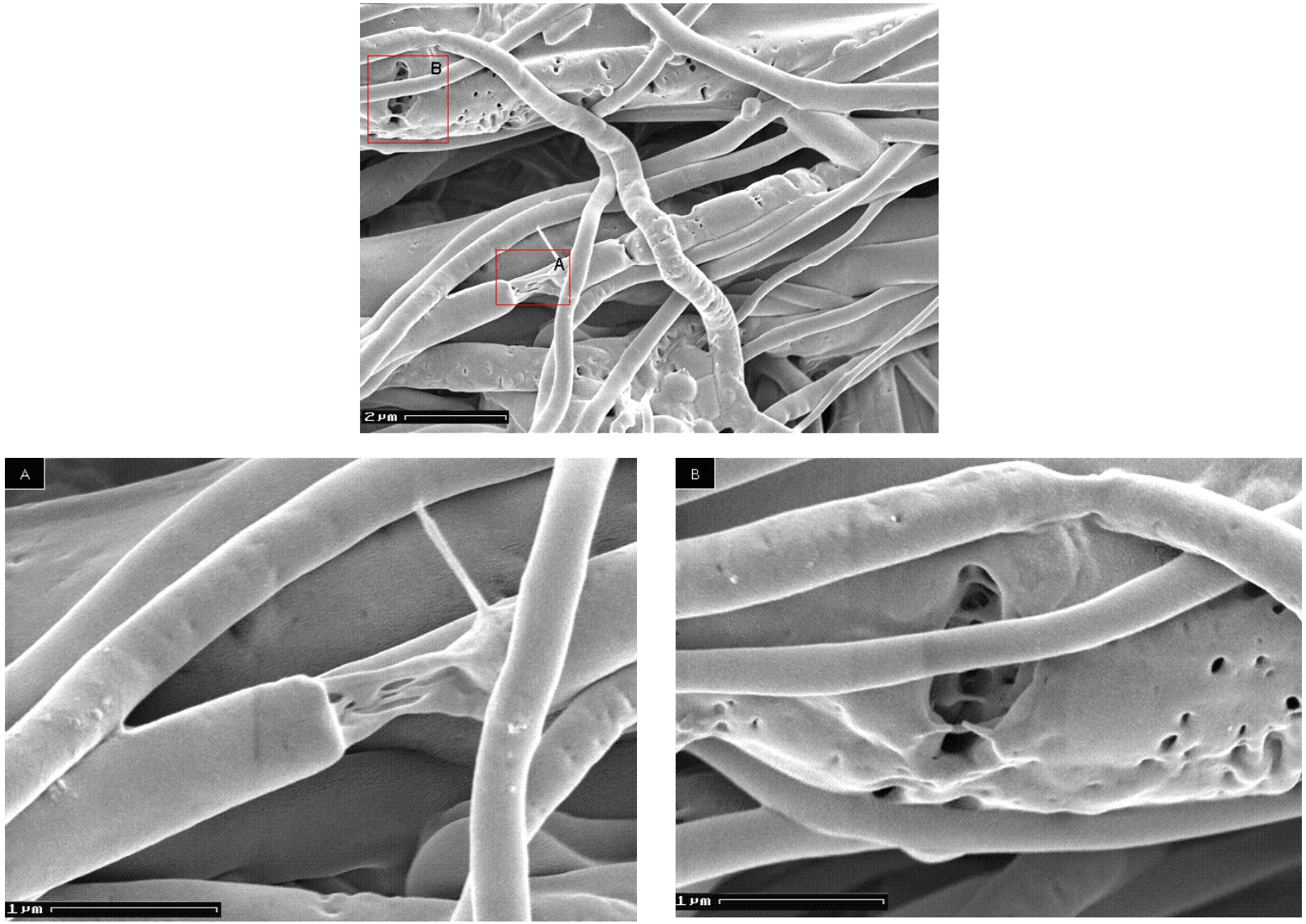

Figure 4.43 SEM Images of Degraded Fiber Samples Showing Microfibrils

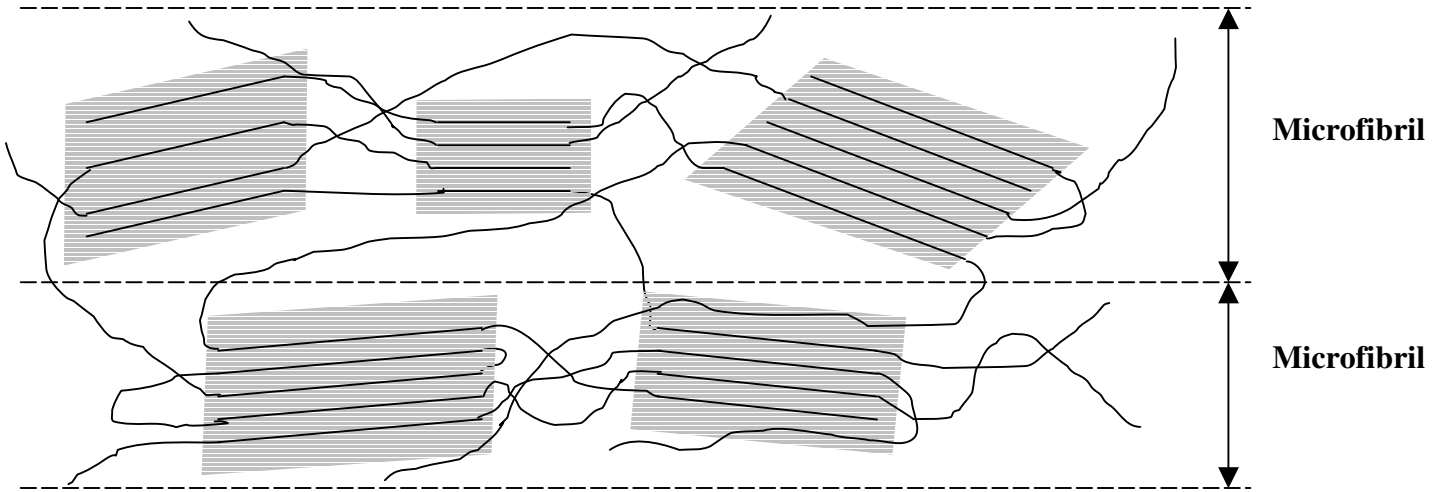

Figure 4.44 Schematic of the Fringed Fibril Model of the Fiber Structure

Chapter 5. Conclusion and Future Work

5.1 Conclusion

As we move into the 21st century, the process of making continuous nanofibers, electrospinning, has attracted the interest of many researchers from a variety of areas, including chemistry, physics, materials, bioengineering, and textiles. Intensive efforts have been made to develop this versatile and seemingly simple technique: determining its mechanisms, improving its performance, and expanding its applications. Electrospinning is currently the only technique available to make continuous nanofibers and fabricate various fiber assemblies, in which the orientation of fibers is controllable. The importance of electrospinning is vital in areas where orientated fibers are required, such as fiber-reinforced materials and most textile biomaterials, including sutures.

As very few published research reports are available that concentrate on the significance of the application of nanofibers to textile biomaterials, this study focused on the use of electrospinning to produce biodegradable suture fibers with antimicrobial properties. The polymer used to produce fibers in this study was polycaprolactone, and the antimicrobial agent was ampicillin sodium salt. This research was carried out in three steps: 1) the design of the electrospinning apparatus, 2) the production of fiber samples, and 3) the evaluation of selected fiber properties. The results and implications of each of these steps are discussed below.

The high voltage supply, the syringe pump, and the fiber collector are the three main components in the electrospinning apparatus. Each one controls some part of the spinning process parameters. The alignment of the collected fibers is primarily determined by the

collector. In this study, the fiber collector was designed to collect well-aligned fibers bundles. This goal was achieved by using a rotating thin disk as the collector. After the collected fiber bundles are twisted into yarns, they can be handled as conventional textile yarns. As has been done in this study, the yarns were tested for their antimicrobial properties, the release of the antimicrobial agent, and tensile properties. The results of this testing indicated that the yarns should be able to withstand other tests or treatments. Taking sutures as an example of the final product, the twisted yarns can be coated to improve the surface smoothness and sterilized to kill microorganisms that contaminate the yarns.

Using the electrospinning equipment in this study, continuous fibers with diameters between 0.26 μm and 1.59 μm were produced by varying the polymer concentration, the ampicillin concentration, and the electrospinning processing parameters, which included the applied voltage, distance between the needle tip and the collector, and feedrate. The fiber diameter increased by increasing the polymer concentration, decreasing the ampicillin concentration, reducing the voltage, shortening the distance, and increasing the feedrate. The diameter of the fibers was directly influenced by the extent to which the polymer jet was stretched under the electric field and the amount of polymer solution available at the tip of the needle.

As to the alignment of fibers in the fiber bundle, no quantitative measurement had been made on the degree of alignment since when the rotating speed of the collector was set to 1500 rpm the fibers had good alignment. The alignment was observed using an optical microscope, and the collected fibers were oriented along the rotating direction of the collector.

The stretching of the polymer jet influenced not only the diameter of fibers but also their internal fiber structure. A more stretched polymer jet resulted in a higher percentage of fiber

crystallinity. For example, when the voltage increased, the crystallinity increased; and when the distance was increased, the crystallinity increased. However, the incorporation of ampicillin in the polymer solution decreased the crystallinity of the fibers, and this decrease was more pronounced when the voltage was low. The crystallinity of the fibers produced in this study ranged approximately from 14% to 56%. The wide range of crystallinity suggested that fibers with various mechanical properties could be manufactured, such as fibers with different stress-strain profiles and different elasticity. The semi-crystalline structure of the fibers provided the fibers with flexibility and toughness. When the voltage was 9 kV and the distance was 8 cm, the crystallinity of the fibers was between 40% and 60%, which was in the textile-usable range.

The tensile properties of the electrospun fiber yarns were measured. The influence of ampicillin concentration on tensile properties was studied. The pure PCL fibers (spinning conditions: FR = 0.3 ml/h; D = 8 cm; V = 9 kV) had a mean elongation of approximately 66% and a mean load of 2.12 N. With the addition of ampicillin, the elongation did not change significantly, but the load of the yarns increased significantly. The yarns of fibers with 16% ampicillin had the largest load at almost 4 N. The load-elongation curves of the electrospun yarns were typical of the stress-strain curves of the usual fiber yarns, which indicated that the breaking mechanism of electrospun yarns was similar to that of the traditional fiber yarns. Thus, as in the traditional yarns, both the physical and mechanical properties of the fibers and the arrangement of the fibers in the yarns influenced the yarn tensile properties. The elongation of the yarns was a little higher than the commercially used sutures. But this could be improved by pre-drawing, by coating yarn surfaces, or by increasing the yarn twist. These treatments would also affect the load that yarns could withstand.

One of the most important attributes of the fibers produced in this study, the antimicrobial properties, were also tested *in vitro* for the yarns. The effectiveness of as-spun yarns on two microorganisms, gram-positive *S. aureus* and gram-negative *K. pneumoniae*, and the release profile of ampicillin from yarns were evaluated. The results on the zone of inhibition suggested that the ampicillin retained its antimicrobial effectiveness after being incorporated into the polymer solution, spun into fibers, and released from the fibers. This antimicrobial agent worked more effectively on *S. aureus* than on *K. pneumoniae*. The release profile showed that the ampicillin was almost completely released from the fibers in 48 hours. A burst depletion of more than 75% was observed in the first hour, which indicated an accumulation of ampicillin on the fiber surfaces. Overall, the incompatibility of hydrophilic ampicillin in lipophilic PCL resulted in the quick release. Extending the release time or decreasing the release speed, using other antimicrobial agents, which have better compatibility with PCL, could be considered. The release profile could not be explained by any of the popular models typically used in drug release studies. The mechanism(s) of ampicillin release from electrospun PCL fiber needs further investigation.

The *in vitro* degradation of the electrospun yarns was accessed from two aspects, mass loss and surface morphology change. The mass loss of yarns with various ampicillin concentrations in 12 weeks was less than 3%. For those yarns containing ampicillin, the higher the ampicillin concentration, the faster the rate of degradation. All fibers had faster release rates in the first three weeks of the study than in the following time period. But, generally speaking, PCL degraded slowly. The surface morphology change of fibers was first observed after six weeks' degradation. Microcracks were observed on fiber surfaces. The morphological changes revealed the attributes of the degradation. First, the degradation started from some "defects" on

the fibers, where the access of water was easier. Second, the degradation was localized. Microfibrils connecting two adjacent fiber blocks were observed. The existence of microfibrils further verified the semi-crystalline structure of the fibers and the orientation of molecular chains along the direction of the fiber length.

In conclusion, electrospinning is a very useful technique for producing continuous fibers and producing fibers with inherent antimicrobial properties by incorporating antimicrobial agents in the polymer solution before spinning. Using appropriate spinning conditions and collecting methods, the produced electrospun nanofibers can be fabricated into yarn. This is a significant breakthrough benefiting the expansion of nanofiber applications. Currently, the application of nanofibers is limited to where nanofiber webs can be used since single fibers cannot be physically manipulated due to their small size. This method of forming nanofiber yarns may provide the basic technique necessary for the application of nanofibers as conventional fibers while taking advantage of the superior physical and mechanical properties of nanofibers. By using degradable polymers, the electrospun nanofiber products will be degradable, which will be environmentally beneficial, and the products could be used on bioimplants. Finally, the successful incorporation of the antimicrobial agent into electrospun nanofibers suggests that it is efficient to use electrospinning to produce fibers with the incorporation of some agents to provide fibers with the desirable inherent properties.

5.2 Recommendations for Future Work

Based on the work that has been done in this study, the recommendations that the author would like to propose for future work include the following:

1) The results showed that the polymer solution properties and spinning processing parameters influenced fiber diameter. Further investigation of the fiber diameter

distribution will provide additional information on fiber diameter evenness beyond that provided by standard deviation.

2) Other antimicrobial agents, especially those with better compatibility than the ampicillin sodium salt to PCL, should be investigated to study the antimicrobial release profile.

3) The change in fiber morphology during degradation, such as the percentage of crystallinity, may provide additional information that will contribute to better understanding of the degradation mechanisms of the electrospun PCL fibers.

4) The study of tensile properties indicated that nanofiber yarns with ampicillin could withstand a higher load than pure PCL yarns. This should be further investigated for a better understanding of this relationship.

REFERENCES

1. MedicineNet.com, Definition of suture. http://www.medterms.com/script/main/art.asp?articlekey=5604 (Accessed August 1 2005).

2. Meyer, R. D., and Antonini, C. J., A review of suture materials, Part I. *Compendium of Continuing Education in Dentistry* **1989,** X, (5), 260-265.

3. Dumitriu, S., *Polymeric biomaterials*. 2nd ed.; Marcel Dekker: New York, 2002.

4. Cheng, Sutures-resorption. http://www.me.berkeley.edu/ME117/S05/finalproject.html (Accessed August 10 2005).

5. Rater, B. D., Hoffman, A.S., Schoeon, F.J., and Lemons, J.E., *Biomaterials Science (2nd Ed.)*. Elsevier Academic Press: New York, 2004.

6. Chu, C. C., *Wound closure biomaterials and devices*. 2nd ed.; CRC Press: New York, 1997.

7. Ratner, B. D., Hoffman, A. S., Schoeon, F. J. and Lemons, J. E., *Biomaterials Science (2nd Ed.)*. Elsevier Academic Press: New York, 2004.

8. Elek, S. D. and Conen, P. E., The virulence of *S. pyogenes* for man. A study of the problems of wound infection *British Journal of Experimental Pathology* **1957,** 38, 573-586.

9. Bide, M., Bachuwar, A., Phaneuf, M., Phaneuf, T., Aggarwal, P., Sousa, K., and LoGerfo, F., Fiber-antibiotic interactions in the development of infection resistant sutures. *American Association of Chemist and Colorist, International Conference Proceedings* **2005**, 291-296.

10. Mangram, A. J., Horan, T.C., Pearson, M.L., Silver, L.C., and Jarvis, W.R., Guideline for prevention of surgical site infection, 1999. *Infection Control and Hospital Epidermiology* **1999,** 20, (4), 247-278.

11. Ford, H. R., Jones, P., Gaines, B., Reblock, K. and Simpkins, P. L., Intraoperative handling and wound healing: controlled clinical trial comparing coated Vicryl® Plus antibacterial suture (coated polyglactin 910 suture with triclosan) with coated Vicryl® suture (coated polyglactin 910 suture) *Surgical infections* **2005,** 6, (3), 313-321.

12. Gómez-Alonso, A. and Garcia-Criado, F. J., Study of the efficacy of coated Vicryl Plus® antibacterial suture (coated polyglactin 910 suture with triclosan) in two animal models of general surgery. *Journal of Infection* **2006,** 52, 82-88.

13. Ethicon:a johnson & johnson company, Ethicon receiveds FDA clearance to market Vicryl* Plus, first ever antibacterial suture. www.ethicon.com/bgdisplay.jhtml?itemname=News_Vicrylplus_02 (Accessed July 1 2006).

14. Chu, C. C., Tsai, W. C., Yao, J. Y. and Chiu, S. S., Newly made antibacterial braided nylon sutures. I. *In vitro* qualitative and *in vivo* preliminary biocompatibility study. *Journal of Biomedical Materials Research* **1987,** 21, (11), 1281-1300.

15. King, M. W., Jones, A.D., and Shalaby, S.W., Sutures with antimicrobial performance. *Clemson University Conference on Medical Textiles, Westin Poinsett Hotel, Greenville, SC* **2004**.

16. Sergeev, V. P., Development of method of manufacturing modified sutures corresponding to current requirements in medicine. *Fibre Chemistry* **2002,** 34, (6), 433-439.

17. Tsai, W. C., Chu, C. C., Chiu, S. S. and Yao, J. Y., *In Vitro* quantitative study of newly made antibacterial braided nylon sutures. *Surgery Gynecology & Obstetrics* **1987,** 165, (3), 207-211.

18. Capperauld, I., Suture materials: a review. *Clinial Materials* **1989,** 4, 3-12.

19. Chu, C. C., Textile-based biomaterials for surgical applications. In *Polymeric biomaterials*, Dumitriu, S., Ed. Marcel Dekker, Inc. : New York, 2002.

20. Ethicon:a johnson & johnson company, Ethicon brands. http://www.ethicon.novartis.us/brands/en/vicryl_plus.shtml (Accessed June 24 2006).

21. Forrester, J. C., Suture mateirals and their use. *British Journal of Hospital Medicine* **1972,** 8, (5), 578-592.

22. Hendrickson, A., Sutures: Past, present, and future. *Innovations in Veterinary Surgery* **2004**, (10), 10-14.

23. Jerrmann, J. B., Changes in tensile strength and knot security of surgical sutures *in vivo*. *Archives of Surgery* **1973,** 106, (5), 707-710.

24. Terhune, M., Materials for wound closure. http://www.emedicine.com/derm/tipic825.htm (Accessed June 24 2006).

25. Freudenberg, S., Rewerk, S., Kaess, M., Weiss, C., Dorn-Beinecke, A. and Post, S., Biodegradation of absorbable sutures in body fluids and pH buffers. *European Surgical Research* **2004,** 36, 376-385.

26. Chu, C. C., *Wound Closure Biomaterials and Devices*. 2nd ed.; CRC Press: New York, 1997.

27. Chu, C. C., Mechanical properties of suture mateirals: an important characterization. *Annals of Surgery* **1981,** 193, 365-371.

28. Holmlund, E. W., Physical properties of surgical suture materials: stress-strain relationship, stress relaxation and irreversible elongation. *Annals of Surgery* **1976,** 184, 189-193.

29. Thacker, J. G., Rodeheaver, G. T. and Morre, J. W., Mechanical performance of surgical sutures. *American Journal of Surgery* **1975,** 130, 374-380.

30. Stone, I. K., von Fraunhofer, J. A. and Masterson, B. J., Mechanical properties of coated absorbable multifilament suture materials. *Surgery Gynecology & Obstetrics* **1986,** 67, 737-740.

31. von Fraunhofer, J. A., Storey, R. S., Stone, I. K. and Masterson, B. J., Tensile strength of suture materials. *Journal of Biomedical Materials Research* **1985,** 19, (5), 595-600.

32. Chu, C. C., *Wound closure biomaterials and devices*. 2nd ed.; CRC Press: New York, 1997.

33. Chu, C. C. and Kizil, Z., Quantitative evaluation of stiffness of commercial suture materials. *Surgery Gynecology & Obstetrics* **1989,** 168, 233-238.

34. Metz, S. A., von Fraunhofer, J.A., and Masterson, B.J., Stress relaxation of organic suture materials. *Biomaterials* **1990,** 11, (4), 197-199.

35. van Rijssel, E. J., Brand, R., Admiraal, C., Smit, I. and Trimbos, J. B., Tissue reaction and surgical knots: the effect of suture size, knot configuration, and knot volume. *Obstetrics Gynecology* **1989,** 74, (1), 64-68.

36. Trimbos, J. B., Brohim, R. and van Rijssel, E. J., Factors relating to the volume of surgical knots. *International Journal of Gynaecology & Obstetertrics* **1989,** 30, (4), 355-359.

37. Rodeheaver, G. T., Thacker, J. G. and Edlich, R. F., Mechanical performance of polyglycolic acid and polyglactin 910 synthetic absorbable sutures. *Surgery, Gynecology & Obstetrics* **1981,** 153, (6), 835-841.

38. Geiger, D., Debus, E. S., Ziegler, U. E., Larena-Avellaneda, A., Frosch, M., Thiede, A. and Dietz, U. A., Capillary activity of surgical sutures and suture-dependent bacterial transport: a qualitative study. *Surgical Infections (Larchmt)* **2005,** 6, (4), 377-83.

39. Lilly, G. E., Osbon, D.B., Clinial and bacteriological aspects of polyglycolic acid sutures. *Journal of Oral Surgery* **1973,** 31, 103-105.

40. Meyer, R. D., and Antonini, C. J., A review of suture materials, Part II. *Compendium of Continuing Education in Dentistry* **1989,** 10, (6), 360-364.

41. Shishatskaya, E. I., Volova, T. G., Puzyr, A. P. and Mogilnaya, O. A., Tissue response to the implantation of biodegradable polyhydroxyalkanoate sutures. *Journal of Materials Science: materials in Medicine* **2004,** 15, 719-728.

42. Juszkiewicz, M., Experiments on new synthetic and non-absorbable surgical threads. *Polim Med* **1998,** 28, (1-2), 33-58.

43. Molea, G., Schonauer, F., Bifulco, G. and D'Angelo, D., Comparative study on biocompatibility and absorption times of three absorbable monofilament suture materials (Polydioxanone, Poliglecaprone 25, Glycomer 631). *British Journal of Plastic Surgery* **2000,** 53, 137-141.

44. Smit, I. B., Witte, E., Brand, R. and Trimbos, J. B., Tissue reaction to suture materials revisited: is there argument to change our views? *European Surgical Research* **1991,** 23, (5-6), 347-354.

45. Karaca, E., Kochenberger, A.S., and Yildiz, H., Investigating changes in mechanical properties and tissue reaction of silk, polyester, polyamide and polypropylene sutures *in vivo*. *Journal of Textile Research* **2005,** 75, (4), 297-303.

46. Rodeheaver, G. T., Beltran, K. A., Green, C. W., Fraulkner, B. C., Stiles, B. M., Stanamir, G. W., Traeland, H., Fried, G. M., Brown, H. C. and Edllich, R. F., Biomechanical and clinical performance of a new synthetic monofilament absorbable suture. *Journal of Long-term Effects Med. Implants* **1996,** 6, (3-4), 181-198.

47. Shalaby, S. W. and Burg, K. J. L., *Absorbable and Biodegradable Polymers*. CRC Press: New York, 2004.

48. Athanasiou, K. A., Niederauer, G. G. and Agrawal, C. M., Sterilization, toxicity, biocompatibility and clinical applications of polylactic acid/polyglycolic acid copolymers. *Biomaterials* **1996,** 17, (2), 93-102.

49. Kulkarni, R. K., Pani, K., C., Neuman, C. and Leonard, F., Polylactic acid for surgical implants. *Archives of Surgery* **1966,** 93, 839-843.

50. Postlethwait, R. W., Polyglycolic acid surgical suture. *Archives of Surgery* **1970,** 101, 489-494.

51. Frazza, E. J. and Schmitt, E. E., A new absorbable suture. *Journal of BIomaterials Research Symposium* **1971,** 1, 43-58.

52. Cutright, D. E., Hunsuck, E. E. and Veasley, J. D., Fracture reduction using a biodegradable material, polylactic acid. *Journal of Oral and Maxillofacial Surgury* **1971,** 29, 393-397.

53. Schakenraad, J. M., Oosterbaan, J. A. and Nieuwenduis, P., Biodegradable hollow fibers for the controlled release of drugs. *Biomaterials* **1988,** 9, 116-120.

54. Schakenraad, J. M., Hardonk, M. J., Feijen, J., Molenaar, I. and Nieuwenhuis, P., Enzymatic activity toward poly(L-lactic acid) implants. *Journal of Biomedical Materials Research* **1990,** 24, 529-545.

55. Cutright, D. E. and Hunsuck, E. E., Tissue reaction to the biodegradable polylactic acid suture. *Journal of Biomedical Materials Research* **1971,** 31, 169-181.

56. Shikanov, A., Kumar, N. and Domb, A. J., Biodegradable polymers: An update. *Isreal Journal of Chemistry* **2005,** 45, 393-399.

57. Vigo, T. R. and Turbak, A. F., *Hi-Tech Fibrous Materials*. American Chemical Society Symp. Ser. 457: Washington, D.C., 1991.

58. Browning, A. and Chu, C. C., The effect of annealing treatments on the tensile properties and hydrolysis degradatio properties of polyglycolic acid stuures. *Journal of Biomedical Materials Research* **1986,** 20, 613-632.

59. Chu, C. C. and Louie, M., A chemical means to examine the degradation phenomena of polyglycomlic acid fibers. *Journal of Applied Polyer Science* **1985,** 30, 3133-3141.

60. Fredericks, R. J., Melveger, A. J. and Dolegiewetz, L. J., Morphological and structural changes in a copolymer of glycolide and lactide occurring as a result of hydrolysis. *Journal of polymer science. Polymer physics edition.* **1984,** 22, 57-66.

61. Chu, C. C., The effect of pH on the *in vitro* degradation of poly(glycolide-lactide) co-polymer absorbable sutures. *Journal of Applied Polymer Science* **1982,** 16, 117-124.

62. Chu, C. C., *In-vitro* degradation of polyglycolic acid sutures: effect of pH. *Journal of Biomedical Materials Research* **1981,** 15, 794-804.

63. Chu, C. C., A comparison of the effect of pH on the biodegradation of two synthetic absorbable sutures. *Annals of Surgery* **1982,** 195, 55-59.

64. Chu, C. C. and Moncrief, G., An *in-vitro* evaluation of the stability of mechanical properties of srugical suture materials in various pH conditions. *Annals of Surgery* **1983,** 198, 223-228.

65. Tomihata, K., Suzuki, M. and Ikada, Y., The pH dependent of monofilament sutures on hydrolytic degradation. *Journal of Biomedical Materials Research, Applied Biomaterials* **2001,** 58, (5), 511 - 518.

66. Chu, C. C., *Wound Closure Biomaterials and Devices*. 2nd ed.; CRC Press: New York, 1997.

67. Pratt, L., Chu, C., Auer, J., Chu, A., Kim, J., Zollweg, J. A. and Chu, C. C., The effect of ionic electrolytes on hydrolytic degradation of biodegradable polymers: mechanical properties, thermodynamics and molecular modeling. *Journal of polymer science. Chemistry edition.* **1993,** 31, 1759-1769.

68. Hall, C. W., *Surgical Research -- Recent Developments*. Pergamon Press: New York, 1985.

69. Zhong, S. P., Doherty, P. J. and Williams, D. F., The effect of applied strain on the degradation of absorbable suture *in vivo*. *Clinical Materials* **1993,** 14, 183-189.

70. Miller, N. D., and Williams, D.F., The *in vivo* and *in vitro* degradation of poly(glycolic acid) suture material as a function of applied strain. *Biomaterials* **1984,** 5, 365-368.

71. Shikanov, A., Caisman, B., Krasko, M. Y., Nyska, A. and Domb, A. J., Poly(sebacic acid-co-ricinoleic acid) biodegradable carrier for paclitaxel: *In vitro* release and *in vivo* toxicity. *Journal of Biomedical Materials Research Part A* **2004,** 69A, (1), 47 - 54.

72. Giunchedi, P., Conti, B., Scalia, S. and Conte, U., *In vitro* degradation study of polyester microspheres by a new HPLC method for monomer release determination *Journal of Controlled Release* **1998,** 56, (1), 53-62.

73. Miyajima, M., Koshika, A., Okada, J., Kusai, A., and Ikeda, M., The effects of drug physico-chemical properties on release from copoly (lactic/glycolic acid) matrix *International Journal of Pharmaceutics* **1998,** 169, (2), 255-263.

74. Li, S. M., Girod-Holland, S., Vert, M., Hydrolytic degradation of poly(-lactic acid) in the presence of caffeine base *Journal of Controlled Release* **1996,** 40, (1), 41-53.

75. Athanasiou, K. A., Niederauer, G. G. and Agrawal, C. M., Sterilization, toxicity, biocompatibility and clinical applications of polylactic acid/polyglycolic acid copolymers. *Biomaterials* **1996,** 17, 93-102.

76. Costerton, J. W., Cheng, K. J., Geesey, G. G., Ladd, T. I., Nickel, J. C., Dasgupta, M. and Marrie, T. J., Bacterial biofilms in nature and disease. *Annual Review of Microbiology* **1987,** 41, 435-464.

77. Donlan, R. M. and Costerton, J. W., Biofilms: Survival mechanisms of clinically relevent microorganisms. *Clinial Microbiology Reviews* **2002,** 15, (2), 167-193.

78. Costerton, J. W., Stewart, P. S. and Greenberg, E. P., Bacterial biofilms: a common cause of persistent infections. *Science* **1999,** 284, 1318-1322.

79. Marrie, T. J., Nelligan, J., and Costerton, J.W., A scanning and transmission electron microscopic study of an infected endocardical pacemaker lead. *Circulation* **1982,** 66, 1339-1341.

80. Otten, J. E. and Wiedmann-Al-Ahmad, M., Bacterial colonization on different materials - A potential risk for introoral dentoalveolar surgery. *Journal of Biomedical Materials Research, B: Applied Biomaterials* **2005,** 74, (1), 627-635.

81. Mainil-Varlet, P., Hauke, C., Maquet, V., Printzen, G., and Arens, S., Polylactide implants and bacterial contamination: an animal study. *Journal of Biomedical Materials Research* **2001,** 54, (3), 335-343.

82. Chu, C. C., and Williams, D.F., Effects of physical configuration and chemical structure of suture materials on bacterial adhesion. *American Journal of Surgery* **1984,** 147, (2), 197-204.

83. Katz, S., Izhar, M., and Mirelman, D., Bacterial adherence to surgical sutures. *Annals of Surgery* **1981,** 194, (1), 35-41.

84. Todar, K., Antimicrobial agents used in treatment of infectious disease. http://textbookofbacteriology.net/antimicrobial.html (Accessed Feburary 13 2006).

85. Prescott, L. M., Harley, J. P. and Klein, D. A., *Microbiology, 5th Ed.* McGraw Hill: New York, 2002.

86. Echeverria, A. E. and Olivares, L., Clinical and experimental evaluation of suture materials treated with antibiotics. *The American Journal of Surgery* **1957,** 98, (11), 695-701.

87. Blaker, J. J., Nazhat, S. N. and Boccaccini, A. R., Development and characterisation of silver doped bioactive glass coated sutures for tissue engineering and wound healing applications. *Biomaterials* **2004,** 25, 1319-1329.

88. Kovtun, E. A., Plygan, E. P., Gudz, O.V., and Sergeev, V.P., Creation of sutures with antimicrobial properties. *Fibre Chemistry* **2000,** 32, (4), 287-292.

89. Kovtun, E. A., Baglei, N. N, Plygan, E. P., Sergeev, V.P., Study of the kinetics of release of decametoxin from modified surgical sutures in aqueous medium. *Fibre Chemistry* **1999,** 31, (5), 374-379.

90. Kovtun, E. A., Plygan, E. P., and Sergeev, V.P., Study of the stability of modified sutures in biological medium. *Fibre Chemistry* **2000,** 32, (6), 441-443.

91. Storch, M., Scalzo, H., Van Lue, S. and Jacinto, G., Physical and functional comparison of Coated VICRYL* Plus Antibacterial Suture (coated polyglactin 910 suture with triclosan) with Coated VICRYL* Suture (coated polyglactin 910 suture). *Surgical Infections (Larchmt)* **2002,** 3 Suppl 1, S65-77.

92. Rothenburger, S., Spangler, D., Bhende, S. and Burkley, D., *In vitro* antimicrobial evaluation of Coated VICRYL* Plus Antibacterial Suture (coated polyglactin 910 with triclosan) using zone of inhibition assays. *Surgical Infections (Larchmt)* **2002,** 3 Suppl 1, S79-87.

93. Storch, M. L., Rothenburger, S. J. and Jacinto, G., Experimental efficacy study of coated VICRYL plus antibacterial suture in guinea pigs challenged with Staphylococcus aureus. *Surgical Infections (Larchmt)* **2004,** 5, (3), 281-288.

94. Ethicon:a johnson & johnson company, Human clinical trials indicate Vicryl* Plus sutures provide added benefits while achieving standard suture safety, handling and healing performance. www.ethicon.com/bgdisplay.jhtml?itmname-News_Vicrylplus_01 (Accessed July 1 2006).

95. Storch, M., Perry, L. C., Davidson, J. M. and Ward, J. J., A 28-day study of the effect of Coated VICRYL* Plus Antibacterial Suture (coated polyglactin 910 suture with triclosan) on wound healing in guinea pig linear incisional skin wounds. *Surgical Infections (Larchmt)* **2002,** 3 Suppl 1, S89-98.

96. Defazio, A., M., D. and C., N., Does the use of Vicryl™ Plus Antibacterial Suture Decrease the Incidence of Umbilical Infection When Compared to Vicryl™ Suture? *Fertiligy & Sterility* **2005,** 84, (Supplement 1), S161.

97. Lewin, M., and Sello, S., *Handbook of Fiber Science and Technology: Volume II Chemical Processing of Fibers and Fabrics, Functional Finishes: Part A: Protection of Textiles from Biological Attack*. Marcel Dekker Inc,: New York, 1984.

98. Bide, M., Phaneuf, M., Ozaki, C., Quist, W. and LoGerfo, F., The use of dyeing technology in biomedical applications. *Textile Chemists and Colorists* **1993,** 25, (1), 15-19.

99. Choi, H. M. and Bide, M., Antibiotic treatment of silk to produce novel infection-resistant biomaterials. *Textile Research Journal* **2004,** 74, (3), 333-342.

100. Huang, Z., Zhang, Y., Kotaki, M. and Ramakrishna, S., A review on polymer nanofibers by electrospinning and their applications in nanocomposites. *Composites Science and Technology* **2003,** 63, 2223-2253.

101. Doshi, J. and Reneker, D. H., Electrospinning process and applications of electrospun fibers. *Journal of Electrostatics* **1995,** 35, 151-160.

102. Hegde, C. C., Dahiya, A. and Kamath, M. G., Nanofiber nonwovens. http://web.utk.edu/~mse/pages/Textiles/Nanofiber%20Nonwovens.htm (Accessed August 13 2006).

103. Formhals, A. Process and apparatus for preparing artifical threads. US Patent: 1975504, 1934.

104. Formhals, A. Method and apparatus for spinning. US Patent: 2160962, 1939.

105. Formhals, A. Artifical thread and method of producing same. US Patent: 2187306, 1940.

106. Formhals, A. Production of artifical fibers from fiber forming liquids. US Patent: 2323025, 1943.

107. Formhals, A. Method and apparatus for spinning. US Patent: 2349950, 1944.

108. Kalayci, V. K., Patra, P.K. and Warner, S.B., Electrostatic spinning and properties of ultrafine fibers. In http://www.umassd.edu/engineering/textiles/research/electrospinning: 2005.

109. Caruso, R. A., Schattka, J. H. and Greiner, A., Titanium dioxide tubes from sol-gel coating of electrospun polymer fibers. *Advanced Materials* **2001,** 13, (20), 1577-1579.

110. Bognitzki, M., Czado, W., Frese, T., Schaper, A., Hellwig, M., Steinhart, M., Greiner, A. and Wendorff, J. H., Nanostructured fibers via electrospinning *Advanced Materials* **2001,** 13, 70-72.

111. Megelski, S., Stephens, J.S., Chase, D.B., and Rabolt, J.F., Micro- and nanostructured surface morphology on electrospun polymer fibers. *Macromolecules* **2002,** 35, (22), 8456-8466.

112. Casper, C. L., Stephens, J. S., Tassi, N. G., Chase, D. B. and Rabolt, J. F., Controlling surface morphology of electrospun polystyrene fibers: Effect of humidity and molecular weight in the electrospinning process. *Macromolecules* **2004,** 37, 573-578.

113. Zhao, S. L., Wu, X. H., Wang, L. G. and Huang, Y., Electrospinning of ethylcyanoehtyl cellulose/tetrahydrofuran solutions. *Journal of Applied Polyer Science* **2004,** 91, 242-246.

114. Fong, H., Liu, W. D., Wang, C. S. and Vaia, R. A., Beaded nanofibers formed during electrospinning. *Polymer* **1999,** 40, 4585-4592.

115. Kameoka, J., Orth, R., Yang, Y., Czaplewski, D., Mathers, R., Coates, G and Craighead, H.G., A scanning tip electrospinning source for deposition of oriented nanofibers. *Nanotechnology* **2003,** 14, 1124-1129.

116. Zhong, X. H., Kim, K. S., Fang, D. F., Ran, S. F., Hsiao, B. S. and Chu, B., Structure and process relationship of electrospun bioabsorbable nanofiber membrances. *Polymer* **2002,** 43, 4403-4412.

117. Ramakrishna, S., Fujihara, K., Teo, W. E., Lim, T. C. and Ma, Z. W., *An introduction to electrospinning and nanofibers*. World Scientific Publishing Co.Pte. Ltd.: Hackensack, NJ., 2005.

118. Zeng, J., Xu, X., C., X., Liang, Q., Bian, X., Yang, L. and Jing, X., Biodegradable electrospun fibers for drug delivery. *Journal of Controlled Release* **2003,** 92, 227-231.

119. Huang, L., Nagapudi, K., Apkarian, R. P. and Chaikof, E., Engineered collagen-PEO nanofibers and fabrics. *Journal of Biomaterials Science Polymer Edition* **2001,** 12, (9), 979-993.

120. Zong, X., Kim, K., Fang, D., Ran, S., Hsiao, B.S. and Chu, B, Structure and process relationship of electrospun bioabsorbable nanofiber membranes. *Polymer* **2002,** 43, 4403-4412.

121. Taylor, G., Disintegration of water drops in an electric field. *Proceedings of the Royal Society A* **1964,** 280, 383-397.

122. Lee, J. S., CHoi, K.H., Ghim, H.D., Kim, S.S., Chun, D.H., Kim, H.Y., and Lyoo, W.S., Role of molecular weight of atactic poly(vinyl alcohol) (PVA) in the structure and properties of PVA nanofabric prepared by electrospinning. *Journal of Applied Polyer Science* **2004,** 93, 1638-1646.

123. Deitzel, J. M., Kleinmeyer, J., Harris, D. and Tan, N. C. B., The effect of processing variables on the morphology of electrospun nanofibers and textiles. *Polymer* **2001,** 42, 261-272.

124. Casper, C. L., Stephens, J. S., Tassi, N. G., Chase, D. B. and Rabolt, J. F., Controlling surface morphology of electrospun polystyrene fibers: Effect of humidity and molecular weight in the electrospinning process. *Macromolecules* **2004,** 37, (2), 573-578.

125. Doshi, J., and Reneker, D.H., Electrospinning process and applications of electrospun fibers. *Journal of Electrostatics* **1995,** 35, 151-160.

126. Graham, K., Schreuder-Gibson, H. and Gogins, M. In *Incorporation of electrospun nanofibers into functional structures*, International Nonwoven Technical Conference, Baltimore, MD., September 15-18, 2003; Technical Association of the Pulp& Paper Industry: Baltimore, MD., 2003; pp 1-16.

127. Zeng, J., Xu, X., Chen, X., Liang, Q., Bian, X., Yang, L. and Jing, X., Ultrafine fibers electrospun from biodegradable polymers. *Journal of Applied Polyer Science* **2003,** 89, 1085-1092.

128. Tsai, P. P., Schreuder-Gibson, H. and Gibson, P., Different electrostatic methods for making electret filters. *Journal of Electrostatics* **2002,** 54, 333-341.

129. Acatay, K., Simsek, E., Akel, M. and Menceloglu, Y. Z., Electrospinning of low surface energy quaternary ammonium salt containing polymers and their antibacterial activity. In *Nanoengineered Nanofibrous Materials*, Guceri, S. I., Gogotsi, Y.and Kuzentsov, V., Eds. Kluwer Academic: Dordrecht, Netherlands, 2004; pp 97-106.

130. Lee, S. W., and Belcher, A.M., Virus-based fabrication of micro- and nanofibers using electrospinning. *Nano Letters* **2004,** 4, (3), 387-390.

131. Xu, X., Yang, Q., Wang, Y., Hu, H., Chen, X. and Jing, X., Biodegradable electrospun poly(L-lactide) fibers containing antibacterial silver nanoparticles. *European Polymer Journal* **2006,** 42, 2081-2087.

132. Kim, K., Luu, Y. K., Chang, C., Fang, D., Hsiao, B. S., Chu, B. and Hadjiargyrou, M., Incorporation and controlled release of a hydrophilic antibiotic using poly(lactide-co-glycolide)-based electrospun nanofibrous scaffolds. *Journal of Controlled Release* **2004,** 98, 47-56.

133. Theron, S. A., Zussman, E. and Yarin, A. L., Electrostatic field-assisted alignment of electrospun nanofibers. *Nanotechnology* **2001,** 12, 384-390.

134. Sundaray, B., Subramanian, V., Natarajan, T. S., Xiang, R. Z., Chang, C. C. and Fann, W. S., Electrospinning of continuous alinged polymer fibers. *Applied Physics Letters* **2004,** 84, (7), 1222-1224.

135. Bornat, A. Production of electrostatically spun products. Patent: 4689186, 1987.

136. Deitzel, J. M., Kleinmeyer, J., Harris, D., Hirvonen, J. K. and Tan, N. C. B., Controlled deposition of eelctrspun poly(ethylene oxide) fibers. *Polymer* **2001,** 42, 8163-8170.

137. Pan, H., Li, L., Hu, L. and Cui, X. J., Continuous aligned polymer fibers produced by a modified electrospinning method. *Polymer* **2006,** 47, 4901-4904.

138. Li, D., Wang, Y.L., and Xia, Y.N., Electrospinning nanofibers as uniaxially aligned arrays and layer-by-layer stacked films. *Advanced Materials* **2004,** 16, (4), 361-366.

139. Smit, E., Buttner, U. and Sanderson, R. D., Continous yarns from electrospun fibers. *Polymer* **2005,** 46, 2419-2423.

140. Dalton, P. D., Klee, D. and Moller, M., Electrospinning with dual collection rings. *Polymer* **2005,** 46, 611-614.

141. International Labour Organization, International Chemical Safty Card 0027. http://www.ilo.org/public/english/protection/safework/cis/products/icsc/dtasht/_icsc00/icsc0027.htm (Accessed January 17 2008).

142. International Labour Organization, International Chemical Safty Card 0057. http://www.ilo.org/public/english/protection/safework/cis/products/icsc/dtasht/_icsc00/icsc0057.htm (Accessed January 17 2008).

143. Nava, D., Salom, C., Prolongo, M.G., and Masegosa, R.M., Thermal properties and interactions in blends of poly(e-caprolactone) with unsaturated polyester resins. *Journal of Materials Processing Technology* **2003,** 143, (122), 171-174.

144. Williamson, M. R., Adams, E. F. and Coombes, A. G. A., Cell attachment and proliferation on novel polycaprolactone fibres having application in soft tissue engineering. *European Cells and Materials* **2002,** 4, (Suppl.2), 62-63.

145. Rutledge, G. C. and Shin, M. Y. *A fundamental investigation of the formation and properties of electrospun fibers*; NTC M98 -D01; 2001.

146. Rutledge, G. C., LI, Y., Fridrikh, S., Warner, S. B., Kalayci, V. E. and Patra, P. In *Electrostatic spinning and properties of ultrafine fibers*, National Textile Center, 2000; 2000.

147. Warner, S. B., *Fiber Science*. Prentice Hall: Englewood Cliffs, NJ, 1995.

148. Zong, X., Kim, K., Fang, D., Ran, S., Hsiao, B. and Chu, B., Structure and process relationship of electrospun bioabsorbable nanofiber membranes. *Polymer* **2002,** 43, 4403-4412.

149. Miyajima, M., Koshika, A., Okada, J., Kaess, M. and Ikada, Y., Factors influencing the diffusion-controlled release of papaverine from poly(l-lactic acid) matrix. *Journal of Controlled Release* **1998,** 56, 85-94.

150. Zurita, R., Puiggali, J. and Rodriguez-Galan, A., Triclosan release from coated polyglycolide threads. *Macromol Biosci* **2006,** 6, (1), 58-69.

151. Ford, J. L., Rubinstein, M. H. and Hogan, J. E., Formulation of sustained release promethazine hydrochloride tablets using hydroxypropylmeethycellulose matrices. *International Journal of PHarmaceutics* **1985,** 24, 327-338.

152. Ritger, P. L. and Peppas, N. A., A simple equation for description of solute release I. Fickian and non-Fickian release from non-swellable devices in the form of slabs, spheres, cylinders or discs. *Journal of Controlled Release* **1987,** 5, 23-36.

153. Zurita, R., Puiggali, J. and Rodriguez-Galan, A., Triclosan release from coated polyglycolide threads. *Macromolecular Bioscience* **2006,** 6, (1), 58-69.

154. Miyajima, M., Koshika, A., Okada, J. and Ikeda, M., Mechanism of drug release from poly(L-lactic acid) matrix containing acidic or neutral drugs. *Journal of Controlled Release* **1999,** 60, 199-209.

155. Hsu, Y. Y., Gresser, J. D., Trantolo, D. J., Lyons, C. M., Gangadharam, P. R. J. and Wise, D. L., *In vitro* controlled release of isoniazid from poly(lactide-co-glycolide) matrices. *Journal of Controlled Release* **1994,** 31, 223-228.

156. Warner, S. B., *Fiber Science*. Prentice Hall: Englewood Cliffs, NJ, p 55.

APPENDICES

Appendix A: The Influence of Spinning Parameters on Fiber Diameters

1. Polymer Concentration

SAS Program

```
Data Diameter;
input group $ dia;
datalines;
14%  0.53
14%  0.43
14%  0.33
14%  0.69
14%  0.52
14%  0.48
14%  0.79
14%  0.60
14%  0.50
14%  0.47
14%  0.40
14%  0.33
14%  0.52
14%  0.46
14%  0.40
14%  0.60
14%  0.51
14%  0.40
15%  0.64
15%  0.47
15%  0.37
15%  0.79
15%  0.63
15%  0.50
15%  1.59
15%  1.11
15%  0.55
15%  0.56
15%  0.44
15%  0.35
15%  0.61
```

```
15%    0.56
15%    0.53
15%    0.76
15%    0.60
15%    0.44
;

Proc npar1way data=Diameter Wilcoxon;
class group;
var dia;
run;
```

SAS Output

The NPAR1WAY Procedure

Wilcoxon Scores (Rank Sums) for Variable dia
Classified by Variable group

group	N	Sum of Scores	Expected Under H0	Std Dev Under H0	Mean Score
14%	18	273.0	333.0	31.574402	15.166667
15%	18	393.0	333.0	31.574402	21.833333

Average scores were used for ties.

Wilcoxon Two-Sample Test

Statistic	273.0000
Normal Approximation	
Z	-1.8844
One-Sided Pr < Z	0.0298
Two-Sided Pr > |Z|	0.0595
t Approximation	
One-Sided Pr < Z	0.0339
Two-Sided Pr > |Z|	0.0678

Z includes a continuity correction of 0.5.

2. Feedrate

SAS Program

```
Data Diameter;
input group $ dia;
datalines;
0.3ml/h     0.53
0.3ml/h     0.43
0.3ml/h     0.33
0.3ml/h     0.64
0.3ml/h     0.47
0.3ml/h     0.37
0.3ml/h     0.47
0.3ml/h     0.40
0.3ml/h     0.33
0.3ml/h     0.56
0.3ml/h     0.44
0.3ml/h     0.35
0.4ml/h     0.79
0.4ml/h     0.60
0.4ml/h     0.50
0.4ml/h     1.59
0.4ml/h     1.11
0.4ml/h     0.55
0.4ml/h     0.60
0.4ml/h     0.51
0.4ml/h     0.40
0.4ml/h     0.76
0.4ml/h     0.60
0.4ml/h     0.44
;

Proc npar1way data=Diameter Wilcoxon;
class group;
var dia;
run;
```

SAS Output

The NPAR1WAY Procedure

Wilcoxon Scores (Rank Sums) for Variable dia
Classified by Variable group

group	N	Sum of Scores	Expected Under H0	Std Dev Under H0	Mean Score
0.3ml/h	12	102.0	150.0	17.290359	8.50
0.4ml/h	12	198.0	150.0	17.290359	16.50

Average scores were used for ties.

Wilcoxon Two-Sample Test

Statistic	102.0000
Normal Approximation	
Z	-2.7472
One-Sided Pr < Z	0.0030
Two-Sided Pr > |Z|	0.0060
t Approximation	
One-Sided Pr < Z	0.0057
Two-Sided Pr > |Z|	0.0115

Z includes a continuity correction of 0.5.

3. Voltage

SAS Program

```
Data Diameter;
input group $ dia;
datalines;
7k      0.53
7k      0.69
7k      0.79
7k      0.64
7k      0.79
7k      1.59
7k      0.47
7k      0.52
7k      0.60
7k      0.56
7k      0.61
7k      0.76
8k      0.43
```

```
8k      0.52
8k      0.60
8k      0.47
8k      0.63
8k      1.11
8k      0.40
8k      0.46
8k      0.51
8k      0.44
8k      0.56
8k      0.60
;

Proc npar1way data=Diameter Wilcoxon;
class group;
var dia;
run;
```

SAS Output

The NPAR1WAY Procedure

Wilcoxon Scores (Rank Sums) for Variable dia
Classified by Variable group

group	N	Sum of Scores	Expected Under H0	Std Dev Under H0	Mean Score
7k	12	189.50	150.0	17.290359	15.791667
8k	12	110.50	150.0	17.290359	9.208333

Average scores were used for ties.

Wilcoxon Two-Sample Test

Statistic	189.5000

Normal Approximation

Z	2.2556
One-Sided Pr > Z	0.0120
Two-Sided Pr > |Z|	0.0241

t Approximation

One-Sided Pr > Z	0.0170
Two-Sided Pr > |Z|	0.0339

Z includes a continuity correction of 0.5.

SAS Program

```
Data Diameter;
input group $ dia;
datalines;
7k      0.53
7k      0.69
7k      0.79
7k      0.64
7k      0.79
7k      1.59
7k      0.47
7k      0.52
7k      0.60
7k      0.56
7k      0.61
7k      0.76
9k      0.33
9k      0.48
9k      0.50
9k      0.37
9k      0.50
9k      0.55
9k      0.33
9k      0.40
9k      0.40
9k      0.35
9k      0.53
9k      0.44
;

Proc npar1way data=Diameter Wilcoxon;
class group;
var dia;
run;
```

SAS Output

The NPAR1WAY Procedure

Wilcoxon Scores (Rank Sums) for Variable dia
Classified by Variable group

group	N	Sum of Scores	Expected Under H0	Std Dev Under H0	Mean Score

7k	12	213.50	150.0	17.301671	17.791667
9k	12	86.50	150.0	17.301671	7.208333

Average scores were used for ties.

Wilcoxon Two-Sample Test

Statistic 213.5000

Normal Approximation
Z 3.6413
One-Sided Pr > Z 0.0001
Two-Sided Pr > |Z| 0.0003

t Approximation
One-Sided Pr > Z 0.0007
Two-Sided Pr > |Z| 0.0014

Z includes a continuity correction of 0.5.

SAS Program

```
Data Diameter;
input group $ dia;
datalines;
8k 0.43
8k 0.52
8k 0.60
8k 0.47
8k 0.63
8k 1.11
8k 0.40
8k 0.46
8k 0.51
8k 0.44
8k 0.56
8k 0.60
9k 0.33
9k 0.48
9k 0.50
9k 0.37
9k 0.50
9k 0.55
9k 0.33
```

```
9k      0.40
9k      0.40
9k      0.35
9k      0.53
9k      0.44
;

Proc npar1way data=Diameter Wilcoxon;
class group;
var dia;
run;
```

SAS Output

The NPAR1WAY Procedure
Wilcoxon Scores (Rank Sums) for Variable dia
Classified by Variable group

group	N	Sum of Scores	Expected Under H0	Std Dev Under H0	Mean Score
8k	12	189.50	150.0	17.290359	15.791667
9k	12	110.50	150.0	17.290359	9.208333

Average scores were used for ties.

Wilcoxon Two-Sample Test

Statistic	189.5000

Normal Approximation

Z	2.2556
One-Sided Pr > Z	0.0120
Two-Sided Pr > |Z|	0.0241

t Approximation

One-Sided Pr > Z	0.0170
Two-Sided Pr > |Z|	0.0339

Z includes a continuity correction of 0.5.

4. Ampicillin

SAS Program

```
Data Diameter;
input group $ dia;
datalines;
w/o     0.53
w/o     0.43
w/o     0.33
w/o     0.69
w/o     0.52
w/o     0.48
w/o     0.79
w/o     0.60
w/o     0.50
w/o     0.64
w/o     0.47
w/o     0.37
w/o     0.79
w/o     0.63
w/o     0.50
w/o     1.59
w/o     1.11
w/o     0.55
w/      0.47
w/      0.40
w/      0.33
w/      0.52
w/      0.46
w/      0.40
w/      0.60
w/      0.51
w/      0.40
w/      0.56
w/      0.44
w/      0.35
w/      0.61
w/      0.56
w/      0.53
w/      0.76
w/      0.60
w/      0.44
;

Proc npar1way data=Diameter Wilcoxon;
```

```
class group;
var dia;
run;
```

SAS Output

The NPAR1WAY Procedure

Wilcoxon Scores (Rank Sums) for Variable dia
Classified by Variable group

group	N	Sum of Scores	Expected Under H0	Std Dev Under H0	Mean Score
w/o	18	386.0	333.0	31.574402	21.444444
w/	18	280.0	333.0	31.574402	15.555556

Average scores were used for ties.

Wilcoxon Two-Sample Test

Statistic	386.0000
Normal Approximation	
Z	1.6627
One-Sided Pr > Z	0.0482
Two-Sided Pr > |Z|	0.0964
t Approximation	
One-Sided Pr > Z	0.0526
Two-Sided Pr > |Z|	0.1053

Z includes a continuity correction of 0.5.

Appendix B. The influence of Ampicillin Concentration on Percentage of Crystallinity of Fibers

SAS Program

```
data Percentcry;
input group $ crystal;
datalines;
noamp     43.21
noamp     47.14
noamp     49.52
noamp     39.54
noamp     42.65
noamp     46.44
noamp     44.71
noamp     47.98
noamp     56.27
amp      28.11
amp      35.00
amp      41.76
amp      12.66
amp      14.07
amp      27.08
amp      34.84
amp      37.12
amp      50.43
;

proc npar1way data=Percentcry Wilcoxon;
class group;
var crystal;
run;
```

SAS Output

The NPAR1WAY Procedure

Wilcoxon Scores (Rank Sums) for Variable crystal
Classified by Variable group

group	N	Sum of Scores	Expected Under H0	Std Dev Under H0	Mean Score
noamp	9	117.0	85.50	11.324752	13.0

amp	9	54.0	85.50	11.324752	6.0

Wilcoxon Two-Sample Test

Statistic	117.0000
Normal Approximation	
Z	2.7374
One-Sided Pr > Z	0.0031
Two-Sided Pr > |Z|	0.0062
t Approximation	
One-Sided Pr > Z	0.0070
Two-Sided Pr > |Z|	0.0140

Z includes a continuity correction of 0.5.

Appendix C. The Influence of Ampicillin Concentration on Yarn Tensile Properties

SAS Program

```
Data Tensile;
Input group $ elong load;
datalines;
0%      62.21   1.316
0%      50.70   2.501
0%      60.30   1.448
0%      48.79   1.580
0%      72.00   2.501
0%      79.27   2.764
0%      73.27   2.369
0%      74.13   2.501
0%      75.53   2.764
0%      67.53   1.448
8%      77.00   3.027
8%      63.65   3.554
8%      59.02   2.369
8%      66.10   3.159
8%      69.20   2.896
8%      51.01   2.106
8%      64.11   3.159
8%      63.85   3.291
8%      64.58   3.027
8%      60.50   3.949
;

Proc npar1way data=Tensile Wilcoxon;
class group;
var elong;
var load;
run;
```

SAS Output

The NPAR1WAY Procedure

Wilcoxon Scores (Rank Sums) for Variable elong
Classified by Variable group

group	N	Sum of Scores	Expected Under H0	Std Dev Under H0	Mean Score
0%	10	114.0	105.0	13.228757	11.40
8%	10	96.0	105.0	13.228757	9.60

Wilcoxon Two-Sample Test

Statistic 114.0000

Normal Approximation
Z 0.6425
One-Sided Pr > Z 0.2603
Two-Sided Pr > |Z| 0.5205

t Approximation
One-Sided Pr > Z 0.2641
Two-Sided Pr > |Z| 0.5282

Z includes a continuity correction of 0.5.

The NPAR1WAY Procedure

Wilcoxon Scores (Rank Sums) for Variable load
Classified by Variable group

group	N	Sum of Scores	Expected Under H0	Std Dev Under H0	Mean Score
0%	10	66.50	105.0	13.183922	6.650
8%	10	143.50	105.0	13.183922	14.350

Average scores were used for ties.

Wilcoxon Two-Sample Test
Statistic 66.5000

Normal Approximation
Z -2.8823
One-Sided Pr < Z 0.0020
Two-Sided Pr > |Z| 0.0039

t Approximation
One-Sided Pr < Z 0.0048
Two-Sided Pr > |Z| 0.0095

Z includes a continuity correction of 0.5.

SAS Program

```
Data Tensile;
Input group $ elong load;
datalines;
0%    62.21  1.316
0%    50.70  2.501
0%    60.30  1.448
0%    48.79  1.580
0%    72.00  2.501
0%    79.27  2.764
0%    73.27  2.369
0%    74.13  2.501
0%    75.53  2.764
0%    67.53  1.448
12%   54.12  2.238
12%   70.87  2.896
12%   53.57  2.633
12%   58.87  3.554
12%   78.07  3.027
12%   55.83  4.081
12%   58.13  4.081
12%   50.03  2.896
12%   47.08  3.159
12%   58.51  3.170
;

Proc npar1way data=Tensile Wilcoxon;
class group;
var elong;
var load;
run;
```

SAS Output

The NPAR1WAY Procedure

Wilcoxon Scores (Rank Sums) for Variable elong
Classified by Variable group

group	N	Sum of Scores	Expected Under H0	Std Dev Under H0	Mean Score
0%	10	128.0	105.0	13.228757	12.80
12%	10	82.0	105.0	13.228757	8.20

Wilcoxon Two-Sample Test

Statistic 128.0000

Normal Approximation
Z 1.7008
One-Sided Pr > Z 0.0445
Two-Sided Pr > |Z| 0.0890

t Approximation
One-Sided Pr > Z 0.0526
Two-Sided Pr > |Z| 0.1053

Z includes a continuity correction of 0.5.

The NPAR1WAY Procedure

Wilcoxon Scores (Rank Sums) for Variable load
Classified by Variable group

group	N	Sum of Scores	Expected Under H0	Std Dev Under H0	Mean Score
0%	10	63.0	105.0	13.188911	6.30
12%	10	147.0	105.0	13.188911	14.70

Average scores were used for ties.

Wilcoxon Two-Sample Test

Statistic 63.0000

Normal Approximation
Z -3.1466
One-Sided Pr < Z 0.0008
Two-Sided Pr > |Z| 0.0017

t Approximation
One-Sided Pr < Z 0.0027
Two-Sided Pr > |Z| 0.0053

Z includes a continuity correction of 0.5.

SAS Program

```
Data Tensile;
Input group $ elong load;
datalines;
0%    62.21  1.316
0%    50.70  2.501
0%    60.30  1.448
0%    48.79  1.580
0%    72.00  2.501
0%    79.27  2.764
0%    73.27  2.369
0%    74.13  2.501
0%    75.53  2.764
0%    67.53  1.448
16%   85.67  4.344
16%   71.07  4.081
16%   66.61  5.002
16%   80.73  3.554
16%   70.07  4.870
16%   66.49  3.949
16%   74.07  3.291
16%   58.44  3.027
16%   78.33  3.818
16%   49.96  3.685
;

Proc npar1way data=Tensile Wilcoxon;
class group;
var elong;
var load;
run;
```

SAS Output

The NPAR1WAY Procedure

Wilcoxon Scores (Rank Sums) for Variable elong
Classified by Variable group

group	N	Sum of Scores	Expected Under H0	Std Dev Under H0	Mean Score
0%	10	98.0	105.0	13.228757	9.80
16%	10	112.0	105.0	13.228757	11.20

Wilcoxon Two-Sample Test

Statistic 98.0000

Normal Approximation
Z -0.4914
One-Sided Pr < Z 0.3116
Two-Sided Pr > |Z| 0.6232

t Approximation
One-Sided Pr < Z 0.3144
Two-Sided Pr > |Z| 0.6288

Z includes a continuity correction of 0.5.

The NPAR1WAY Procedure

Wilcoxon Scores (Rank Sums) for Variable load
Classified by Variable group

group	N	Sum of Scores	Expected Under H0	Std Dev Under H0	Mean Score
0%	10	55.0	105.0	13.198884	5.50
16%	10	155.0	105.0	13.198884	15.50

Average scores were used for ties.

Wilcoxon Two-Sample Test

Statistic 55.0000

Normal Approximation
Z -3.7503
One-Sided Pr < Z <.0001
Two-Sided Pr > |Z| 0.0002

t Approximation
One-Sided Pr < Z 0.0007
Two-Sided Pr > |Z| 0.0014

Z includes a continuity correction of 0.5.

SAS Program

```
Data Tensile;
Input group $ elong load;
datalines;
0%    62.21  1.316
0%    50.70  2.501
0%    60.30  1.448
0%    48.79  1.580
0%    72.00  2.501
0%    79.27  2.764
0%    73.27  2.369
0%    74.13  2.501
0%    75.53  2.764
0%    67.53  1.448
20%   66.87  2.369
20%   70.93  3.818
20%   47.75  2.764
20%   52.76  2.106
20%   60.97  2.633
20%   58.83  2.501
20%   60.42  5.002
20%   72.80  3.818
20%   62.64  3.027
20%   71.13  4.081
;

Proc npar1way data=Tensile Wilcoxon;
class group;
var elong;
var load;
run;
```

SAS Output

The NPAR1WAY Procedure

Wilcoxon Scores (Rank Sums) for Variable elong
Classified by Variable group

group	N	Sum of Scores	Expected Under H0	Std Dev Under H0	Mean Score
0%	10	121.0	105.0	13.228757	12.10
20%	10	89.0	105.0	13.228757	8.90

Wilcoxon Two-Sample Test

Statistic 121.0000

Normal Approximation
Z 1.1717
One-Sided Pr > Z 0.1207
Two-Sided Pr > |Z| 0.2413

t Approximation
One-Sided Pr > Z 0.1279
Two-Sided Pr > |Z| 0.2558

Z includes a continuity correction of 0.5.

The NPAR1WAY Procedure

Wilcoxon Scores (Rank Sums) for Variable load
Classified by Variable group

group	N	Sum of Scores	Expected Under H0	Std Dev Under H0	Mean Score
0%	10	73.0	105.0	13.143940	7.30
20%	10	137.0	105.0	13.143940	13.70

Average scores were used for ties.

Wilcoxon Two-Sample Test
Statistic 73.0000

Normal Approximation
Z -2.3965
One-Sided Pr < Z 0.0083
Two-Sided Pr > |Z| 0.0166

t Approximation
One-Sided Pr < Z 0.0135
Two-Sided Pr > |Z| 0.0270

Z includes a continuity correction of 0.5.

SAS Program

```
Data Tensile;
Input group $ elong load;
datalines;
8%    77.00  3.027
8%    63.65  3.554
8%    59.02  2.369
8%    66.10  3.159
8%    69.20  2.896
8%    51.01  2.106
8%    64.11  3.159
8%    63.85  3.291
8%    64.58  3.027
8%    60.50  3.949
12%   54.12  2.238
12%   70.87  2.896
12%   53.57  2.633
12%   58.87  3.554
12%   78.07  3.027
12%   55.83  4.081
12%   58.13  4.081
12%   50.03  2.896
12%   47.08  3.159
12%   58.51  3.170
;

Proc npar1way data=Tensile Wilcoxon;
class group;
var elong;
var load;
run;
```

SAS Output

The NPAR1WAY Procedure

Wilcoxon Scores (Rank Sums) for Variable elong
Classified by Variable group

group	N	Sum of Scores	Expected Under H0	Std Dev Under H0	Mean Score
8%	10	130.0	105.0	13.228757	13.0
12%	10	80.0	105.0	13.228757	8.0

Wilcoxon Two-Sample Test

Statistic 130.0000

Normal Approximation
Z 1.8520
One-Sided Pr > Z 0.0320
Two-Sided Pr > |Z| 0.0640

t Approximation
One-Sided Pr > Z 0.0398
Two-Sided Pr > |Z| 0.0796

Z includes a continuity correction of 0.5.

The NPAR1WAY Procedure

Wilcoxon Scores (Rank Sums) for Variable load
Classified by Variable group

group	N	Sum of Scores	Expected Under H0	Std Dev Under H0	Mean Score
8%	10	101.50	105.0	13.158947	10.150
12%	10	108.50	105.0	13.158947	10.850

Average scores were used for ties.

Wilcoxon Two-Sample Test

Statistic 101.5000

Normal Approximation
Z -0.2280
One-Sided Pr < Z 0.4098
Two-Sided Pr > |Z| 0.8197

t Approximation
One-Sided Pr < Z 0.4110
Two-Sided Pr > |Z| 0.8221

Z includes a continuity correction of 0.5.

SAS Program

```
Data Tensile;
Input group $ elong load;
datalines;
8%      77.00   3.027
8%      63.65   3.554
8%      59.02   2.369
8%      66.10   3.159
8%      69.20   2.896
8%      51.01   2.106
8%      64.11   3.159
8%      63.85   3.291
8%      64.58   3.027
8%      60.50   3.949
16%     85.67   4.344
16%     71.07   4.081
16%     66.61   5.002
16%     80.73   3.554
16%     70.07   4.870
16%     66.49   3.949
16%     74.07   3.291
16%     58.44   3.027
16%     78.33   3.818
16%     49.96   3.685
;

Proc npar1way data=Tensile Wilcoxon;
class group;
var elong;
var load;
run;
```

SAS Output

The NPAR1WAY Procedure

Wilcoxon Scores (Rank Sums) for Variable elong
Classified by Variable group

group	N	Sum of Scores	Expected Under H0	Std Dev Under H0	Mean Score
8%	10	81.0	105.0	13.228757	8.10
16%	10	129.0	105.0	13.228757	12.90

Wilcoxon Two-Sample Test

Statistic 81.0000

Normal Approximation
Z -1.7764
One-Sided Pr < Z 0.0378
Two-Sided Pr > |Z| 0.0757

t Approximation
One-Sided Pr < Z 0.0458
Two-Sided Pr > |Z| 0.0917

Z includes a continuity correction of 0.5.

The NPAR1WAY Procedure

Wilcoxon Scores (Rank Sums) for Variable load
Classified by Variable group

group	N	Sum of Scores	Expected Under H0	Std Dev Under H0	Mean Score
8%	10	67.50	105.0	13.188911	6.750
16%	10	142.50	105.0	13.188911	14.250

Average scores were used for ties.

Wilcoxon Two-Sample Test

Statistic 67.5000

Normal Approximation
Z -2.8054
One-Sided Pr < Z 0.0025
Two-Sided Pr > |Z| 0.0050

t Approximation
One-Sided Pr < Z 0.0056
Two-Sided Pr > |Z| 0.0113

Z includes a continuity correction of 0.5.

SAS Program

```
Data Tensile;
Input group $ elong load;
datalines;
8%    77.00  3.027
8%    63.65  3.554
8%    59.02  2.369
8%    66.10  3.159
8%    69.20  2.896
8%    51.01  2.106
8%    64.11  3.159
8%    63.85  3.291
8%    64.58  3.027
8%    60.50  3.949
20%   66.87  2.369
20%   70.93  3.818
20%   47.75  2.764
20%   52.76  2.106
20%   60.97  2.633
20%   58.83  2.501
20%   60.42  5.002
20%   72.80  3.818
20%   62.64  3.027
20%   71.13  4.081
;

Proc npar1way data=Tensile Wilcoxon;
class group;
var elong;
var load;
run;
```

SAS Output

The NPAR1WAY Procedure

Wilcoxon Scores (Rank Sums) for Variable elong
Classified by Variable group

group	N	Sum of Scores	Expected Under H0	Std Dev Under H0	Mean Score
8%	10	110.0	105.0	13.228757	11.0
20%	10	100.0	105.0	13.228757	10.0

Wilcoxon Two-Sample Test

Statistic 110.0000

Normal Approximation
Z 0.3402
One-Sided Pr > Z 0.3669
Two-Sided Pr > |Z| 0.7337

t Approximation
One-Sided Pr > Z 0.3687
Two-Sided Pr > |Z| 0.7375

Z includes a continuity correction of 0.5.

The NPAR1WAY Procedure

Wilcoxon Scores (Rank Sums) for Variable load
Classified by Variable group

group	N	Sum of Scores	Expected Under H0	Std Dev Under H0	Mean Score
8%	10	105.0	105.0	13.188911	10.50
20%	10	105.0	105.0	13.188911	10.50

Average scores were used for ties.

Wilcoxon Two-Sample Test

Statistic 105.0000

Normal Approximation
Z 0.0000
One-Sided Pr < Z 0.5000
Two-Sided Pr > |Z| 1.0000

t Approximation
One-Sided Pr < Z 0.5000
Two-Sided Pr > |Z| 1.0000

Z includes a continuity correction of 0.5.

SAS Program

```
Data Tensile;
Input group $ elong load;
datalines;
12%    54.12   2.238
12%    70.87   2.896
12%    53.57   2.633
12%    58.87   3.554
12%    78.07   3.027
12%    55.83   4.081
12%    58.13   4.081
12%    50.03   2.896
12%    47.08   3.159
12%    58.51   3.170
16%    85.67   4.344
16%    71.07   4.081
16%    66.61   5.002
16%    80.73   3.554
16%    70.07   4.870
16%    66.49   3.949
16%    74.07   3.291
16%    58.44   3.027
16%    78.33   3.818
16%    49.96   3.685
;

Proc npar1way data=Tensile Wilcoxon;
class group;
var elong;
var load;
run;
```

SAS Output

The NPAR1WAY Procedure

Wilcoxon Scores (Rank Sums) for Variable elong
Classified by Variable group

group	N	Sum of Scores	Expected Under H0	Std Dev Under H0	Mean Score
12%	10	76.0	105.0	13.228757	7.60
16%	10	134.0	105.0	13.228757	13.40

Wilcoxon Two-Sample Test

Statistic 76.0000

Normal Approximation
Z -2.1544
One-Sided Pr < Z 0.0156
Two-Sided Pr > |Z| 0.0312

t Approximation
One-Sided Pr < Z 0.0221
Two-Sided Pr > |Z| 0.0443

Z includes a continuity correction of 0.5.

The NPAR1WAY Procedure

Wilcoxon Scores (Rank Sums) for Variable load
Classified by Variable group

group	N	Sum of Scores	Expected Under H0	Std Dev Under H0	Mean Score
12%	10	73.0	105.0	13.193898	7.30
16%	10	137.0	105.0	13.193898	13.70

Average scores were used for ties.

Wilcoxon Two-Sample Test

Statistic 73.0000

Normal Approximation
Z -2.3875
One-Sided Pr < Z 0.0085
Two-Sided Pr > |Z| 0.0170

t Approximation
One-Sided Pr < Z 0.0138
Two-Sided Pr > |Z| 0.0275

Z includes a continuity correction of 0.5.

SAS Program

```
Data Tensile;
Input group $ elong load;
datalines;
12%    54.12   2.238
12%    70.87   2.896
12%    53.57   2.633
12%    58.87   3.554
12%    78.07   3.027
12%    55.83   4.081
12%    58.13   4.081
12%    50.03   2.896
12%    47.08   3.159
12%    58.51   3.170
20%    66.87   2.369
20%    70.93   3.818
20%    47.75   2.764
20%    52.76   2.106
20%    60.97   2.633
20%    58.83   2.501
20%    60.42   5.002
20%    72.80   3.818
20%    62.64   3.027
20%    71.13   4.081
;

Proc npar1way data=Tensile Wilcoxon;
class group;
var elong;
var load;
run;
```

SAS Output

The NPAR1WAY Procedure

Wilcoxon Scores (Rank Sums) for Variable elong
Classified by Variable group

group	N	Sum of Scores	Expected Under H0	Std Dev Under H0	Mean Score
12%	10	86.0	105.0	13.228757	8.60
20%	10	124.0	105.0	13.228757	12.40

Wilcoxon Two-Sample Test

Statistic 86.0000

Normal Approximation
Z -1.3985
One-Sided Pr < Z 0.0810
Two-Sided Pr > |Z| 0.1620

t Approximation
One-Sided Pr < Z 0.0890
Two-Sided Pr > |Z| 0.1781

Z includes a continuity correction of 0.5.

The NPAR1WAY Procedure

Wilcoxon Scores (Rank Sums) for Variable load
Classified by Variable group

group	N	Sum of Scores	Expected Under H0	Std Dev Under H0	Mean Score
12%	10	110.0	105.0	13.188911	11.0
20%	10	100.0	105.0	13.188911	10.0

Average scores were used for ties.

Wilcoxon Two-Sample Test

Statistic 110.0000

Normal Approximation
Z 0.3412
One-Sided Pr > Z 0.3665
Two-Sided Pr > |Z| 0.7330

t Approximation
One-Sided Pr > Z 0.3684
Two-Sided Pr > |Z| 0.7367

Z includes a continuity correction of 0.5.

SAS Program

```
Data Tensile;
Input group $ elong load;
datalines;
16%    85.67   4.344
16%    71.07   4.081
16%    66.61   5.002
16%    80.73   3.554
16%    70.07   4.870
16%    66.49   3.949
16%    74.07   3.291
16%    58.44   3.027
16%    78.33   3.818
16%    49.96   3.685
20%    66.87   2.369
20%    70.93   3.818
20%    47.75   2.764
20%    52.76   2.106
20%    60.97   2.633
20%    58.83   2.501
20%    60.42   5.002
20%    72.80   3.818
20%    62.64   3.027
20%    71.13   4.081
;

Proc npar1way data=Tensile Wilcoxon;
class group;
var elong;
var load;
run;
```

SAS Output

The NPAR1WAY Procedure

Wilcoxon Scores (Rank Sums) for Variable elong
Classified by Variable group

group	N	Sum of Scores	Expected Under H0	Std Dev Under H0	Mean Score
16%	10	125.0	105.0	13.228757	12.50
20%	10	85.0	105.0	13.228757	8.50

Wilcoxon Two-Sample Test

Statistic 125.0000

Normal Approximation
Z 1.4741
One-Sided Pr > Z 0.0702
Two-Sided Pr > |Z| 0.1405

t Approximation
One-Sided Pr > Z 0.0784
Two-Sided Pr > |Z| 0.1568

Z includes a continuity correction of 0.5.

The NPAR1WAY Procedure

Wilcoxon Scores (Rank Sums) for Variable load
Classified by Variable group

group	N	Sum of Scores	Expected Under H0	Std Dev Under H0	Mean Score
16%	10	129.50	105.0	13.193898	12.950
20%	10	80.50	105.0	13.193898	8.050

Average scores were used for ties.

Wilcoxon Two-Sample Test

Statistic 129.5000

Normal Approximation
Z 1.8190
One-Sided Pr > Z 0.0345
Two-Sided Pr > |Z| 0.0689

t Approximation
One-Sided Pr > Z 0.0424
Two-Sided Pr > |Z| 0.0847

Z includes a continuity correction of 0.5.